

**W-PM-SymIV-1 MODEL FOR THE FLAGELLAR ROTARY MOTOR.** H.C. Berg, Division of Biology, California Institute of Technology, Pasadena, CA 91125

A bacterial flagellum is driven at its base by a reversible rotary motor powered by a proton flux. Data on the structure and function of this device have led to a model for the motor (Berg & Khan, *In Mobility and Recognition in Cell Biology*, Sund & Veeger, eds., de Gruyter, Berlin, 1983, pp. 485-497) in which transmembrane particles linked elastically to the S-ring (the stator) move from site to site along the periphery of the M-ring (the rotor). Each particle executes a random walk with a bias determined by the elastic constraints and the occupancy of adjacent sites. Protons from the outside or the inside of the cell reach these sites via a pair of channels, one of which acts as a proton well. A particle can advance only when the site at the bottom of the outer channel is occupied and the site at the bottom of the inner channel is unoccupied; as a result, its motion is tightly coupled to proton flow. At equilibrium, the work done against the elastic constraints is balanced by the energy available when a proton moves down its electrochemical gradient; the elastic restoring force is balanced by the external load. The model predicts a stall torque proportional to the protonmotive force, the absence of exponential thermal effects, and smooth displacement, all of which are observed in practice. It leads to several predictions about variation in speed as a function of protonmotive force, pH, and external load. The model will be described in detail, and experiments that confirm some of these predictions will be discussed.

**W-PM-SymIV-2 MECHANOELECTRICAL TRANSDUCTION BY HAIR CELLS OF THE INTERNAL EAR.** A. J. Hudspeth, Department of Physiology S-762, University of California, San Francisco CA 94143.

The function of mechanoreceptors is the inverse of that in motile systems; rather than converting chemical energy into mechanical work, receptors produce an output that represents work done on them by the environment. The response is generally an electrical signal, or receptor potential, produced by the flow of ionic current gated by the mechanical input. The sensory receptors of the internal ear, or hair cells, have on their apical surfaces 30-300 stereocilia, regularly arranged derivatives of microvilli, which are the sites of transduction. Using *in vitro* preparations from the ears of lower vertebrates, we are investigating mechanoelectrical transduction. Hair cells are extraordinarily sensitive: responses can be obtained with stimuli of atomic dimensions, that is, by approximately 100-pm deflections of the hair bundle's tip. Although the transducer saturates with stimuli larger than about  $\pm 200$  nm, the cells possess an adaptation mechanism that allows them to respond to small, transient stimuli in the presence of large, static ones. The mechanosensitivity is highly directional, a property that may be conferred by the complex arrangement of the stereocilia. The rate of opening of transduction channels increases with increasing stimulus size, suggesting that hair-bundle deflection gates channels by altering the free-energy difference between their closed and open states. Ion-substitution experiments indicate that the channel's ionophore is relatively non-selective, passing not only  $K^+$  and  $Na^+$ , but even small organic cations. The pattern of current flow through the medium surrounding a hair bundle indicates that active channels occur in the distal portions of the stereocilia, perhaps where contiguous cilia interact. (Supported by NIH grants NS13154 and NS20429)

**W-PM-SymIV-3 HYDRODYNAMICS AND THE FUNCTIONAL ROLES OF CYTOPLASMIC FLOWS.** Watt W. Webb, Applied Physics, Cornell University, Ithaca, NY 14853, and Eugene A. Nothnagel, Botany and Plant Science, University of California, Riverside, CA 92521.

The giant algae *Chara* and *Nitella* have served as approachable archetypes for studies of a general mechanism of active pumping of cytoplasmic flow. Their pumps consist of aligned stationary actin microfilaments that couple with myosin to provide a mechanical traction that propels the myosin and the structures to which it is attached. Hydrodynamic coupling between myosin-bearing gels and/or vesicles and the cytoplasm induces systematic, cooperative plug flow of the cytoplasm (Nothnagel and Webb, *J. Cell Biol.* 94:444, 1982). The hydrodynamic interaction between particles and flows can work in both directions; pumped streams of fluid can convect the entrained particles just as cooperatively driven particle motion can induce a flow. In vertebrate cells there are numerous systematic intracellular flows and cooperative particulate motions that are subject to similar hydrodynamic constraints. We hypothesize that the actin-myosin traction mechanism and/or its analogs may be ubiquitous too, and we consider their applicability to axoplasmic streaming, saltatory vesicle and particle motions in motile cells, interorganelle protein traffic, mass transport supplying and/or propelling growth zones, secretion and endocytosis.

Supported by NSF grant 83-03404.

**W-PM-SymIV-4**    PLASMODIAL OSCILLATIONS IN PHYSARUM AND THE MECHANOCHEMISTRY OF ACTOMYOSIN GELS. G. Oster, Department of Biophysics, University of California. Berkeley, CA 94720: G. Odell. Department of Mathematics, Rensselaer Polytechnic Institute. Troy, NY 12181.

Plasmodial strands of the slime mold *Physarum* exhibit rhythmic mechanical contractions which drive an alternating flow of cytoplasm ("shuttle-streaming"). We present a mechanochemical model for the plasmodial cytogel which can mimic the periodic mechanical and chemical behavior of the plasmodial rhythms. The model is built around the observation that calcium ions both solate actomyosin gels and stimulate active contraction of the gel.

**W-PM-A1** EFFECTS OF A SUBSTANCE RELEASED FROM A SINGLE CARDIAC CELL ON THE ELECTRICAL AND CONTRACTILE ACTIVITY OF SINGLE FROG ATRIAL CARDIAC CELLS. M. Tarr, and J.W. Trank. Physiology Dept., Univ. of Kansas College of Health Sciences and Hospital, Kansas City, KS. 66103.

In 1978 (Nature 34:1472) we reported a rather unexpected result that a substance released from a dying cardiac cell can induce spontaneous contractile activity in other isolated single cardiac cells within the vicinity of the dying cell. We have now found that this spontaneous contractile activity can occur without any coincident membrane depolarization although occasionally a spontaneous action potential does occur coincident with the spontaneous contraction. We have also found that the contractile response of the cell to electrical stimulation is enhanced for several contractions and that this enhanced contractility is often associated with action potentials having more positive plateau potentials. The enhanced contractility in response to electrical stimulation can occur even when the substance does not induce spontaneous contractile activity in the cell. A depression of contractility follows the enhanced contractility and this depression is generally associated with action potentials having less positive plateau potentials. The spontaneous contractile activity, the enhanced contractility associated with electrical stimulation, and the enhancement of the plateau potential are not blocked by the calcium channel blocker D600 (3  $\mu\text{g/ml}$ ) suggesting that these effects are not mediated by the slow channel calcium current. Preliminary experiments indicate that all of the above effects also occur when the isolated cell is superfused with ATP (10  $\mu\text{M}$ ) suggesting that the substance released from the dying cardiac cell may be ATP. (Supported by a Grant-in-Aid from the American Heart Association with funds contributed in part by the Kansas Affiliate, Inc.)

**W-PM-A2** ON IMPULSE RESPONSES OF AUTOMATICITY IN THE PURKINJE FIBERS

Teresa Ree Chay and Young Seek Lee, Department of Biological Sciences, University of Pittsburgh, Pittsburgh, PA 15260.

We have examined the effects of brief current pulses on the pacemaker oscillations of the Purkinje fibers using the model of McAllister, Noble, and Tsien (1976. J. Physiol. 251: 1-57). This model is used to construct phase response curves vs. brief electric stimuli to predict the size of "black holes," where rhythmic activity of the Purkinje fiber ceases. In our computer simulation, a brief current stimulus of the right magnitude and timing annihilates oscillations in membrane potential. The model also reveals a sequence of alternating periodic and chaotic regimes as the strength of a biasing current is increased. The results of our computer simulations agree very well with experimental work on Purkinje fibers. This work was supported by NSF PCM 79-22483.

**W-PM-A3** THE INFLUENCE OF  $\beta$ -ADRENERGIC STIMULATION ON THE RELATION BETWEEN INTRACELLULAR  $[\text{Ca}^{2+}]$  AND TENSION IN INTACT MAMMALIAN CARDIAC MUSCLE. E. Marban and W.G. Wier. Dept. of Physiology, University of Maryland, School of Medicine, Baltimore, Maryland, and the Johns Hopkins University Cardiology Division, Baltimore, Maryland.

We examined the relation between  $[\text{Ca}^{2+}]$  and tension in intact canine Purkinje fibers micro-injected with the  $\text{Ca}^{2+}$ -sensitive bioluminescent protein aequorin.  $\text{Ca}^{2+}$ -activated aequorin luminescence was recorded during slow tension changes induced by decreasing external  $[\text{Na}^+]$  from 140mM to 24mM, after exposure to a zero  $\text{K}^+$  solution for three minutes. Ryanodine ( $10^{-6}\text{M}$ ) was present to prevent oscillations in  $[\text{Ca}^{2+}]_i$  which can occur under such conditions (Wier, et al., 1983, PNAS, in press). Aequorin luminescence and tension were each sampled at 100 msec intervals; the  $[\text{Ca}^{2+}]$  was calculated from the aequorin luminescence at each point and an apparent  $[\text{Ca}^{2+}]$ -tension relation was constructed. Experiments were accepted for analysis only if the  $\text{Ca}^{2+}$ -tension relation was identical before and after exposure to isoproterenol ( $5 \times 10^{-7}\text{M}$ ). In two of three acceptable experiments, the  $[\text{Ca}^{2+}]$  associated with a given tension was less in the presence of isoproterenol than in its absence. In these experiments, the peak tension during the procedure was 30% less in the presence of isoproterenol than in its absence. The third fiber showed no response to isoproterenol. Our results suggest that  $\beta$ -adrenergic stimulation causes either an increase in the maximum  $\text{Ca}^{2+}$ -activated tension or an increase in the  $\text{Ca}^{2+}$ -sensitivity of the myofilaments. A decrease in  $\text{Ca}^{2+}$ -sensitivity of the myofilaments cannot be ruled out, but such a decrease must occur together with an increase in maximum  $\text{Ca}^{2+}$ -activated tension.

**W-PM-A4** RECONSTRUCTION OF PROPAGATING DEPOLARIZATION IN CARDIAC MUSCLE BASED ON VOLTAGE CLAMP DATA: Madison S. Spach, Joseph D. Sloan, and J. Mailen Kootsey. Duke University, Durham, NC.

The time course of  $g_{Na}$ ,  $I_{Na}$ ,  $I_{Cm}$ , and transmembrane potential  $V$  were computed for membrane action potentials (MAP) and uniformly propagating action potentials (PAP) based on the fast Na current kinetics in cardiac muscle described by Ebihara and Johnson. The linear relationship between peak  $g_{Na}$  or peak  $I_{Na}$  and  $\bar{G}_{Na}$  (number of sodium channels) during voltage clamp was not present during a MAP.  $g_{Na}$  and  $I_{Na}$  followed different time courses in a MAP; also, peak  $g_{Na}$  decreased more rapidly than peak  $I_{Na}$  and  $\dot{V}_{max}$  for similar decreases in  $\bar{G}_{Na}$ . The dissociation of  $g_{Na}$ - $I_{Na}$  in a MAP was related to the effective addition of  $C_m$  to the electrical circuit and the additional feed-back effect of the changing rate constants of  $I_{Na}$  activation and inactivation ( $m$  and  $h$ ) as  $V$  changed.  $I_{Na}$  and  $\dot{V}$  had the same time course in a MAP, but became dissociated during propagation. This further dissociation of  $g_{Na}$ - $I_{Na}$ - $\dot{V}$  in a PAP was due to the downstream  $C_m$  of the foot, an additional effective RC component. The results reproduced the voltage dependency of  $\dot{V}_{max}$  in TTX experiments (Baer, Best, Reuter. *Nature* 263:344, 1976) without any voltage dependency of peak  $g_{Na}$ . Further, for any baseline state that reduced  $\dot{V}$  ( $\uparrow g_{Leak}$  or  $\uparrow C_m$ ), the same decrease in  $\bar{G}_{Na}$  produced relatively greater decreases in  $\dot{V}_{max}$  in both a MAP and a PAP, as well as relatively greater decreases in velocity of a PAP. The different effects for a similar decrease in  $\bar{G}_{Na}$  were accounted for by uncoupling of  $g_{Na}$ - $I_{Na}$ - $\dot{V}$  as the effective electrical circuit changes from voltage clamp to membrane to propagated action potential. The results show that a concentration of a Na-channel blocking drug can have minimal effects on propagation in normal cardiac muscle, but produce marked conduction changes under abnormal conditions -- all due to the same decrease in the number of sodium channels.

**W-PM-A5** LINEAR IMPEDANCE OF CANINE PURKINJE STRANDS. Richard T. Mathias and Ira S. Cohen. Rush Medical College, Chicago 60612 and SUNY at Stony Brook 11794.

Linear frequency domain impedance studies were performed on short ( $\sim 1.3$ mm) Purkinje strands of narrow radius ( $\sim 0.16$ mm). The strands, obtained from mongrel dogs, were recovered for several hours in a Tyrode solution containing  $8\text{mM } [K^+]_o$  and  $4\text{mM } [Ca^{2+}]_o$  prior to initiating the experimental protocol. The strands were then impaled with two microelectrodes separated by 0.2-0.5 mm. One electrode passed current while the other electrode recorded the induced voltage. Whenever possible one electrode was moved in order to obtain the length constant. A wide band noise current was injected intracellularly and the impedance was recorded in accordance with techniques described in Mathias et al., 1981, *Biophys. J.* 36:221. The data were analyzed assuming the strand was a short transmission line, with zero current flow from either of the cut, healed over ends.

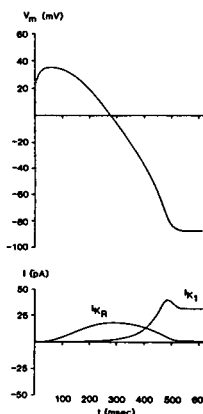
The strands are encased by a sheath of connective tissue which obscured the actual myocytes and therefore introduced uncertainty in our estimate of length, diameter and the existence of branching. However, to the accuracy of our data the sheath appears to provide zero series resistance. The effective extracellular resistance of the space within a strand, but between cells, appears to be quite variable, particularly from animal to animal. Sometimes its value is negligibly small, but in other preparations it was surprisingly large. The phase delay between the two electrodes was also variable. Implications of the structure to the spatial and temporal control of voltage will be presented. Also the effects of holding potential, extracellular  $[K^+]_o$ , and D600 will be summarized. Supported by NIH grants HL29205 and HL20558.

**W-PM-A6** REPOLARIZATION IN CARDIAC MUSCLE: AN EXPERIMENTAL AND THEORETICAL STUDY USING SINGLE CELLS FROM BULLFROG ATRIUM. W. Giles, K. Robinson, E.F. Shibata and J.R. Hume, University of Texas Medical Branch, Galveston, Texas 77550 and University of Calgary School of Medicine, Calgary, Canada T2N 4N1.

The mechanism of action potential repolarization in cardiac muscle is unknown. Recent hypotheses invoke three different transmembrane ionic currents: (1) a voltage- and time-dependent increase in a "delayed rectifier"  $K^+$  current, (2) an inactivation of  $i_{Si}$ , or  $i_{Ca}$ , and (3) an activation of an electrogenic pump current. We have studied the basis of repolarization in single bullfrog atrial cells by first performing voltage clamp measurements of each of these currents (1-3 above), and then simulating the repolarization process.

Our data and modelling strongly suggest that repolarization is initiated or triggered by a "delayed rectifier" current,  $i_{KR}$ , and is also modulated in the potential range  $-70$  to  $-90$  mV by an inwardly rectifying "background"  $K^+$  current,  $i_{K1}$  (See Fig.). The TTX-insensitive transient inward current,  $i_{Ca}$ , inactivates much too rapidly to produce repolarization. Our present action potential model indicates that no significant  $\Delta a(Na_1)$  ( $<0.5$  mM, from 5 mM) occurs at physiological heart rates; therefore, no significant phasic changes in electrogenic pump current would be expected in frog atrium.

Supported by DHHS-HL-27454, AHA-81-835, The Canadian MRC, and the Alberta Heritage Foundation.



**W-PM-A7 EVALUATION OF SINGLE SUCTION PIPETTE VOLTAGE CLAMP TECHNIQUE IN FROG VENTRICULAR MYOCYTES.** Leslie Tung and Martin Morad, Univ. of Penna., Dept. of Physiology, Philadelphia, PA

Isolated myocytes were obtained from frog ventricle (*Rana pipiens*) using enzymatic techniques (collagenase, trypsin). A single suction pipette was attached to a cell and had a seal resistance of 1-10 G $\Omega$ . Electronics were constructed which included: (1) compensation for current lost through the seal, and (2) electronic switching between voltage and current clamp modes, so that action potential (AP) and clamp currents could be recorded. Seal current compensation resulted in an increase in measured resting potential, elevation of plateau, shortening of AP, and increase in phase 3 repolarization. Cells (typically 300-350  $\mu$ m, length; 4-9  $\mu$ m, diameter) had resting potentials of -70 to -80 mV, overshoots of +30 to +40 mV, and input resistances of 80-125 M $\Omega$  (measured in hyperpolarizing direction). Total membrane capacitance was about 100 pF (measured from the time constant of decay of membrane potential in current clamp mode). These values compare favorably to those obtained in bulk preparations using the single sucrose gap voltage clamp technique. The isochronal I-V relation (at 400 ms) exhibited marked inward rectification of currents around resting potential, with a negative slope region for potentials between -50 and 0 mV. Two populations of cells were observed as defined by AP: those with a pronounced and sustained phase 2 plateau, and those with a rapidly decaying plateau. For a clamp step to 0 mV, both groups showed an initial fast inward current, followed by a slowly decreasing inward current for the first group and a transient outward current for the second group. These results suggest that measurement of AP and careful compensation of the seal leakage current are critical for a reliable study of the ionic currents in isolated cells.

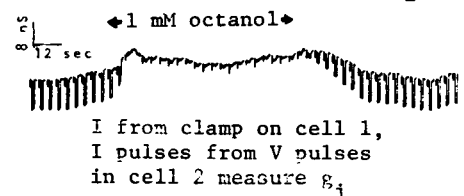
**W-PM-A8 INTRACELLULAR INJECTION OF cGMP, PrK INHIBITOR: FURTHER EVIDENCE FOR PHOSPHORYLATION OF MYOCARDIAL SLOW CHANNELS.** Ghassan Bkaily and Nick Sperelakis. Department of Physiology, University of Cincinnati College of Medicine, Cincinnati, OH 45267.

We have recently demonstrated in our laboratory, by intracellular injection of cyclic AMP (cAMP) via microiontophoresis and pressure injection, that cAMP is involved in the regulation of the myocardial slow channels. This effect is mediated presumably by activation of cAMP-dependent protein kinase (cAMP-PrK) and phosphorylation of the slow channels or an associated regulatory protein. To test this hypothesis, injection of cAMP, cGMP, PrK inhibitor, and the catalytic subunit of cAMP-PrK in cultured heart cells (reaggregates) was done using the liposome method. Automaticity and excitability of the cells were blocked by high K<sup>+</sup> (20 mM). Superfusion with phosphatidylcholine liposomes containing 10<sup>-6</sup> M cAMP restored excitability within 1-3 min. These restored slow APs were blocked by verapamil or nifedipine. Injection of 10<sup>-5</sup> or 10<sup>-3</sup> M cGMP blocked the naturally-occurring slow APs within 20 min. Addition of 10<sup>-6</sup> M isoproterenol did not reverse the effects of the injected cGMP. Prior exposure to cAMP (10<sup>-3</sup> M) did prevent the inhibitory effects of cGMP injection. Injection of PrK inhibitor rapidly and completely blocked the inward slow current (2-6 min) and depolarized the membrane to -15 mV. Hyperpolarizing current pulses did not restore the slow APs; neither did addition of histamine or isoproterenol. Injection of the catalytic subunit of cAMP-PrK did reverse the effects of PrK inhibitor. The data show that cGMP and cAMP may play opposing roles in regulation of the myocardial slow channels, and support the hypothesis that the slow channels must be phosphorylated in order to be available for voltage activation. (This study was supported by N.I.H. grant HL-31942 and Dr. Bkaily had a fellowship from the Canadian Heart Foundation.)

**W-PM-A9 SOME PHYSIOLOGICAL AND PHARMACOLOGICAL PROPERTIES OF CARDIAC GAP JUNCTIONS.**

R.L. White, D.C. Spray, G.J. Schwartz, B.A. Wittenberg, M.V.L. Bennett Depts. of Neuroscience, Pediatrics, and Physiology, Albert Einstein College of Medicine, Bronx, New York 10461.

Properties of gap junctions between cardiac cells have been difficult to study because of the complex geometry of the tissue. We have directly measured gap junctional conductance ( $g_j$ ) using pairs of myocytes isolated from rat ventricle (Wittenberg and Robinson '81, *Cell Tissue Res.* 16: 231.) Dissociated cells exhibit -70 mV resting and 110 mV action potentials in medium with 1-3 mM Ca. Soon after dissociation some cell pairs show electrotonic coupling; when maintained overnight, virtually all contiguous cells become coupled. Whole cell patch recordings from coupled cell pairs reveal  $g_j$  generally 5-100 nS.  $g_j$  is reversibly decreased to zero by brief extracellular application of CO<sub>2</sub> solution which acidifies the cell cytoplasm. Junctional conductance is also reversibly decreased to zero by millimolar concentrations of octanol (Fig.), and is unaffected by transjunctional and inside-outside voltages at least  $\pm$  50 mV around resting potential. Intracellular pH (pH<sub>i</sub>) is being measured using 6-carboxyfluorescein (ratio of emission at 530 nm at excitation wavelengths 490 and 460 nm; the diacetate derivative used for membrane permeation) and liquid ion exchange microelectrodes (WPI ligand) Normal pH<sub>i</sub> is 7.1-7.3. We conclude that physiological and pharmacological properties of cardiac gap junctions are similar but not identical to those of other well studied systems. Supported by a Grant-in-Aid from the American Heart Association (to DCS).



**W-PM-A10 COMPUTER MODELING OF DIASTOLIC POTENTIAL AND ELECTROGENIC PUMPING IN DISEASED HUMAN HEART**

D. Mogul, N. Thakor, J. McCullough, D. Singer, H. Rasmussen and R. TenEick (Intr. by A. Veis).  
Depts. of EECS, Med. (Reingold ECG Ctr.) and Pharmacology, Northwestern U., Evanston/Chicago, IL

Mathematical models exist to describe ionic conductances and currents underlying normal nerve and cardiac action potentials in a number of animal species. We developed detailed algorithms which model possible changes in membrane ionic conductances and electrogenic  $\text{Na}^+ - \text{K}^+$  pump flux ( $J_{ep}$ ) in these tissues and which permit reconstruction of the response of the diastolic potential ( $E_m^D$ ) to changes in  $[\text{K}^+]_o$  in diseased human atrial and ventricular myocardium (DHA+VM).

A common finding in diseased myocardium is cells with low  $E_m$ , some of which exhibit a 25-35 mV hyperpolarization of  $E_m$  in response to an increase in  $[\text{K}^+]_o$  from 4 to 7 mM.  $E_m$  depends upon membrane permeability to potassium ( $P_K$ ) and sodium ( $P_{Na}$ ); contributions by a  $J_{ep}$  have also been postulated. Computer simulations determined the contribution of  $J_{ep}$  to  $E_m$ , the effects of  $[\text{K}^+]_o$  on  $P_K$  and thus  $E_m$ . Moreton's equation was used to model the dependence of  $E_m$  on these factors. Newton's method provided solutions to Moreton's equation.  $P_K$  and  $J_{ep}$  were made dependent upon  $[\text{K}^+]_o$  in separate relationships according to:

$$P_K = 4 \times 10^{-8} [\text{K}^+]_o^{0.5} \quad \text{and} \quad J_{ep} = 4 \times 10^{-7} [\text{K}^+]_o.$$

Temperature effects on these relationships were also modeled. These solutions satisfactorily modeled changes in  $E_m$  in DHA+VM. We conclude that an increase in  $P_{Na}/P_K$  ratios may underlie the reduced level in diastolic potentials. Further, the model predicts that the hyperpolarization upon increasing  $[\text{K}^+]_o$  from 4 to 7 mM can result from the  $P_K$  dependency on  $[\text{K}^+]_o$ ; a pump contribution also may influence the relationship between  $E_m$  and  $[\text{K}^+]_o$ .

**W-PM-B1** COMPARISON OF THE EFFECTS OF GIZZARD AND SKELETAL MUSCLE TROPOMYOSINS ON ACTO-S-1 ATPase AND BINDING. D.L. Williams, Jr., L.E. Greene, and Evan Eisenberg, NHLBI, NIH, Bethesda, MD.

Gizzard tropomyosin (GZTM) has been reported to increase the skeletal muscle acto-S-1 ATPase activity under conditions where skeletal muscle tropomyosin (SKTM) inhibits this activity (Sobieszek (1982), *JMB* 157, 275). We now find that, while SKTM inhibits the ATPase activity by 60-70% at all ionic strengths tested, the effect of GZTM is dependent on ionic strength. At low ionic strength (20 mM) GZTM inhibits the ATPase activity by 60%, while at high ionic strength (120 mM) GZTM increases the ATPase activity 2.5-fold. It is known that increasing the S-1 to actin ratio cooperatively increases the tropomyosin-inhibited ATPase rate. However, this cannot be why the GZTM increases the ATPase activity since our studies were performed at very low S-1 to actin ratios, and over a 4-fold range of [S-1] there was no change in the ATPase rate. Thus under our conditions even the GZTM-actin complex is as "turned off" as it can be. To determine if the "turned on" rates were different for GZTM and SKTM, we used S-1 extensively modified by NEM to attain high S-1 to actin ratios. At both low and high ionic strength, the fully "turned on" rates were the same for both tropomyosins. Therefore, the difference in the effect of GZTM and SKTM seems to arise from a greater fraction of the GZTM-actin system being "turned on" at high ionic strength in the absence of S-1 than is the case with SKTM-actin. This interpretation was confirmed by equilibrium binding studies of S-1 to actin in the absence of ATP at I=120 mM. These studies suggested that even in the absence of S-1, more actin is in the strong binding form with GZTM than with SKTM. Hence our data provide evidence that the fraction of tropomyosin-actin in the strong binding form correlates with the effect of tropomyosin on the actin-activated ATPase rate.

**W-PM-B2** LIGAND EFFECTS ON ACTO-S1 ATPASE OF FAST MUSCLE MYOSIN ISOZYMES. I. PREFERENTIAL ANION EFFECTS AND DIFFERENCES IN LIGHT CHAIN ISOZYMES. M. Balish and P. Dreizen, Biophysics Graduate Program and Department of Medicine, SUNY Downstate Medical Center, Brooklyn, N.Y.

In studies on steady-state actin activated ATPase of rabbit fast muscle myosin S1 we reported that ATP is a competitive inhibitor with respect to actin activation, acting at 2 independent allosteric sites linked to the acto-S1 interaction zone and away from the hydrolytic site. We have further explored effects of anionic ligands on acto-S1 ATPase at 25° C, pH 8. There are striking differences in the extent of inhibition of acto-S1 ATPase by different salts. The extent of inhibition is very much anion dependent ( $\text{SCN}^-$ ,  $\text{I}^- > \text{Cl}^- > \text{CH}_3\text{COO}^-$ ), but essentially independent of cation ( $\text{Na}^+$ ,  $\text{K}^+$  or  $\text{Tris}^+$ ) over the range 0-50 mM. In the absence of actin there are no appreciable effects on S1 MgATPase over the same range of salt concentration. The selective anion effects are inconsistent with a simple Debye-Hückel ionic-strength effect on the acto-S1 interaction. Kinetic analysis shows that the salt effects involve apparent  $K_m$  and not  $V_m$  for actin activation. Dixon plots are non-linear, indicating multiple inhibition sites. A model of four identical, independent anion inhibitory sites gives excellent fit to the data, with  $K_i$  70mM for  $\text{CH}_3\text{COO}^-$ , 40mM for  $\text{Cl}^-$ , and 30mM for  $\text{SCN}^-$ , in the case of acto S1-L1. In order to determine whether the ATP inhibitory sites are identical with the monovalent anion sites, or instead are independent sites, we conducted kinetic studies at fixed actin and varying ATP/ $\text{Cl}^-$  ratios. The results are consistent with a model in which ATP and monovalent anions occupy the same inhibitory sites. Studies of actin activation of S1-L1 and S1-L3 indicate similar kinetic behavior for both; however, in all cases, the inhibition constants for ATP and monovalent anions are significantly stronger for S1-L1 than for S1-L3.

**W-PM-B3** LIGAND EFFECTS ON ACTO-S1 ATPASE OF FAST MUSCLE MYOSIN ISOZYMES. II. CATIONIC EFFECTS AND THE FUNCTIONAL ROLE OF LIGHT CHAIN ISOZYMES. M. Balish and P. Dreizen, Biophysics Graduate Program and Department of Medicine, SUNY Downstate Medical Center, Brooklyn, N.Y.

We have reported that  $\text{MgCl}_2$  is a multisite competitive inhibitor with respect to actin activation of S1 ATPase of rabbit fast muscle, and that the isozymes, S1-L1 and S1-L3, differ as to the extent of inhibition.  $\text{MgCl}_2$  inhibition is considerably greater than inhibition by  $\text{NaCl}$ ,  $\text{KCl}$  or  $\text{TrisCl}$ , even when normalized to the same ionic strength. However, the question arises whether  $\text{MgCl}_2$  inhibition includes some contribution from  $\text{Cl}^-$ , in view of the observed preferential anion effects (paper I). Anion effects must be considered since the extent of inhibition varies for  $\text{MgCl}_2$ ,  $\text{Mg}(\text{SCN})_2$ , and  $\text{Mg}(\text{CH}_3\text{COO})_2$ . In order to distinguish  $\text{Mg}^{2+}$  and anion effects, kinetic studies were done in which  $\text{Mg}^{2+}$  and  $\text{K}^+$  concentrations were varied, with  $\text{Cl}^-$  concentration fixed. The kinetic data can be analyzed in terms of competitive inhibition by free  $\text{Mg}^{2+}$  with a single inhibition site;  $K_{mg}$  is stronger for acto S1-L1 (1mM) than acto S1-L3 (2mM). The ligand effect on apparent  $K_m$  can be described as a product of terms relating to  $\text{Mg}^{2+}$  inhibition and anion inhibition. Significantly, when anion effects are taken into account, we find that  $K_{mg}$  is approximately the same at 0-30mM  $\text{KCl}$ , differing between acto S1-L1 and acto S1-L3 throughout. These kinetic data provide a plausible explanation for the functional role of the 2 light chain isozymes in muscle in vivo. In the resting state the apparent  $K_m$  is similar for the two isozymes; however, during marked glycolysis there is considerable increase of anion concentration that could result in diminished ATPase for S1-L1 but much less change for S1-L3. Thus the L3 isozyme may serve as back-up during anaerobic glycolysis, a condition characteristic of fast muscle under sudden, severe exertion.

**W-PM-B4** DEPOLYMERIZATION AND REPOLYMERIZATION OF ACTO-S1 CROSS-LINKED COMPLEX. Takamitsu Ikkai and Paul Dreizen. (Intr. by Manfred Brust). Biophysics Graduate Program, State University of New York Downstate Medical Center, Brooklyn, New York.

Cross-linking of actin and myosin subfragment-1 (S1) by 1-ethyl-3-(3-dimethylaminopropyl) carbodiimide (EDC) has been utilized by Mornet and associates and Sutoh to investigate the binding sites of actin and S1. We here report studies of depolymerization and repolymerization of the acto-S1 cross-linked complex. S1 was obtained by chymotryptic digestion of rabbit fast-muscle myosin and used as the light chain isoforms before and after chromatographic separation. EDC-activated actin was reacted with S1 for 10 min at 25°C, and the reaction mixture was precipitated in 0.1M KCl, 5mM MgCl<sub>2</sub>, 10mM pyrophosphate, 50mM HEPES, pH 7.5, at 4°C. In all cases, SDS-gel electrophoresis shows the presence of acto-95K complex as a doublet at 170-180K, actin, light chain(s), and 95K heavy-chain fragment. Stored samples of unfractionated S1 may also contain a band at 70K, presumably degraded 95K fragment, and generate 155K band after EDC reaction. Actin was depolymerized by dissolving and dialyzing the pellet in 0.2mM ATP, 0.2mM CaCl<sub>2</sub>, 0.5mM β-mercaptoethanol, 2mM Tris, pH 8.0. After centrifugation at 140,000 g for 45 min at 4°C, the supernatant contained actin-95K complex and free actin, whereas the pellet also contained a doublet band at ca. 265K and the 155K band, for stored S1. The supernatant fraction (G-actin and acto-S1 complex) was repolymerized in 0.1M KCl, 1 mM MgCl<sub>2</sub>, and the actin polymer, as recovered on centrifugation at 140,000 g at 23°C, was found to contain both actin-95K complex and free actin on SDS-gel electrophoresis. These results indicate that acto-S1 complex can undergo depolymerization and repolymerization, as does actin alone. However, the 155K and 265K cross-linked products do not undergo comparable polymerization cycles.

**W-PM-B5** EVIDENCE FOR TETHERED ACTO-HEAVYMEROMYOSIN (HMM) AT LOW ATP LEVEL. David D. Hackney and Patrick K. Clark. Department Biological Sciences, Carnegie-Mellon Univ., Pittsburgh, PA 15213.

Subfragment-1 (S1) or HMM alone, when assayed with pyruvate kinase and phosphoenolpyruvate (PEP) to regenerate ATP, exhibits a linear increase in ATPase rate on addition of ATP until a sharp break occurs at the equivalence point of 1 ATP/active site above which no further increase in ATPase rate occurs. (Hackney and Clark, *Biophys. J.* 41, 92a (1983)). When a similar titration is performed with 1.7μM S1 in the presence of 4μM actin, the ATPase rate again exhibits a sharp break at the equivalence point with a higher plateau rate. With acto-HMM, however, the turnover rate per site at low ATP is increased over acto-S1, but then decreases at higher ATP levels to the acto-S1 rate. This increased ATPase rate with acto-HMM at approximately stoichiometric levels of ATP can be accounted for by "tethered" HMM molecules which remain bound to actin by a rigor bond with one head even though the other head contains bound ATP or ADP, Pi. This tethered head will observe a high local actin concentration and will release products at close to the V<sub>max</sub> rate. Binding of ATP to both heads will cause net release of the HMM and conversion to the slower pattern observed with S1. Analysis of the P<sub>i</sub>→HOH oxygen exchange reaction using (<sup>18</sup>O)PEP supports this interpretation. Acto-HMM hydrolyzes ATP with a low extent of exchange at low ATP levels and reverts at high ATP to the extensive exchange observed with acto-S1 at these low actin concentrations.

These results, obtained with purified actin, represent a distinct phenomenon from the well known activation of the ATPase at low ATP with regulated actin in the absence of Ca<sup>2+</sup>.

Supported by grant AM 25980 from the USPHS and by an Established Investigatorship from the American Heart Association to DDH.

**W-PM-B6** A LATTICE OF CHEMICAL POINTS IN MYOSIN S-1. By Jean Botts, Reiji Takashi, and Peter M. Torgerson. CVRI, UCSF, San Francisco.

In several instances it is possible to attach a donor fluorophore to a specific residue in S-1 (or actin or acto-S-1) and an acceptor fluorophore or quencher to another residue and then measure *E*, the fraction of energy transferred from donor to acceptor. From *E* it is possible to calculate (with Förster's equation) the scalar distance from attached donor to attached acceptor. In some cases the Dale/Eisinger analysis has also been applied, giving limits on distance estimates. In our and other laboratories a number of distances have been measured between chemically defined points on S-1, actin, and acto-S-1. S-1 labelling sites include: thiols "SH<sub>1</sub>" and "SH<sub>2</sub>", thiol of LC<sub>1</sub> or LC<sub>3</sub>, reactive lysine residue "RLR", nucleotide binding site (ε-ATP or TNP-ATP), & "trapped" ε-ADP; actin has been labelled at thiol 374 and the nucleotide binding site (ε-ADP). Enough distances are now known to begin constructing a 3-D lattice of points. At present, ambiguities remain in the relative positioning of points either because needed measurements have not yet been attempted or because the distances proved too great for the choice of donor-acceptor pair used. But already the model is useful in trying to visualize a path of communication between S-1 nucleotide- and actin-binding sites, a communication probably crucial for energy transduction in muscle. (Research supported by USPHS HL-16683; P.M.T. is MDA Fellow.)



**W-PM-B7** INTERACTION OF FLUORESCENT NUCLEOTIDE WITH MYOSIN AND REGULATED ACTOMYOSIN.

S.S. Rosenfeld and E.W. Taylor, Dept. Biophysics and Theor. Biol., Univ. Chicago, Chicago, IL 60637.

The binding of  $\epsilon$ ATP or  $\epsilon$ ADP in 200 mM acrylamide to skeletal muscle myosin subfragment 1 (SF-1) yields a large increase in fluorescence (Biophys. J., 41, 301a (1983)). The effect of acrylamide on the fluorescent properties of a SF-1:nucleotide complex has been measured by using Stern Volmer plots. These plots show that SF-1: $\epsilon$ ADP exists in equilibrium in two states, that in one of these states the  $\epsilon$ ADP is considerably more accessible to solvent than in the other, and that addition of sodium vanadate ( $V_i$ ) reduces the accessibility of both states but does not change their equilibrium distribution. These conclusions have been confirmed by measuring the effect of acrylamide on the fluorescence decay properties of SF-1: $\epsilon$ ADP and SF-1: $\epsilon$ ADP: $V_i$ .

Actin accelerates the maximum rate of  $\epsilon$ nucleotide release from skeletal muscle SF-1. For SF-1: $\epsilon$ ADP, the maximum accelerated rate is  $550 \text{ sec}^{-1}$ , while for SF-1: $\epsilon$ ATP, it is  $10\text{--}15 \text{ sec}^{-1}$ . The latter results have been confirmed by measuring the release of [ $\gamma$ - $^{32}\text{P}$ ]- $\epsilon$ ATP from acto-SF-1 by using a quench technique. When SF-1+ $\epsilon$ ATP is mixed with a large excess of actin+ATP, a rapid decrease in fluorescence occurs ( $100\text{--}150 \text{ sec}^{-1}$ ), followed by a slower decrease ( $5\text{--}10 \text{ sec}^{-1}$ ). The first phase of the transient is due to the release of products from acto-SF-1, while the second is due to release of unhydrolyzed  $\epsilon$ ATP. The regulatory proteins troponin:tropomyosin (TN:TM) in the absence of calcium reduce the rate constants for both phases of this transient by > ten fold, while they have little effect on the rates of this fluorescence transient in the presence of calcium. These results show that actin accelerates SF-1:nucleotide exchange in a symmetric manner, and that calcium-free TN:TM inhibits this process in a symmetric manner.

**W-PM-B8** PHOTOLABELING OF MYOSIN BY 3'-p-BENZOYL-BENZOYL-ATP TRAPPED AT THE ACTIVE SITE BY BIFUNCTIONAL THIOL REAGENTS. Riaz Mahmood, Kay Nakemaye and Ralph G. Yount, Biochemistry/Biophysics Program, Washington State University, Pullman, WA 99164-4660

As part of a program to characterize the active site of myosin, we have used the title compound, Bz<sub>2</sub>ATP [Williams and Coleman, JBC 257, 2834 (1982)] to photolabel residues at or near the active site of subfragment-one (SF<sub>1</sub>) from skeletal myosin. Bz<sub>2</sub>ATP is trapped stoichiometrically at the active site by the bifunctional thiol cross-linking agent, p-phenylene dimaleimide, or by chelation of two SF<sub>1</sub> cysteines by Co(III)phenanthroline [Wells and Yount, PNAS 76, 4966 (1979)]. Under such conditions, Bz<sub>2</sub>ATP has a half-life on SF<sub>1</sub> of > 7 days at 0°C and the [ $^3\text{H}$ ]Bz<sub>2</sub>ATP-SF<sub>1</sub> complex can be readily purified free of all non-trapped analog. Irradiation of this complex with a 450 W Hg lamp at > 300 nm for 30 min gives ~ 50% covalent incorporation of trapped [ $^3\text{H}$ ]Bz<sub>2</sub>ATP into SF<sub>1</sub>. Analysis by SDS-PAGE showed > 99% of the [ $^3\text{H}$ ]Bz<sub>2</sub>ATP was located in the 95 Kd heavy chain fragment. Similar analyses after limited trypsin treatment showed ~ 75% of the label was in the 50 Kd peptide or its 75 Kd precursor. No label (< 1%) was detected in the 25 Kd N-terminal tryptic peptide previously labeled by two other ATP photoaffinity analogs [Szilagyi et al., BBRC 87, 936 (1979); Okamoto and Yount, Biophys. J. 41, 298a (1983)]. These results indicate that portions of the 50 Kd tryptic peptide previously associated only with an actin binding site are within 6-7 Å of the ATP binding site. Supported by NIH grant AM-05195.

**W-PM-B9** THE KINETICS OF SKELETAL MUSCLE MYOSIN PHOSPHORYLATION AND ITS EFFECT ON ACTIN-ACTIVATED ATPase. A. Persechini and J.T. Stull, Department of Pharmacology, University of Texas Health Science Center at Dallas, Dallas, TX 75235

Time courses of phosphorylation and dephosphorylation were determined using purified myosin light chain kinase, cardiac phosphoprotein phosphatase catalytic subunit, and rabbit skeletal muscle myosin. In contrast with studies of vertebrate smooth muscle myosin (Persechini, A. and Hartshorne, D.J., Biochemistry 22, 470, 1983), we find no evidence of a sequential phosphorylation mechanism. Both phosphorylation and dephosphorylation of at least 90% of the P-LC substrate can be described by a single exponential. It would, therefore, appear that sequential P-LC phosphorylation is not a general property of myosin. We have also studied the effect of P-LC phosphorylation on the actin-activated  $\text{Mg}^{2+}$ -ATPase of myosin purified from Triton-washed myofibrils. Full phosphorylation causes a two-fold decrease in  $K_m$  (from 6  $\mu\text{M}$  to 2.5  $\mu\text{M}$  actin) with no significant effect on  $V_{max}$  ( $1.8 \text{ sec}^{-1}$ ). The relationship between P-LC phosphorylation and activation was found to be linear suggesting that the response of the heads to phosphorylation is independent rather than cooperative as was found with vertebrate smooth and scallop muscle myosins (Persechini, A. and Hartshorne, D.J., Science 213, 1383, 1981; Chantler, P.D. et al., Biochemistry 20, 210, 1981). The magnitude of the phosphorylation effect was found to be dependent upon the age of the myosin preparation used; in preparations stored (at 0°C) for longer than 5 days it was greatly reduced or absent. The effect of aging appeared to be an elevation of activity in the absence of phosphorylation. (Supported by HL23990 and HL06296)

**W-PM-B10** A REGULATED TRYPTIC FRAGMENT OF SCALLOP MYOSIN: H. Shpetner, Graduate Program in Biophysics, Brandeis University, Waltham, Massachusetts 02254.

Brief (90 sec.) digestion of scallop myosin, at 0.6M NaCl and high myosin:trypsin ratio (800:1, w/w) yields a heavy meromyosin (HMM) of mass 420kd. It has high actin-activated ATPase activity ( $V_{max} > 2.5 \mu\text{moles/min.-mg}$ ), and, in 8mM NaCl, is 90% calcium sensitive. The HMM runs homogeneously on non-denaturing gels; its principal component is a heavy chain of 174kd. Its regulatory light chains may be removed by gel-permeation chromatography, at 0°, in 10mM EDTA; concomitantly, its ATPase is rendered calcium insensitive. Desensitized HMM, incubated with excess scallop R-LC, in 2mM DTT and 1mM  $\text{MgCl}_2$ , rebinds R-LC stoichiometrically (2 moles R-LC/mole HMM), with full restoration of calcium sensitivity. Desensitized preparations also rebind foreign R-LCs; the hybrids thus formed exhibit calcium sensitivity, dependent on the source of the R-LCs (Sellers et al., *J. Mol. Biol.* 144: 223, 1980). When scallop (Ca,Mg) S-1 is chromatographed under conditions that fully denude HMM, over 75% of the R-LCs remain bound to S1. Thus, in 10mM EDTA, R-LC binds S-1 considerably more tightly than HMM, suggesting head-head interactions in the binding of HMM to R-LC.

The 174kd. heavy chain is subsequently cleaved to 98kd. and 78kd. peptides; the actin-activated ATPase is substantially diminished, though the  $\text{Ca}^{++}$ -ATPase is unchanged. The 78kd. peptide contains the N-terminus of the heavy chain. Nicked and intact HMMs comigrate on native gels. Prolonged digestion causes marked degradation of scallop HMM, as evidenced on native gels; in contrast, rabbit HMM, that has been extensively nicked, appears homogenous on native gels. (Supported by NIH Am-15963 and MDA grants.)

**W-PM-B11** EFFECT OF THE LC2 LIGHT CHAIN ON THE EQUILIBRIUM BETWEEN TWO S-1 STATES IN THE ABSENCE OF NUCLEOTIDE. Ulf Tollemar and John W. Shriver, Department of Medical Biochemistry and Dept. of Chemistry and Biochemistry, Southern Illinois University, Carbondale, IL 62901.

A new fluorine containing sulfhydryl labelling probe has been synthesized, N-[3,5-di(trifluoromethyl)phenyl]iodoacetamide, to allow  $^{19}\text{F}$  NMR studies of the myosin ATPase. This new probe contains six equivalent fluorine NMR probes per sulfhydryl labelled and leads to a four-fold increase in NMR signal-to-noise ratio compared to that previously obtained (Shriver and Sykes, *Biochemistry* 21, 3022 (1982)). Excellent spectra of labelled myosin subfragment-1 (100  $\mu\text{M}$ ) can now be obtained in approximately five minutes when using this new probe.

Papain S-1 was prepared in the presence of Mg and contained intact LC2 as indicated by SDS gel electrophoresis. Papain S-1 was 50% labelled with the above reagent under benign conditions (0.1 M KCl, 50 mM Tris, pH 7.9, 0.1 mM DTE, 4°C) for five minutes. The  $^{19}\text{F}$  NMR spectrum of the labelled protein showed a single major peak. The chemical shift of the NMR resonance was sensitive to temperature in a manner indistinguishable from that of chymotryptic S-1. Papain S-1 exists in two possible states with  $K=1$  near physiological temperature. The NMR data could be fit with the van't Hoff equation to give an apparent enthalpy change for the transition between the two states of 35 kcal/mol and  $\Delta S=120$  e.u. The addition of calcium had no effect on the energetics of the transition. These results indicate that the LC2 light chain does not play a role in determining the energetics of the two-state conformational change in S-1. (Supported by NIH AM 30712).

**W-PM-B12** EFFECTS OF SH MODIFICATIONS ON MYOSIN SUBFRAGMENT-2. R.C. Lu and S.S. Lehrer. Dept. of Muscle Res., Boston Biomed. Res. Inst. and Dept. of Neuro., Harvard Med. Sch., Boston, MA. 02114

Short myosin subfragment-2 (SS2, chain wt= 40 kd) has the same N-terminal sequence as the long S2 (LS2, chain wt= 60 kd) and the presumptive hinge region in the myosin rod is therefore in the C-terminal portion of LS2 (Lu, *PNAS* 77 2010, 1980). There are 3 SH/chain in LS2: two in SS2 and the third near the C-terminus of LS2. Since the reaction with  $\text{Nbs}_2$  has been used successfully to produce interchain S-S crosslinks (XL) and to explore the local conformation in tropomyosin, another coiled-coil helical molecule (Lehrer, *PNAS* 72 3327, 1975; *JMB* 118 209, 1978), we decided to examine the ability of  $\text{Nbs}_2$  to form XL in LS2 and SS2. The reaction with  $\text{Nbs}_2$  was biphasic and indicated that each chain of SS2 contains one rapidly and one slowly reacting SH and that LS2 has an additional slowly reacting SH. Since rapidly reacting SHs did not form XL, it appears that dimer chains were only formed via slowly reacting SHs. Mild tryptic digestion on native (reduced) LS2 produced SS2 whereas the XL-LS2 produced 2 protein bands having mobilities corresponding to 100 kd and 90 kd. When either of the proteins was cut out from the gel and reelectrophoresed under reducing conditions, a single band with the same mobility equivalent to 48 kd was found. Thus, the differing mobilities of the XL-products must be due to the presence of S-S bonds at different locations in the same peptide. Prolonged tryptic treatment of XL-LS2 and XL-SS2 produced the same XL-product with chain wt 25 kd whereas the native SS2 remained undegraded under these conditions. N-terminal analyses indicated that the first cleavage of XL-LS2 occurred at the C-terminal region whereas the second cleavage involved the loss of N-terminal peptides. These data show that reaction of these coiled-coil structures with  $\text{Nbs}_2$  changes the conformation resulting in a new pattern of tryptic cleavage. Supported by grants from NIH, AHA and MDA.

**W-PM-C1** THREE AGENTS THAT PROLONG Na CHANNEL OPENING INCREASE BINDING OF VERATRIDINE TO Na CHANNELS. Jeffrey Sutro (intr. by B. Hille), Physiol. & Biophys., U. of Wash., Seattle, WA 98195.

Veratridine bath-applied to frog muscle makes inactivation of  $I_{Na}$  incomplete during a depolarizing pulse. Following the pulse, a persistent "veratridine-induced tail" current continues to flow. During repetitive depolarizations the size of successive veratridine-induced tail currents grows at first, but eventually a maximum size is reached, and successive tails gradually decrease again. When pulsing is stopped, the veratridine-induced Na current returns exponentially to zero ( $\tau \approx 3$  s). Higher rates of stimulation result in a faster growth of the veratridine-induced tail current, and a larger maximum value. I suggest that veratridine binds only to open channels and, when bound, prevents normal fast inactivation and rapid shutting of the channel on return to rest. Veratridine-modified channels are also subject to a "slow" inactivation during long depolarizations or extended pulse trains. At rest veratridine unbinds with  $\tau \approx 3$  s. Two tests confirm these hypotheses: 1) The time course of the development of veratridine-induced tail currents parallels a running time integral of  $g_{Na}$  during the pulse, as expected for binding to open channels but not to resting or inactivated channels. 2) Chloramine-T, N-bromoacetamide, and scorpion toxin, agents that decrease inactivation in sodium channels, each greatly enhance the veratridine-induced tail currents. The time course of the appearance of the veratridine-induced tails now parallels the larger integral of the much prolonged  $g_{Na}$  during the pulse, as predicted by the hypothesis. As others have reported with aconitine and batrachotoxin, veratridine-modified channels shut following strong hyperpolarizations to below -120 mV, and reopen on repolarization to rest, a process resembling shifted activation gating. (Supported by USPHS grants NS-08174 and GM-07270.)

**W-PM-C2** PERMEANT ORGANIC CATIONS MODIFY SODIUM CHANNEL INACTIVATION KINETICS IN FROG NODE OF RANVIER. Sherrill Spires and Peter Shrager, Department of Physiology, University of Rochester, Rochester, NY 14642.

Inactivation kinetics of sodium channel current in frog myelinated nerve were studied using the Vaseline gap voltage clamp technique. These kinetics were examined in external solutions containing sodium or a permeant organic cation. Since the organic cations used (ammonium, guanidinium, and formamidinium) are less permeant than sodium, controls were done in a low sodium solution. When the external permeant cation is sodium, the declining phase of sodium channel current at negative potentials is well described by the sum of two exponentials. There is no change in the kinetics of inactivation when the external sodium is replaced with ammonium. When formamidinium is the external permeant cation, the declining phase of the sodium channel current at negative potentials is still fit by the sum of two exponentials but the time constant of the fast component has increased by a factor of two; the time constant of the slow phase is not significantly changed. The declining phase of the sodium channel current when guanidinium is the external permeant cation is well fit by a single exponential having a time constant similar to that of the slow component in sodium, ammonium, and formamidinium Ringer's solutions; the fast exponential is absent. These results indicate that inactivation of the sodium channel is not solely a voltage-dependent process but is dependent on the species of the external permeating cation. Supported by USPHS grant NS 17965.

**W-PM-C3** CHEMICAL CROSSLINKING OF AMINO GROUPS ALTERS SODIUM CHANNEL INACTIVATION GATING. P.A. Pappone and M.D. Cahalan, Dept. of Animal Physiology, Univ. of Calif., Davis, CA, 95616, and Dept. of Physiology and Biophysics, Univ. of Calif., Irvine, CA, 92717. We have examined the effects of 4-acetamido-4'-isothiocyano-2,2'-disulfonic acid stilbene (SITS) and 4,4'-diisothiocyano-2,2'-disulfonic acid stilbene (DIDS) on the Na currents of voltage-clamped frog myelinated nerve and skeletal muscle fibers. Both SITS and DIDS contain thiocyno moieties which react covalently with amino groups. The two reagents are almost identical chemically, except that SITS contains one reactive group, while DIDS contains two. Hence DIDS can potentially crosslink reacted groups. External exposure of nerve or muscle membranes to 10-20 mM SITS at pH 9 causes a shift in the voltage dependence of steady-state inactivation ( $h_{\infty}$ ) to more hyperpolarized potentials.  $h_{\infty}$  remains shifted by 5-10 mV following washout of the SITS. The shift in  $h_{\infty}$  is a simple translation of the relation along the voltage axis, with no change in the steepness or shape of the  $h_{\infty}$  curve. Other gating parameters of Na currents are unaffected by treatment with SITS—rates of activation, inactivation, and the voltage dependence of activation of Na currents are not altered by the reagent. Exposure of nerve and muscle fibers to DIDS causes irreversible changes in Na current inactivation which are qualitatively different than those produced by SITS. DIDS also shifts  $h_{\infty}$  to more hyperpolarized potentials, but in addition there is a dramatic decrease in the steepness of the  $h_{\infty}$  relation. The apparent voltage dependence of  $h_{\infty}$  is decreased 2-5 fold by reaction with 0.2-3 mM DIDS for 3-15 min at pH 9. In addition,  $h_{\infty}$  measured using 200 msec conditioning pulses no longer saturates at hyperpolarized potentials, even for potentials as negative as -190 mV. Like SITS, DIDS has little effect on Na current activation. Since SITS and DIDS are nearly identical chemically, it is likely that the differences in their effects on Na channels are due to crosslinking of reacted groups by DIDS. Supported by NIH Grant NS14609 and an NIH fellowship to P.A.P.

**W-PM-C4 EVIDENCE FOR COVALENT BONDING OF SAXITOXIN TO THE NEURONAL SODIUM CHANNEL.** Gary R. Strichartz, Sherwood Hall, and Yuzuru Shimizu. Anesthesia Res. Labs., Brigham and Women's Hospital, 75 Francis Street, Boston, MA 02115, Woods Hole Oceanographic Institute, Woods Hole, MA, 02543, and Dept. of Pharmacognosy, Univ. of Rhode Island, Kingston, R.I. 02881

Investigations of equilibrium association of saxitoxin (STX) and of 9 derivative toxins to neuronal Na<sup>+</sup> channels were conducted using both electrophysiological and [<sup>3</sup>H]-STX binding experiments. The order of toxin affinities (relative to that of STX) agreed well when determined by each method; neo-STX (4.4) > GTXIII (1.8) > STX ( $\approx 1.0$ ) > GTXII (0.34) > GTX VIII (0.093) > B2 (0.077) > 12 $\alpha$ OH-H<sub>2</sub>STX (0.052) > B1 (0.029) > C1 (0.003) > 12 $\beta$ OH-H<sub>2</sub>STX (0.0015). In solution neo-STX carries a much higher fraction of the unhydrated ketone at position C12 than does STX, wherein the ketone is more than 99% hydrated, but ketone dehydration is induced in STX by the binding of that toxin to anionic sites on resins and on membranes. We posit that such ionic bonding initiates the dehydration of the C12 ketone which then forms a covalent bond with the receptor. Inhibition of binding by the selective reagent trinitrobenzene sulfonic acid indicates the necessity of free amino groups on the receptor for the binding reaction and suggests that a Schiff's base may be formed. In binding experiments, elevation of [Ca<sup>2+</sup>] or [Ni<sup>2+</sup>] lowers the affinity of the divalent cationic toxin (STX) more than those of the monovalent species (GTXII, III), consistent with an involvement of surface charge in STX/TTX binding. But in the case of toxins sulfated at the nitrogen (N21) of the carbamyl "tail", raising the concentration of Ca<sup>2+</sup> actually increases the toxin affinity, implying that the metal cations may form a ternary complex with toxins and receptor sites. Supported by USPHS grants NS 18467 (to GRS) and GM-28754 (to Y.S.).

**W-PM-C5 BLOCKADE OF MUSCLE Na<sup>+</sup> CHANNELS BY GUANIDINIUM TOXINS: A VOLTAGE DEPENDENT BLOCK INDEPENDENT OF THE CHARGE ON THE TOXIN MOLECULE.** E. Moczydlowski & C. Miller (Grad. Dept. of Biochem., Brandeis Univ., Waltham, MA 02154) S. Hall (Dept. of Biology, Woods Hole Oceanographic Inst., Woods Hole, MA 02543) G. Strichartz (Dept. of Anesthesiology, Harvard Medical School, Boston, MA 02115)

Blockade of batrachotoxin-modified Na<sup>+</sup> channels from rat skeletal muscle was studied in neutral planar phospholipid (8 PE: 2 PC) bilayers cast from decane (0.2 M NaCl, pH 7.4). Binding rate constants as a function of voltage (+60 to -60 mV) for various toxins were measured by statistical analysis of discrete blocking events in bilayers containing one or two channels of known orientation. The toxins studied were: TTX (+1), STX (+2), neo-STX (+1.2) and four other STX derivatives isolated from *Protogonyaulax* that contain one or two -OSO<sub>3</sub>(-1) groups. All of these toxins exhibited a voltage dependent block with k<sub>off</sub> increasing (e-fold per 79 mV) and k<sub>on</sub> decreasing (e-fold per 81 mV) with depolarizing applied voltages. The actual magnitude of the rate constants was dependent on toxin structure with k<sub>off</sub> ranging from 0.011-0.76 s<sup>-1</sup> and k<sub>on</sub> ranging from 0.61-14x10<sup>6</sup> M<sup>-1</sup>s<sup>-1</sup> at 0 mV and 0.2 M NaCl. Varying [NaCl] symmetrically from 40-600 mM had no effect on k<sub>off</sub> for TTX but affected k<sub>on</sub> competitively according to (1+[Na]/K<sub>Na</sub>)<sup>-1</sup>, where K<sub>Na</sub> = 30mM. K<sub>Na</sub>, itself, appears to be voltage independent. Increasing Na only on the side of the bilayer opposite from the TTX site appears to have no effect on TTX binding rate constants. These results tend to eliminate models in which the toxin plugs a pore in the transmembrane electric field, but raise questions concerning the mechanism of the voltage dependent toxin binding. (Supported in part by NIH 6N31768)

**W-PM-C6 LOCAL ANESTHETICS PRODUCE PHASIC BLOCK OF SODIUM CHANNELS DURING ACTIVATION.**

G.K. Wang and G.R. Strichartz. Anesthesia Res. Labs., Harvard Medical School, Brigham and Women's Hospital, 75 Francis St., Boston, MA 02115

Local anesthetics produce cumulative block of Na currents when depolarizing pulses are applied repetitively under voltage-clamp. One hypothesis to explain this phasic block, first proposed by Courtney (1975) and elaborated by Hille (1977), states that local anesthetics bind to the inactivated form of the Na channel more tightly than to the closed or open forms. We have investigated this proposal by applying test pulses of varying duration repetitively to single myelinated fibers of toad exposed to different lidocaine derivatives. Compound GEA-968 produced phasic block of Na currents at 2 Hz which increased as the pulse duration increased, up to 1-2 ms, but then remained the same or slightly decreased with longer pulses, up to 50 ms. Another local anesthetic, QX-572, having a quaternary (4<sup>+</sup>) amine, gave comparable results. Since little channel inactivation occurs during very short pulses, phasic block cannot result from these local anesthetics binding more tightly to the inactivated channels. We also found that the removal of Na inactivation by externally applied N-bromoacetamide (NBA) did not change the phasic block by GEA-968 from pulses with a duration of 1-2 ms, contrary to previous reports using 4<sup>+</sup> QX-314 in squid axons perfused with pronase or NBA. However, when a test pulse longer than 2 ms was applied a significantly smaller phasic block developed. We conclude that the rapidly inactivated conformation of Na channels contributes little to the phasic block by GEA-968 or QX-572. Rather, our results suggest that this phasic block occurs during channel activation.

**W-PM-C7 MECHANISMS OF APPARENT VARIATION OF LOCAL ANESTHETIC AFFINITY FOR IONIC CHANNEL BINDING SITES.** CF Starmer, AO Grant, and HC Strauss (Intr. by E. A. Johnson). Duke University Medical Center. Durham, North Carolina.

In studies of local anesthetic interaction with Na channels in cardiac tissue, dose-response curves have shown voltage dependence with apparent  $K_d$ 's varying more than 40-fold for a 60 mV shift in holding potential. This variation has been interpreted as support for the modulated receptor hypothesis. Apparent affinity variation can result when ligand access to the channel binding site is restricted by the channel gating particles. Assuming that binding takes place in open conducting sodium channels, and that m gates are immobilized in drug complexed channels, one can describe the equilibrium fraction of blocked channels as

$$b = (1 + (r e^{-zVF/RT}) / (k m^3 D))^{-1}$$

where k and r are the forward and reverse rate constants for drug binding, z is the drug charge, V is the potential difference between the cell interior and the receptor site,  $m^3$  is the fraction of channels with 3 open conformation m particles, and D is drug dose. Peak sodium current reflects both the fraction of blocked channels prior to stimulation as well as the fraction of channels blocked during early test pulse depolarization, thus providing a biased estimate of equilibrium channel block. Using the Ebihara-Johnson sodium model, simulated dose-response curves based on a true  $K_d$  of 10 nM for lidocaine demonstrated apparent  $K_d$ 's of 350  $\mu$ M at  $V_{mem} = -125$  mV and 10  $\mu$ M at  $V_{mem} = -44$  mV, which are in quantitative agreement with published data. We conclude that use- and voltage-dependent channel blocking can be adequately characterized by a first order model of drug binding to open channels where m gates in drug complexed channels are immobilized.

**W-PM-C8 FUNCTIONAL RECONSTITUTION OF THE VOLTAGE-REGULATED SODIUM CHANNEL PURIFIED FROM ELECTROPHORUS ELECTRICUS.** R.L. Rosenberg, S.A. Tomiko and W.S. Agnew. Dept. of Physiology, Yale University School of Medicine, New Haven, CT. 06510.

The voltage-regulated Na channel was solubilized from electroplax membranes and purified as described by Agnew, et. al. (PNAS 75:2606, 1978). Reconstitution of the channel into egg phosphatidylcholine (PC) vesicles was achieved by detergent adsorption to BioBeads SM-2 followed by freeze-thaw-sonication with additional PC liposomes. Whereas solubilized [<sup>3</sup>H]-TTX binding sites were completely inactivated after 5 minutes at 37°C, after reconstitution >75% of the sites survived for >30 minutes at this temperature. Veratridine stimulated the <sup>22</sup>Na<sup>+</sup> flux into the vesicles 3-fold with a  $K_{1/2}$  of 18  $\mu$ M. Influx was blocked by TTX in parallel with specific [<sup>3</sup>H]-TTX binding ( $K_d=33$  nM). Batrachotoxin (BTX) was more effective than veratridine; 5  $\mu$ M BTX caused a 5-fold stimulation of influx which was complete in 10 seconds. Of the [<sup>3</sup>H]-TTX binding sites, 60-70% face the exterior of the reconstituted vesicles; thus external TTX caused partial inhibition of flux whereas blockade was complete when TTX was also present in the vesicle interior. Lipid-soluble local anesthetics caused complete blockade of the stimulated influx; the charged lidocaine derivative QX-222 blocked only inside-out channels. Peptide toxin ATXII had no effect on influx. The principal glycopeptide of  $M_r > 270,000$ , which accounts for >80% of the protein, appears responsible for the functional activity. This preparation is suitable for analysis of voltage-dependence and single channel properties with the patch-clamp technique. Supported by grants from the NIH (NS 17928) and the National Multiple Sclerosis Society to WSA.

**W-PM-C9 FURTHER CHARACTERIZATION AND RECONSTITUTION OF THE TETRODOTOXIN-BINDING POLYPEPTIDE FROM EEL ELECTROPLAX.** S. Rock Levinson, Daniel S. Duch, Kirsten A. McKennett, & Emilia A. Ripoll, Dept. of Physiology, U. Colorado Medical School, Denver CO 80262.

We report here further evidence that the tetrodotoxin-binding protein (TTXR) of eel electroplax sodium channels consists only of a single, compositionally complex, large polypeptide species, and that it probably contains anomalous regions of hydrophobicity. Using rabbit antisera and monoclonal antibodies raised to purified TTXR, we have shown that only this large polypeptide is specifically co-immunoprecipitated with TTX binding activity. In addition, other detergents have been used in the purification of TTXR from crude electroplax membranes; in each case high specific activity fractions of TTX binding protein were obtained which demonstrated only the large polypeptide on SDS-PAGE. We have also shown that the anomalous electrophoretic mobility of this molecule on SDS-PAGE is not due to the comparatively large amount of negatively charged sialic acid residues associated with the protein. Rather, we have determined that the polypeptide binds at least 4 times as much SDS as "well-behaved" soluble proteins. It seems likely that this unusually high binding of the detergent is due to specialized regions of the molecule which can order SDS into extended micellar structures. We have also developed highly efficient techniques to reconstitute purified TTXR in high yield and specific activity into lipid vesicles. While the reconstituted TTXR regains the heat and freeze-thaw stability seen in the original membrane, the slow TTX binding kinetics of detergent extracts remain after insertion into liposomes. The TTXRs reconstituted by these methods appear to be nearly all "right side out" in the vesicles. Finally, as a prelude to functional studies, the TTXR has been incorporated into large liposomes of defined lipid composition. Supported by NIH (NS-15879, NS-00529) and the Muscular Dystrophy Association.

**W-PM-C10 SOLUBILIZATION WITH CHOLATE AND RECONSTITUTION OF THE Na<sup>+</sup> CHANNEL FROM RAT BRAIN.**

J. S. Weiner and B. Rudy. Dept. Physiol. &amp; Biophys., N.Y.U. Med. Ctr., N.Y., N.Y.

Brain Na<sup>+</sup> channels purified in neutral detergents such as Triton X-100 are unsuitable for electrical studies in lipid bilayers because of artifacts introduced by residual detergent (Fig. A). Unlike these detergents, cholate does not introduce electrical artifacts and the bilayers are more stable. Vesicles reconstituted with channels partially purified by WGA agarose chromatography in cholate were fused with lipid bilayers. We observed batrachotoxin-activated 20 pS channels (Fig. B) which were voltage dependent and blocked by TTX. In addition, a second Na-selective channel, with twice the conductance was occasionally observed. Further purification of the channel has been hampered by the instability of the cholate-solubilized channel. Although the channel is stable upon reconstitution into vesicles, several factors, which improve the stability of channels in neutral detergents, are insufficient (such as lecithin) or without effect on the cholate preparation (such as STX) or deleterious (such as Ca<sup>++</sup>). However, we have found that the stability can be dramatically improved if the suspension is supplemented with phosphatidylserine or asolectin. In the presence of asolectin the cholate solubilized channel is as stable as the one in Triton with lecithin. This will finally allow further fractionation of the cholate-solubilized protein. Supported by grant GM 26976. We thank Drs. J. Daly for BTX and R. Barchi for <sup>3</sup>H-STX.



**W-PM-D1** THE RESOLUTION OF NUCLEIC ACID-LIGAND BINDING SITES BY CD FIRST-NEIGHBOR ANALYSIS.

Fritz S. Allen  
Department of Chemistry  
University of New Mexico

Donald M. Gray  
The Molecular Biology Program  
The University of Texas at Dallas

We present a technique which can determine which first-neighbor units in a double stranded polynucleotide are favorable binding sites for a ligand in the event that the binding is non-specific. The binding at the first-neighbor units ApA:TpT and CpC:GpG may be unequivocally resolved. The first-neighbor method provides six different measures of the CD contribution of the eight remaining first-neighbor units. If four or in some cases five of these measures are altered, the pattern of which first-neighbor unit are bound can be resolved. If all six of these measures change, then no further progress can be made in the resolution of the binding; this case may be characterized as nonspecific. We present the techniques which allow the analysis.

**W-PM-D2** LOCATIONS OF HIGH AFFINITY BINDING SITES OF CARCINOGENS ON  $\phi$ X174RF DNA AND ON THE PLASMID PBR322. Stephen A. Winkle, Nicholas Combates, Megerditch Kiledjian, Gary Langieri and Michael Mallamaci, Department of Chemistry, Rutgers, The State University of New Jersey, New Brunswick, New Jersey 08903.

Previous work (Winkle, Mallamaci and Reed [1983] *Biophysical J.* 41, 287 a) using  $^3\text{H}$ -labeled carcinogen and restriction enzymes indicates that the carcinogen N-acetoxy-N-acetyl-2-aminofluorene (AAAF) binds preferentially to small numbers of "high affinity" sites on  $\phi$ X174RF DNA and on the plasmid pBR 322. We have isolated restriction fragments from these DNAs to more exactly localize the AAAF binding sites. One method used was digestion of  $^3\text{H}$ -AAAF - bound fragments ( $^3\text{H}$ -AAAF,  $\sim 1$  Ci/mmol) with second restriction enzymes (e.g. digestion of the Alu I 100 bp fragment of  $\phi$ X174RF with Hha I yielding subfragments of 34 and 66 base pairs) followed by isolation of the subfragments on electrophoresis gels for liquid scintillation counting of the  $^3\text{H}$  in each subfragment. Secondly, fragments containing the bound carcinogen were digested with exonuclease III or DNase I in "foot-print" experiments to localize the carcinogen binding sites. We have used restriction enzyme digests to locate the binding sites of the photochemically induced DNA adducts of the carcinogen 4-nitroquinoline-1-oxide (NQO,  $^3\text{H}$ -labeled,  $\sim 1$  Ci/mmol). The  $^3\text{H}$ -NQO-DNA adducts were produced by broad band irradiation at 340-420 nm and both experimental sequences were employed: 1) restriction enzyme digestion (with Alu I, Hae III, Hha I, Hinf I or Hpa II) followed by 2) NQO reaction and the reverse. As was the case with AAAF, NQO has small numbers of high affinity sites on  $\phi$ X174RF and pBR 322 and the site specificity is similar to that for AAAF. This work supported by NCI Grant CA 34762-01 and Research Corporation Grant 9723.

**W-PM-D3** BINDING OF ETHIDIUM AND BIS(METHIDIUM)SPERMINE TO Z DNA, Richard H. Shafer, Stephen C. Brown, Donald Wade, and Alain Delbarre, Department of Pharmaceutical Chemistry, University of California, San Francisco, CA 94143.

The interaction of ethidium bromide, a DNA intercalating drug, and bis(methidium)spermine (BMSp), a DNA bis-intercalating compound, with the left-handed, Z form of poly(dG-dC) has been examined in 4.4 M NaCl. Spectrophotometric analysis of the visible absorption and fluorescence properties of both ethidium and BMSp in the presence of excess concentrations of the high salt form of poly(dG-dC) show changes similar to those observed with calf thymus DNA under similar conditions. Circular dichroism spectra of these complexes in the UV region are the same as those seen for the left-handed polynucleotide form in the absence of any ligand. Quantitative treatment of the binding data suggests that the B or right-handed form binds ethidium only 5-10 times more strongly than the Z or left-handed form. In the case of the bifunctional compound BMSp, the behavior of the induced CD intensity in the 315 nm region with r, the amount of drug per base pair, is consistent with bis-intercalation in Z as well as B forms of DNA.  $^{31}\text{P}$  NMR has been used to follow the transition from left-handed to right-handed form induced by increasing concentrations of ethidium. These results have significant implications regarding the ability of drugs to bind to Z DNA.

**W-PM-D4** BASE PROTONATION FACILITATES THE SALT INDUCED B-Z TRANSITION OF POLY(dG-dC):POLY(dG-dC). Fu-Ming Chen, Department of Chemistry, Tennessee State University, Nashville, Tennessee 37203.

Comparative studies on the salt titration of poly(dG-dC):poly(dG-dC) in neutral and acidic solutions reveal that base protonation facilitates the salt induced B to Z transition of this polynucleotide. The B-Z transition mid-point decreased from 3 M at pH 7 to 2.2 M NaCl at pH 3.8. In contrast to the nearly equal negative and positive characteristic CD bands at 290 and 260 nm in neutral solution, the inverted CD spectrum of the protonated Z duplex exhibits 4 and 12 nm red shifts on the respective bands with the intensity of the positive maximum to be about three times higher than that of the negative. These features of CD spectra for poly(dG-dC):poly(dG-dC) in the acidic high salt solutions are very similar to those exhibited by the guanine N-7 methylated derivative of this polymer, giving credence to the suggestion by Guschulbauer that protonation occurs at N-7 of guanine with subsequent rearrangement of this base to syn conformation and the formation of Hoogsteen's base pair. The salt induced B to Z conversion as well as the actinomycin D induced reverse Z to B transition are about five times faster at pH 3.8 than at pH 7.

**W-PM-D5** COOPERATIVE TRANSITION BETWEEN TWO DNA HELICAL CONFORMATIONS, B  $\leftrightarrow$  Z.

Shousun Chen Szu and Elliot Charney, Laboratory of Chemical Physics, NIADDC, National Institutes of Health, Bethesda, MD 20814.

The temperature induced B to Z transition was used to study the cooperativity of this one dimensional system. Fragments of poly(dG-dC).poly(dG-dC) and poly(dG-m<sup>5</sup>dC).poly(dG-m<sup>5</sup>dC) of various chain length (molecular weight) were isolated by preparative gel electrophoresis. Equilibrium transition curves induced by temperature variation for four different chain lengths were examined. The results show that, in contrast to DNA strand melting, shorter fragments convert from the B to Z conformation at higher temperature. Least square fits of the transition curve, with calculations based on Schwartz's formulation of the linear Ising model with nearest neighbor interaction between two ordered states, show that the B form is more stable at the ends than the Z form. This may be explained by the stronger solvent interaction with the end groups which favors the more hydrated B form. Equilibrium constants and cooperativity coefficient,  $\sigma_i$ , for the ends and interior of the chain have been estimated. Thermodynamic parameters (enthalpy, entropy and free energy) related to the B-Z transition have also been calculated.

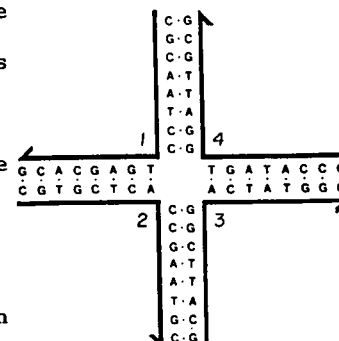
**W-PM-D6** FLEXIBILITY OF HAIRPIN LOOP STRUCTURES.- THE ANTICODON LOOP OF t-RNA<sup>Phe</sup>. N. L. Marky and W. K. Olson, Department of Chemistry, Rutgers University, New Brunswick, New Jersey 08903

The flexibility of hairpin loops containing n bases (residues) has been examined using a recently developed theoretical model (*Biopolymers*, 21, 2329-2344, 1982) of oligonucleotide loop closure. The study is based on correlated probabilities of chain separation and terminal residue orientation outlined previously. The probabilities are calculated using standard statistical mechanical methods as functions of local conformational changes of the chain backbone. Our results for an RNA chain of 9 residues suggest that the anticodon loop is a dynamic structure capable of assuming a variety of different spatial conformations. Free energy values related to the various conformations span a narrow range of values (2-4 Kcal mol<sup>-1</sup>) and compare well to experimental observations in aqueous solution. Conformational transitions between the loop conformations may have potential relevance to the molecular translation of the genetic code. (Supported by USPHS Grant 20861).



**W-PM-D7**  $^1\text{H}$  NMR AND CD STUDIES ON FOURTH RANK IMMOBILE NUCLEIC ACID JUNCTIONS. \*N.C. Seeman, <sup>†</sup>M. Maestre, <sup>††</sup>R.I. Ma, <sup>††</sup>A.J. Wand and <sup>††</sup>N.R. Kallenbach, \*Department of Biology, SUNY Albany, Albany, NY 12222, <sup>†</sup>Biology and Medicine Division, Lawrence Berkeley Lab, Berkeley, CA 94720 and <sup>††</sup>Department of Biology, University of Pennsylvania, Philadelphia, PA 19104.

Fourth rank immobile nucleic acid junctions are stable oligonucleotide models for Holliday recombination intermediates. An algorithm for predicting oligonucleotide sequences capable of forming these structures has recently been tested using chemically synthesized oligonucleotides, including the sequences shown on the right. This set of four hexadecamers forms a stable complex in solution, with definite 1:1:1:1 stoichiometry of the four component strands (1,2). We have used CD spectroscopy in the UV, and  $^1\text{H}$  NMR of the H-bonded ring protons of the bases to characterize the structure of the double helical arms about the junction center. The CD data are consistent with uninterrupted B-DNA helix in all arms of the complex, suggesting no significant loss of structure. The presence of ring proton resonances shifted upfield in the junction, relative to the separate arms, supports the notion that the arms surrounding the junction are involved in some sort of stacking interaction with each other.



- (1) N.R. Kallenbach, R.I. Ma and N.C. Seeman (1983), *Nature*, in press.
- (2) N.R. Kallenbach, R.I. Ma, A.J. Wand, G.H. Veeneman, J.H. van Boom and N.C. Seeman (1983), *J. Biomol. Struct. & Dyn.*, in press.

This work has been supported by grants GM-29554, ES-00117 and CA-31027 from the NIH.

**W-PM-D8** 2D NMR STUDIES OF THE STRUCTURES OF POLY(dA-dT) AND POLY(dI-dC).

D.R. Kearns, N. Assa-Munt and P. Mirau, Department of Chemistry, University of California, San Diego, La Jolla, California 92093.

The structures of poly(dA-dT) and poly(dI-dC) in solution have been probed using 2D NOE spectroscopy. Truncated driven nuclear Overhauser effects in  $\text{H}_2\text{O}$  solution demonstrate that the base pairs of both molecules are Watson-Crick rather than the Hoogsteen-type. Cross-relaxation patterns arising from inter-nucleotide and intra-nucleotide interactions are used to assign the sugar proton resonances and to deduce various structural features including the helical sense. The numerous proton-proton interactions that are observed indicate that both poly(dA-dT) and poly(dI-dC) form right-handed helices with a B-type conformation with bases in the anti conformation. In the case of poly(dA-dT), slight differences in the purine-sugar and pyrimidine-sugar intra-nucleotide interactions are observed, but the large differences in the sugar pucker of the adenine vs. thymine nucleotide suggested by some models (Klug et al., 1979) are not evident in the solution structure of poly(dA-dT). In the low temperature spectra there is unexpected evidence for cross-strand AH2-AH2 interactions. With poly(dI-dC) the 2D NOE spectra indicate that the alternation in nucleotide conformations is more pronounced. These results indicate that poly(dI-dC) does not have some unusual structure as suggested by its inverted circular dichroism spectrum and fiber x-ray diffraction patterns.

**W-PM-D9** EVIDENCE FOR A COMMON OPEN BASE PAIR STATE IN ADENINE-THYMINE AND ADENINE-URACIL DNA AND RNA DUPLEXES.

P.A. Mirau and D.R. Kearns, Department of Chemistry, University of California, San Diego, La Jolla, California 92093.

High resolution proton NMR relaxation in  $\text{H}_2$  solution has been used to study the exchange behavior of the hydrogen bonded imino protons in adenine-thymine (AT) and adenine-uracil (AU) containing DNA and RNA duplexes. At low temperature the spin-lattice relaxation of the imino protons is due to dipolar interactions with the nearby adenine amino and AH2 protons and at higher temperature to exchange with the unpolarized solvent protons. The activation energy for exchange and the room temperature exchange rates are largely unaffected by changes in the duplex sequence (alternating vs. homopolymer duplexes), the conformation (B form DNA vs. A form RNA) and the nature of the pyrimidine base (thymine vs. uracil). The average value of the activation energy for all of the duplexes studied was  $17.2 \pm 1.4$  kcal/mole. This value is considerably less than that observed for cytosine containing duplexes which are sensitive to the sequence, conformation, and nature of the bases. Taken together, these data indicate that there is some low energy pathway for escape of the thymine or uracil imino protons from the double helix which is not available to the cytosine containing ones. The AT and AU exchange behavior may be rationalized with a propped-open state which has recently been proposed on the basis of molecular mechanics calculations;

**W-PM-E1** PHOTOLYZED RHODOPSIN CATALYZES ATP/ADP EXCHANGE ON THE 48 KILODALTON PROTEIN OF RETINAL ROD OUTER SEGMENTS. Ralph Zuckerman, Bruce Buzdygon, Paul Liebman, Department of Anatomy, University of Pennsylvania, School of Medicine, Philadelphia, PA 19104.

Photolyzed rhodopsin triggers rapid, amplified, reciprocal changes in free ATP and ADP in intact retinal rod outer segments (ROS). It was previously proposed that these changes are mediated by exchange binding on a soluble nucleotide-binding protein<sup>1</sup>. We report here that ~80% of the ATP that disappears from the rod free ATP fraction upon illumination can be recovered in the form of ATP bound to soluble rod outer segment proteins. Also, at saturating intensities, 90 mmol ATP is bound to protein per mol photolyzed rhodopsin, implying that the ATP-binding protein exists in a ratio of 1 binding protein per 11 rhodopsins, assuming a single ATP binding site per protein molecule. Further, by use of the specific ATP photoaffinity ligand, [ $\alpha$ -<sup>32</sup>P]8-azido ATP, the protein on which ATP/ADP exchange takes place was identified as the 48 kilodalton protein of ROS, a major ROS protein of previously unknown function. Gel scans reveal a stoichiometry of one 48K protein per 10 rhodopsins, and a 1:1 ratio of 48K to  $\alpha$  subunit of GTP-binding protein in frog rods. We think it possible that 48K ATP-binding protein and GTP-binding (G) protein compete for the same or spatially contiguous sites on photolyzed rhodopsin. Such competition would decrease the rate of formation of G-GTP to light, and be expressed in a decreased initial velocity of phosphodiesterase (PDE) activation. As such, the 48K protein may be involved in the ATP-dependent quench of PDE activation<sup>2</sup>.

Supported by EY00012, EY01583 and EY07035.

1. Zuckerman, R. et al (1982) *Proc. Nat'l. Acad. Sci. USA*, 79:6414-6418.

2. Sitaramayya, A. and Liebman, P.A. (1983) *J. Biol. Chem.*, 258:1205-1209.

**W-PM-E2** CONTROL OF ROD OUTER SEGMENT DISK CALCIUM BY cGMP - John S. George and Mark W. Bitensky, Division of Life Sciences, Los Alamos National Laboratory, Los Alamos, N. M. 87545

cGMP modulates the metabolism of  $\text{Ca}^{2+}$  by rod outer segment (ROS) disks by at least 2 mechanisms. GMP stimulates the rate of ATP dependent  $\text{Ca}^{2+}$  uptake; cGMP hydrolysis causes the release of accumulated  $\text{Ca}^{2+}$  from ROS disks. Metabolism of  $\text{Ca}^{2+}$  was studied in crude suspensions of isolated, leaky, ROS (10-100  $\mu\text{M}$  rhodopsin) containing .005 mg/ml Ruthenium Red; in some experiments 10  $\mu\text{M}$  each of antimycin and oligomycin were added as another control for mitochondrial  $\text{Ca}^{2+}$  metabolism.  $\text{Ca}^{2+}$  activity (Aca) was monitored with a miniature  $\text{Ca}^{2+}$  sensitive electrode or the distribution of  $^{45}\text{Ca}$  between particles and suspending aqueous was studied by centrifugal filtration of ROS through silicone oil. Concentrations of cGMP from 100  $\mu\text{M}$  to 3mM added to ROS were found to stimulate  $\text{Ca}^{2+}$  uptake in the presence of ATP. 8-Br-cGMP, which is not measurably hydrolyzed under these conditions, also stimulated  $\text{Ca}^{2+}$  uptake weakly. In the presence of cGMP, continuous light rapidly released large quantities of  $\text{Ca}^{2+}$ . If cGMP was not added or was completely hydrolyzed, continuous light had little effect, but subsequent addition of cGMP caused a large  $\text{Ca}^{2+}$  release. Thus the effect did not depend on slowing cGMP stimulated uptake. Activation of phosphodiesterase in the dark by addition of purified ROS GTP-binding protein or protamine also stimulated  $\text{Ca}^{2+}$  release in the presence of cGMP. Thus cGMP hydrolysis directly and profoundly stimulates  $\text{Ca}^{2+}$  release. Basal and cGMP stimulated  $\text{Ca}^{2+}$  uptake appear to depend on the generation of an electrochemical gradient across the disk membrane.  $\text{Ca}^{2+}$  uptake is accompanied by a rise of pH of the suspension; uptake is inhibited and  $\text{Ca}^{2+}$  is released by dinitrophenol. Thus proton/ $\text{Ca}^{2+}$  exchange in the disk membrane might mediate both  $\text{Ca}^{2+}$  uptake and release by light activated cGMP hydrolysis. (Supported by NIH grant number 5 R01 AM31610-02.)

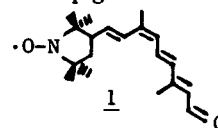
**W-PM-E3** FLASH PHOTOLYSIS STUDIES OF RHODOPSIN FUNCTION IN RECOMBINANT MEMBRANES. J.M. Beach, R.D. Pates, J.F. Ellena, and M.F. Brown. Department of Chemistry, University of Virginia, Charlottesville, VA 22901.

The light-induced Metarhodopsin I  $\rightarrow$  Metarhodopsin II transition is an example of a membrane protein conformational change, possibly linked to visual function, which is sensitive to the nature of the lipid environment (1,2). Previous work has shown that in recombinants of rhodopsin with saturated 1,2-diacyl-sn-glycero-3-phosphocholines, such as di(C14:0)PC, the MI  $\rightarrow$  MII transition is essentially blocked on the time scale of visual phototransduction; in recombinants with longer chain unsaturated PC's, the MI  $\rightarrow$  MII transition proceeds at nearly the same rate as in native retinal ROS membranes (1). To evaluate systematically the role of bilayer structural factors such as the (i) acyl chain length and (ii) position and/or (iii) degree of unsaturation, we have prepared recombinants of rhodopsin with homologous series of saturated and unsaturated PC's. Flash photolysis studies have been performed using an instrument recently constructed in this laboratory. By comparing recombinants of rhodopsin with di(C12:0)PC vs. di(C12:1)PC, di(C14:0)PC vs. di(C14:1)PC, and di(C16:0)PC vs. di(C16:1)PC, we have been able to separate the role of the phospholipid acyl chain length (bilayer thickness) from that of unsaturation in modulating the metarhodopsin transition kinetics. Results for the above recombinants together with the effects of temperature will be discussed.

1) D.F. O'Brien et al., *Biochemistry* 16, 1295 (1977). 2) B.J. Litman et al., *Biochemistry* 20, 631 (1981). Work supported by NIH Fellowship 1F32EY05635 (to J.F.E.), and by NIH Grant EY03754 and the Alfred P. Sloan Foundation (to M.F.B.).

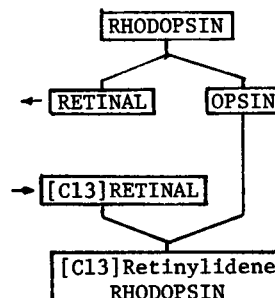
**W-PM-E4 EPR STUDIES OF A SYNTHETIC ISORHODOPSIN USING A SPIN-LABELLED RETINAL**  
 Geoffrey Renk, Yat Sun Or, and Rosalie Crouch, Medical University of South Carolina, Charleston, S.C. 29425

The binding site of bacteriorhodopsin has been studied previously in this laboratory by use of a spin-labelled analog of retinal (JACS 103:7364, 1981), but this molecule failed to form a pigment with bovine opsin. We report here the synthesis of another spin-labelled analog **1** of retinal, lacking the ring double bond, and the successful formation of a photosensitive pigment between the new analog and bovine opsin. The analog was purified and identified by CHN analysis, mass spectrometry and FT-NMR, the latter confirming the isomeric configuration to be 9-*cis*. Pigment was formed by incubation of freshly prepared bovine opsin with an excess of the analog, added as a suspension in EtOH (≤1%), for 12 hours in the dark at 4°C. Unbound analog was removed by successive washes with 2% BSA solution and buffer. Additions of 11- or 9-*cis* retinal to the pigment failed to displace the spin label over 48 hours and the pigment was stable to NH<sub>2</sub>OH in the dark for > 24 hours. Conversely, addition of the analog to fully saturated rhodopsin failed to form a pigment. The UV-VIS spectrum of the pigment showed a broad absorbance peak with λ<sub>max</sub> = 458 nm, which diminished on exposure to visible light. The EPR spectrum of the pigment showed a broad, complex lineshape characteristic of a nitroxide undergoing slow anisotropic motion. After exposure to light, the anisotropic signal disappeared and the characteristic triplet spectrum of a small, rapidly tumbling nitroxide was obtained, representing unbound spin label. Effects of detergents, pH, and small hydrophilic reducing agents will be discussed. (Supported by NIH Grant EY04939 and NSF grant BNS-80-11563)



**W-PM-E5 NUCLEAR MAGNETIC RESONANCE INVESTIGATION OF THE 'OPSIN SHIFT' IN RHODOPSIN AND BACTERIORHODOPSIN.** G. D. Mateescu, D. V. Waterhous, M. Iqbal, W. G. Copan, D. D. Muccio, E. W. Abrahamson, and J. W. Shriver, Department of Chemistry, Case Western Reserve University, Cleveland, Ohio 44106

Carbon-13 and nitrogen-15 constitute sensitive NMR probes of electronic charge distributions in the retinylidene chromophores of visual pigments and halobacteria photoreceptors. Results obtained with pigments regenerated with retinals which were labeled at key carbon atom positions (6, 13, 9, 12, 13, 14, 15) suggest that effects of chromophore-protein interactions in rhodopsin and bacteriorhodopsin are similar near the Schiff base linkage, but different at the corresponding beta-ionone sites. The latter may account for the bathochromic shift of bacteriorhodopsin with respect to rhodopsin. Both C-13 and N-15 NMR data obtained with lyophilized specimens suggest that the degree of protonation of the Schiff base nitrogen depends on the degree of hydration of the specimen. These preliminary results emphasize the necessity of performing *in vivo* experiments with biosynthetically enriched bacteriorhodopsin. Measurements on light and dark adapted *Halobacterium halobium* cells are in progress in our laboratory.



**W-PM-E6 MODIFICATIONS TO THE LIGHT RESPONSE OF LIMULUS VENTRAL PHOTORECEPTORS BY INTRACELLULAR Ca/EGTA.** Richard Payne and Alan Fein, Marine Biological Laboratory, Woods Hole, MA 02543.

10-100 pI of 0.1 M K<sub>2</sub> EGTA (pK=6.3) and sufficient Ca(OH)<sub>2</sub> to buffer calcium concentrations between 0.1 and 10 μM at pH7 were pressure-injected into ventral photoreceptors. Photocurrents were recorded under voltage clamp at the resting potential. After injections of EGTA with 0.1 μM free calcium: (1) Responses to dim flashes were slowed but the areas under the responses were undiminished. (2) Responses could be modelled as the output of 7 exponential stages of delay, having 6 time constants, T<sub>α</sub>, of 39 ± 11 ms and one, T<sub>β</sub>, of 534 ± 128 ms. (3) "Quantum bump" amplitudes decreased ten-fold while their duration increased ten-fold, maintaining a constant bump area. After injection of EGTA with 10 μM free calcium: (1) Response area was reduced 100-fold. (2) A 7-stage model again described the response, but with faster decay time constants, T<sub>α</sub> = 10 ± 1 ms and T<sub>β</sub> = 89 ± 4 ms. (3) The average initial response was at least ten-fold greater than that after injection of 0.1 μM calcium. Calcium therefore increases the rate constants (3) for production as well as for decay of the photocurrent. Dark-adapted responses recorded before injections of EGTA rose too abruptly to be modelled with 6-7 stages of delay. A possible explanation is that EGTA buffers an early, local release of calcium which first accelerates the rising edge of the photocurrent by increasing 3, before reducing sensitivity by reducing T<sub>α</sub> and T<sub>β</sub>.

**W-PM-E7 EFFECTS OF EXTRACELLULAR  $\text{Ca}^{++}$ ,  $\text{K}^+$ , AND  $\text{Na}^+$  ON CONE AND RPE RETINOMOTOR MOVEMENTS IN ISOLATED TELEOST RETINAS.** Allen Dearry and Beth Burnside, Univ. of California, Berkeley 94720.

We have studied the effects of altering external levels of  $\text{Ca}^{++}$ ,  $\text{K}^+$ , and  $\text{Na}^+$  on cone elongation and contraction and on pigment migration in retinal pigment epithelium (RPE) in cultured isolated retinas of green sunfish (*Lepomis cyanellus*). In vivo, cones elongate in darkness and contract in light, while pigment granules aggregate to the base of RPE cells in darkness and disperse into the cells' apical projections in light. During culture in constant darkness, dark-adapted (DA) cones remained in their long DA positions when  $[\text{Ca}^{++}]_o$  was  $<10^{-6}$  M but contracted to their short light-adapted (LA) positions when  $[\text{Ca}^{++}]_o$  was  $10^{-3}$  M. With A23187, DA cones contracted fully at  $[\text{Ca}^{++}]_o >10^{-5}$  M. During culture in light, long cones of DA retinas contracted to LA positions in  $10^{-3}$  M  $\text{Ca}^{++}$ , but DA cones contracted to only half that extent in  $<10^{-8}$  M  $\text{Ca}^{++}$  (1 mM EGTA). Thus, cones initiated contraction in the absence of  $\text{Ca}^{++}$ , but full contraction required  $\text{Ca}^{++}$ . During culture in constant light, LA RPE-retinas exhibited little change in retinomotor positions regardless of  $[\text{Ca}^{++}]_o$ . However, during culture of LA RPE-retinas in darkness, cones elongated and RPE pigment aggregated at  $[\text{Ca}^{++}]_o$  between  $10^{-5}$  and  $10^{-7}$  M. Increasing  $[\text{K}^+]_o$  to  $>27$  mM inhibited both light-induced and light-independent  $\text{Ca}^{++}$ -induced cone contraction. However, decreasing  $[\text{Na}^+]_o$  to 3.5 mM in the presence of  $<10^{-6}$  M  $\text{Ca}^{++}$  did not mimic light onset by inducing cone contraction in the dark. High  $[\text{K}^+]_o$  also promoted dark-adaptive movements in LA RPE-retinas cultured in constant light. Thus, low  $[\text{Ca}^{++}]_o$  or high  $[\text{K}^+]_o$  favored DA retinomotor positions and their effects were shown to be similar to those of agents which elevate  $[\text{cAMP}]_i$ . Supported by EY03575.

**W-PM-E8 ACTION AND ABSORPTANCE SPECTRA MEASURED IN THE SAME ISOLATED VERTEBRATE ROD.** M. Carter Cornwall, E.F. MacNichol, Jr., and Alan Fein. Department of Physiology, Boston Univ. School of Med., Boston, MA 02118 and Marine Biological Laboratory, Woods Hole, MA 02543.

We report experiments designed to examine and compare the action spectrum of photoexcitation of a rod photoreceptor and the absorptance spectrum of the visual pigment in the same cell using the optical system of a photon-counting microspectrophotometer for making both measurements. The inner segment of an isolated dark-adapted rod of the tiger salamander, *Ambystoma tigrinum*, was aspirated into a micropipette connected to a current to voltage converter. The optical density (OD) spectrum of the visual pigment in the outer segment was then determined in a rectangular area ( $10\mu\text{m} \times 2\mu\text{m}$ ) oriented with the long axis of the slit parallel to the long axis of the rod. Individual OD measurements bleached less than 0.3% of the visual pigment in this area and did not desensitize the cell for more than a few seconds following the measurement. Immediately following this, the spectral sensitivity of the cell was determined in the same area of the outer segment in which the OD spectrum was measured by determining at selected wavelengths the number of photons in a brief flash necessary to elicit a criterion response. No significant differences could be found between the pigment absorptance spectrum and the action spectrum except at wavelengths shorter than about 440nm. This discrepancy could be due to wavelength dependent light-scattering or to absorption by photoproducts. Our results suggest that the correspondence between the absorptance spectrum and the action spectrum in these rods is very good when optical and geometrical conditions under which the two measurements are made are identical. Supported by NIH grants EY01157, EY01362, and EY02399.

**W-PM-E9 PHOTOCURRENT AND SPECTRAL SENSITIVITY OF VISUAL RECEPTORS OF MACACA FASCICULARIS.** D.A. Baylor, B.J. Nunn, and J.L. Schnapf. Neurobiology Department, Stanford Medical School, Stanford, CA 94305

Photon capture and visual transduction have been examined by recording membrane current from single rod and cone outer segments in chopped pieces of retina from a monkey thought to have human-like photoreceptors. The rod spectral sensitivity is fitted by the Dartnall nomogram for a rhodopsin of  $\lambda_{\text{max}} 491 \pm 3$  nm and agrees with the human scotopic visibility curve, corrected for lens absorption and self-screening. Measured cone sensitivities fell into two groups with broad peaks at roughly 560 and 540 nm. The two curves coincide with estimates of red and green pigment absorptions derived from human color matching. The gentler descent of the green cone sensitivity at long wavelength explains the paradoxical hue shift observed psychophysically, where light of very long wavelength resembles light of shorter wavelength.

In dim light, the rod photocurrent consists of rounded shot effects 0.7 pA in peak amplitude and 0.2 sec in time to peak; each is triggered by a single  $\text{Rh}^*$ . The average electrical effect of an  $\text{Rh}^*$  is not reduced by steady lights causing up to roughly 100  $\text{Rh}^* \text{ sec}^{-1}$ . Recovery of the photocurrent after bright light is delayed by long step-like events apparently resulting from single molecular transitions. These events have amplitudes of about 1 pA and exhibit widely variable durations.

Cones give photocurrents up to 20 pA in saturating amplitude. The dim flash response is several times faster than that of rods, and background light desensitizes over a wider intensity range.

Supported by USPHS grant EY01543.

**W-PM-E10** SODIUM AND CALCIUM TRANSPORT IN OUTER SEGMENTS ISOLATED FROM ROD PHOTORECEPTORS, Paul P. M. Schnetkamp, Jules Stein Eye Institute, UCLA School of Medicine, Los Angeles, CA 90024. (Introduced by W. Hubbell)

The properties of conductive  $\text{Na}^+$  transport and  $\text{Na}^+$ -stimulated  $\text{Ca}^{2+}$  efflux were compared in intact rod outer segments isolated from bovine retinae (ROS). Conductive  $\text{Na}^+$  transport was progressively inhibited when the external  $\text{Ca}^{2+}$  was raised from 10  $\mu\text{M}$  to 10 mM.  $\text{Na}^+$  could be replaced by  $\text{H}^+$  and  $\text{Li}^+$ , but with decreasing effectiveness. In contrast,  $\text{Na}^+$  stimulated  $\text{Ca}^{2+}$  efflux from  $\text{Ca}^{2+}$ -enriched ROS at maximal rates of  $10^7$   $\text{Ca}^{2+}$ /outer segment/sec, whereas  $\text{Ca}^{2+}$  efflux stimulated by other alkali cations did not exceed  $\text{Ca}^{2+}$  leakage. Conversely,  $\text{Ca}^{2+}$  uptake in  $\text{Ca}^{2+}$ -depleted ROS was only inhibited by  $\text{Na}^+$ , whereas upon addition of gramicidin, all alkali cations abolished  $\text{Ca}^{2+}$  uptake. Under the latter conditions, alkali cations in the medium will cause the release of internal  $\text{Na}^+$  from ROS and can be expected to inhibit  $\text{Ca}^{2+}$  uptake by reverse Na-Ca exchange. These findings are consistent with the notion that  $\text{Ca}^{2+}$  transport through the plasma membrane of ROS is exclusively performed by the Na-Ca exchanger. The conductive  $\text{Na}^+$  transport and Na-Ca exchange showed a very similar and sigmoidal dependence on the external  $\text{Na}^+$  concentration (dissociation constant for  $\text{Na}^+$ : 7 - 10 mM). On the assumption that two  $\text{Na}^+$  are transported simultaneously and using the dissociation constants of the Na-Ca exchanger for  $\text{Na}^+$  and  $\text{Ca}^{2+}$ , the fractional occupancy of the Na-Ca exchanger by these ions can be calculated. The calculated occupancy by two  $\text{Na}^+$  fits closely the variations of the dark current upon variations of the external  $\text{Na}^+$  and  $\text{Ca}^{2+}$  concentrations as observed in toad ROS by Yau et al. [Nature 292:502(1981)]. This could suggest that these variations of the dark current arise from competition between external  $\text{Na}^+$  and  $\text{Ca}^{2+}$  for common sites on the Na-Ca exchanger.

**W-PM-E11** PERMEABILITY OF LIGHT-SENSITIVE CONDUCTANCE IN RETINAL ROD TO MONOVALENT ALKALI CATIONS.

King-Wai Yau and Kei Nakatani, Department of Physiology and Biophysics, The University of Texas Medical Branch, Galveston, Texas 77550.

The permeability of the light-sensitive conductance in toad rod outer segments to monovalent alkali cations was studied by recording membrane current from a single isolated rod with a suction pipet while rapidly exchanging the solution around its outer segment. With a normal external Ca concentration of 1 mM,  $\text{Na}^+$  and  $\text{Li}^+$  carried current equally well through the light-sensitive conductance. However, within a few seconds after complete replacement of external  $\text{Na}^+$  by  $\text{Li}^+$  the light-sensitive current declined to near zero, most probably because  $\text{Li}^+$  was unable to substitute for  $\text{Na}^+$  in driving the Na-Ca exchanger in the rod outer segment membrane which tended to keep the conductance open.  $\text{K}^+$  also carried current very well through the conductance, with an apparent permeability ratio  $P_{\text{K}}/P_{\text{Na}}$  of 0.5 to 0.7. Additionally, increasing external K concentration above normal (2.5 mM) caused a rapid and significant reduction in the light-sensitive current. This reflected a decline in the light-sensitive conductance resulting most probably from an inhibition on the Na-Ca exchanger by external  $\text{K}^+$ .  $\text{Rb}^+$  and  $\text{Cs}^+$  also could carry current through the conductance, though not as well as  $\text{Na}^+$ ,  $\text{Li}^+$  or  $\text{K}^+$ . In addition  $\text{Rb}^+$  had an inhibitory action on the current like  $\text{K}^+$ . With external Ca concentration at 1  $\mu\text{M}$ , the light-sensitive conductance was many times higher but its ionic selectivity seemed unchanged. In conclusion, in normal conditions the light-sensitive (dark) current in rods consists of mainly a mixture of Na (inward) and K (outward) fluxes, and this can explain the reversal potential for the current being at 0 to +10 mV.

**W-PM-E12** "WHOLE CELL RECORDINGS" OF SOLITARY SALAMANDER ROD PHOTORECEPTORS. P.R. Robinson, P.R. MacLeish and J. Lisman. Dept of Biology, Brandeis University, Waltham, MA. and Laboratory of Neurobiology, Rockefeller University, N.Y., N.Y.

Solitary vertebrate rods prepared by enzymatic dissociation of dark-adapted tiger salamander (*Ambystoma tigrinum*) retinas were studied using the whole cell recording mode of the patch clamp technique. This method allowed us to obtain high resolution current recordings from isolated voltage-clamped rods. 1-50 gigohm seals were obtained on both the inner and outer segments of solitary rods suspended in an amphibian salt solution containing 1.8 mM Ca. Patch electrodes were filled with a solution containing 92 mM K-aspartate, 7mM NaCl, 5mM  $\text{MgCl}_2$ , 1 mM  $\text{NaHCO}_3$ , 10 mM taurine, 1mM ATP, 1mM GTP (pH 7.4). After the patch membrane was disrupted, the cell was studied in the whole cell recording mode under voltage-clamp. When the rod was clamped at its dark resting potential (-20 mV to -40 mV) the response to a saturating flash ranged from 14-40 pA with an average of 25 pA. In the dark the input resistance around rest averaged 1.25 gigohms. Dark adapted rods often underwent an irreversible transition in their conductance properties in response to large depolarizing voltage pulses resulting in a decrease in net voltage-dependent outward current. This decrease in outward current was associated with a dramatic change in the light response at very positive voltages. Before the transition no light response was observed at large depolarizing voltages, whereas after the transition light responses with a polarity opposite to that obtained at rest were observed. A possible explanation of these phenomena involving a light-enhanced, but labile outward current will be discussed. (Supported by EY-01496 & EY 03665)

**W-PM-F1 THERMAL INACTIVATION OF MITOCHONDRIAL ELECTRON TRANSPORT CHAIN.**

Barry E. Knox and Tian Yow Tsong, Department of Physiological Chemistry, The Johns Hopkins University School of Medicine, Baltimore, Maryland 21205

In order to investigate the structure-function relationship of the inner mitochondrial membrane, we have done a study of the thermal denaturation of submitochondrial particles (SMP) from beef heart. Several functions of the respiratory chain were assayed at 30°C on samples preheated at certain temperatures for 3 minutes. The denaturation of the respiratory chain took place in at least three distinct stages, and each stage was irreversible. The first stage occurred at 53°C with the inactivation of NADH-linked respiration, ATP-driven reverse electron transport, and ATP/Pi exchange activity of the FoF<sub>1</sub> ATPase. The second stage occurred at 58°C with the loss of succinate-driven ATP synthesis and respiration. The cytochrome oxidase and the oligomycin-sensitive ATP hydrolysis activities persisted until 63°C. These results indicate different stability of the complexes of the electron transport chain and suggest that these complexes may inactivate independently. Surprisingly, ATP/Pi exchange is lost several degrees before loss of the succinate-driven ATP synthesis and the oligomycin-sensitive ATP hydrolysis activity. This indicates that the FoF<sub>1</sub> ATPase may be partially denatured by heat. The thermal denaturation of the SMP was also studied by the differential scanning microcalorimetry (DSC). Under anaerobic conditions, four main irreversible endothermic transitions were observed with T<sub>m</sub> of 53, 58, 62 and 75°C. The first three transitions apparently correspond to the denaturation of the protein complexes described here. The 75°C transition may contribute from denaturation of heat stable proteins such as cytochrome c. (Supported by NIH Grant GM 28795).

**W-PM-F2 EXOTHERMIC TRANSITIONS OF MITOCHONDRIAL INNER MEMBRANES.**

Tian Yow Tsong and Barry E. Knox, Department of Physiological Chemistry, The Johns Hopkins University School of Medicine, Baltimore, Maryland 21205

The thermal denaturation of submitochondrial particles (SMP) prepared from beef heart were endothermic in the presence of mercaptoethanol, dithiothreitol, or under anaerobic conditions. There were several transitions centered around 53, 58, 62 and 75°C, corresponding to the denaturation of certain protein complexes in the respiratory chain (see the accompanying abstract). The total heat absorbed was about 6 mcal/mg. Under aerobic conditions, however, the first three transitions became exothermic and released 20 to 25 mcal/mg. Measurement of oxygen in the SMP suspension by an oxygen electrode revealed the consumption of 200 to 250 nmoles of molecular oxygen per mg protein in the denaturation process. This corresponds to 120 kcal of heat generated per mole of oxygen consumed. Treatment of SMP with detergent followed by trypsin completely abolished the exothermic transitions. An examination of the composition of proteins and lipids in the membrane suggested to us that the heat might have come from an auto-oxidation of iron containing proteins, such as Fe-S and heme proteins. Supporting this idea, a purified Fe-S protein, ferredoxin, also exhibited an exothermic transition at 48°C, with consumption of molecular oxygen and a release of 6 mcal/mg. Oxidation of lipids as the sole source of heat was tentatively ruled out. The implication of these observations on biological molecules or complexes, and the application of microcalorimetry to the study of these molecules will be discussed. (Supported by NIH Grant GM 28795).

**W-PM-F3 RECONSTITUTED CHEMICALLY MODIFIED SUBMITOCHONDRIAL PARTICLES WITH UNEXPECTED RELATIVE SPECIFIC ACTIVITIES.** Karen S. Soong and Jui H. Wang, Bioenergetics Laboratory, Acheson Hall, State University of New York, Buffalo, NY 14214.

Submitochondrial particles reconstituted from [<sup>14</sup>C]DCCD-labeled bovine heart MF<sub>1</sub>-ATPase and MF<sub>1</sub>-depleted inner membrane particles (ASU) were found to catalyze oxidative phosphorylation and ATP hydrolysis at reduced rates. But the ratio of the specific activity (S.A.) of the labeled particles (DCCD-MF<sub>1</sub>-ASU) to that of the control particles (MF<sub>1</sub>-ASU) were found to be higher for oxidative phosphorylation than for ATP hydrolysis. Submitochondrial particles reconstituted from disulfide cross-linked MF<sub>1</sub>(XMF<sub>1</sub>) and ASU catalyze ATP hydrolysis with a rate similar to that for MF<sub>1</sub>-ASU. But the S.A. of the cross-linked particles (XMF<sub>1</sub>-ASU) for oxidative phosphorylation was much lower than that for MF<sub>1</sub>-ASU. When assayed in the normal way for ATP hydrolysis, the S.A. of DCCD-MF<sub>1</sub>-ASU increased with preincubation time without losing the radioactive label. But the S.A. of DCCD-MF<sub>1</sub>-ASU for oxidative phosphorylation was unaffected by preincubation. These results are incompatible with the binding-change mechanism with either 2 or 3 alternating sites. The rate of spontaneous reactivation of DCCD-MF<sub>1</sub>-ASU for ATP hydrolysis was accelerated by proton-flux stimulated exchange of tightly bound ADP and ATP. A new mechanistic model with 1 active site and 2 interacting latent catalytic sites is proposed which assumes that during ATP hydrolysis only 1 of the 3 β-subunits is active because of the unique way it interacts with the γ, δ and ε subunits, and that during oxidative phosphorylation, the protonation-driven dissociation and subsequent rebinding of the ADP on α-subunit repeatedly trigger subunit rearrangement to admit pulses of proton flux for protonating the bound P<sub>i</sub> without protonating the bound nucleophile ADP on the β-subunit in order to facilitate the formation of ATP.

**W-PM-F4** THREE DIMENSIONAL DIFFUSION OF CYTOCHROME c IN MITOCHONDRIA AT PHYSIOLOGICAL IONIC STRENGTH. Sharmila S. Gupte & Charles R. Hackenbrock. Laboratories for Cell Biology, Department of Anatomy, School of Medicine, University of North Carolina, Chapel Hill, NC 27514.

The role of diffusion of cytochrome c for electron transfer in mitochondria at physiological ionic strength was investigated. The ionic strength dependence of the rate of electron transfer from cytochrome bc<sub>1</sub> via cytochrome c to cytochrome oxidase was determined for isolated inner membranes and for whole, intact mitochondria using uncoupled duroquinol oxidase activity. The ionic strength of the assay medium was varied from 0 to 150 mM KCl + 2 mM Hepes, pH 7.4. For isolated, inner membranes, the rate of electron transfer increased progressively when the KCl concentration was raised up to 50 mM; further increase in KCl concentration to 150 mM resulted in a decrease in the rate of electron transfer. In contrast, for whole, intact mitochondria, the rate of electron transfer increased progressively when KCl concentration was raised up to 150 mM. Addition of 20  $\mu$ M cytochrome c to the aqueous medium containing 150 mM KCl resulted in up to 600% increase in the rate of electron transfer for isolated inner membranes. This elevated rate was comparable to that of whole mitochondria without exogenous cytochrome c. These data indicate that cytochrome c is not permanently bound to the surface of the inner membrane at physiological ionic strength but rather is free to diffuse in three dimensions. In whole mitochondria, however, freely diffusing cytochrome c is trapped in the intermembrane space and can collide randomly with the membrane surface and its redox partners. The data suggest that three dimensional diffusion and collisional interaction of cytochrome c with its redox partners is an essential part of the mechanism of electron transfer in mitochondria at physiological ionic strength. Supported by NIH GM28704 and NSF PCM79-10968 to CRH.

**W-PM-F5** TEMPERATURE DEPENDENCE OF THE LATERAL DIFFUSION RATES OF LIPID IN MITOCHONDRIAL INNER MEMBRANES OF VARYING PROTEIN DENSITY. Brad Chazotte and Charles R. Hackenbrock. Laboratories for Cell Biology, Department of Anatomy, University of North Carolina, Chapel Hill, NC 27514

Fluorescence recovery after photobleaching (FRAP) was employed to measure the temperature dependence of the lateral diffusion coefficient (D) of the lipid analogue 3,3'-dihexyldecylindocarbocyanine (diI) in rat liver intact mitochondrial inner membranes (MIM) where the protein density had been varied by the controlled incorporation of exogenous phospholipid. The low pH method of Schneider et al. (PNAS 77:42, 1980) was used for the lipid enrichment. The calcium fusion method of Chazotte et al. (Fed. Proc. 42:2170, 1983) was used to fuse these membranes to a size sufficient for FRAP. Freeze fracture electron microscopy revealed that these fused membranes have randomly distributed proteins with the same protein density as the enriched membrane from which they are made. The diffusion coefficients of diI were analyzed according to an Arrhenius treatment. The temperature dependence as determined by the apparent activation energy of the diffusion coefficients in the native (unenriched membrane) was substantially greater than that of model and other biological membranes. Decreasing the protein density resulted in decreases in the temperature dependence of the diffusion coefficients. This was consistent with previous findings that showed an increase in lipid diffusion as the protein density decreased. These results demonstrate the strong effect of the protein concentration in the mitochondrial inner membrane on bilayer diffusion. Supported by NIH GM28704 and NSF PCM79-10968 to CRH.

**W-PM-F6** RESOLUTION OF CYTOCHROME b-c<sub>1</sub> COMPLEX IN MONOMERIC AND DIMERIC FORM: STRUCTURAL-FUNCTIONAL ANALYSIS. M. J. Nałecz and A. Azzi, Medizinisch-chemisches Institut der Universität Bern, 3012 Bern, Switzerland.

Bovine heart cytochrome b-c<sub>1</sub> complex was prepared by the method of Rieske and dispersed in 0.1% dodecylmaltoside - 10 mM Tris/HCl (pH 7.4) in the presence or absence of 50 mM KCl. As estimated by filtration on Ultrogel ACA 34, an apparent  $M_r$  about 400,000 was observed in the presence of 50 mM KCl and about 170,000 in the absence of added KCl. Similar  $M_r$  values were obtained also from sucrose-gradient centrifugation of the enzyme complexes recovered from the gel filtration experiment. Both species having higher or lower  $M_r$  contained all b-c<sub>1</sub> subunits (eight, using Laemmli's SDS-gel electrophoresis technique). The experiments suggest that the two species represent a dimer and a monomer of the b-c<sub>1</sub> complex. The molecular conversion between monomeric and dimeric state of the enzyme was found to be reversible. Using the reduced form of 2,3-dimethoxy-5-methyl-6-decyl-1,4-benzoquinone and ferricytochrome c as an electron donor and acceptor, respectively, the  $QH_2$ :cytochrome c oxidoreductase activity was measured. Both monomers and dimers of b-c<sub>1</sub> complex were found competent to catalyse the reaction. The apparent  $K_m$  for cytochrome c was slightly higher in the presence of added KCl, but the maximal velocity was virtually the same. Functional models requiring a dimeric b-c<sub>1</sub> complex are not supported by the evidence presented above. Supported by a grant from Schweizerischer Nationalfonds N. 3.739-080 and the Emil-Barell Foundation.

**W-PM-F7** IDENTIFICATION OF AN 82,000 DALTON PROTEIN RESPONSIBLE FOR K<sup>+</sup>/H<sup>+</sup> ANTIPORT IN MITOCHONDRIA. Keith D. Garlid, Andrew D. Beavis and William H. Martin, Dept. Pharmacology, Medical College of Ohio, Toledo 43699.

We have previously shown that the mitochondrial K<sup>+</sup>/H<sup>+</sup> antiporter is inhibited by matrix magnesium ions and have postulated that the carrier-braking action of Mg<sup>++</sup> constitutes the primary mechanism for maintaining mitochondrial volume homeostasis *in vivo* (Garlid, J.B.C. 255, 11273, 1980). In subsequent studies we have obtained evidence for physiological inhibition of the K<sup>+</sup>/H<sup>+</sup> antiporter by protons and pharmacological inhibition by quinine and other hydrophobic amines. Each of these interactions is reversible. We now report that the K<sup>+</sup>/H<sup>+</sup> antiporter is irreversibly inhibited by N,N'-dicyclohexylcarbodiimide (DCCD) and that DCCD inhibition is prevented by physiological (Mg<sup>++</sup> and H<sup>+</sup>) and pharmacological (quinine, propranolol) inhibitors of the antiporter. DCCD treatment under a wide variety of conditions leaves the Na<sup>+</sup>/H<sup>+</sup> antiporter unaffected, confirming our contention that rat liver mitochondria possess two alkali cation/proton antiporters with distinct properties and physiological roles (Nakashima and Garlid, J.B.C. 257, 9252, 1982). The highly selective nature of DCCD inhibition has enabled us to label and identify the 82,000 dalton protein responsible for K<sup>+</sup>/H<sup>+</sup> antiport in intact mitochondria and in submitochondrial particles. The kinetics of the inhibition are consistent with a 1:1 stoichiometry of DCCD binding to the antiporter. To our knowledge, this is the first assignment of alkali cation/proton antiport function to a particular membrane polypeptide. This work was supported by U.S.P.H.S. Grant GM 31086.

**W-PM-F8** O<sub>2</sub><sup>-</sup> FREE RADICAL PRODUCTION BY RAT BRAIN MITOCHONDRIA AS INFLUENCED BY AGE. R.A. Floyd, H. James Harmon, and S.K. Nank. Oklahoma Medical Research Foundation, 825 N. E. 13th St., Oklahoma City, OK 73104 and Dept. of Zoology, Oklahoma State University, Stillwater, OK 74078.

Oxygen free radical damage to neurons could be of importance in many aspects of aging in brain. Mitochondria in other tissues including brain have been shown to produce O<sub>2</sub><sup>-</sup>. We have tested the idea that brain mitochondria from rats of different ages show both metabolic differences as well as differences in O<sub>2</sub><sup>-</sup> production. Synaptic (S) and non-synaptic (NS) mitochondria were isolated from 3, 12, and 27 mo. old Fisher 344 rat brains. Cytochrome c+c contents do not change with age in NS-mito; 27 month S-mito show a 43% decrease in c+c content, Cyt b content does not change in NS- or S-mito. Cyt aa<sub>3</sub> decreases less than 25% in NC-mito with age while S-mito decrease over 50% in aa<sub>3</sub> content. NS-mito do not show significant decreases in succinate oxidase activity (per heme a) with age while S-mito lose approximately 50% of their activity after 27 mo. In 3 month old rats, S-mito generate up to 16 times more O<sub>2</sub><sup>-</sup> sensitive to exogenous superoxide dismutase (SOD) than NS-mito of the same age or 27 month-old S-mito. Malate-glutamate-driven oxygen consumption in NS-mito decreases only slightly with age while activity in S-mito decreases approximately 75% after 27 mo. Up to 100% decrease in SOD-sensitive O<sub>2</sub><sup>-</sup> generation is observed in synaptic mitochondria. Differences in O<sub>2</sub><sup>-</sup> generation are observed if O<sub>2</sub><sup>-</sup> is measured in an antimycin inhibited or in an uninhibited respiratory chain. With age, mitochondria contain less cytochrome, respire at a slower rate, and produce less superoxide. These effects are more pronounced in synaptic mitochondria and may relate to neuronal damage associated with aging.

Supported by NIH Grant No. R01 AG02599 and the Department of the Air Force.

**W-PM-F9** EXAMINATION OF THE EQUIVALENCE OF THE MEMBRANE POTENTIAL ( $\Delta\psi$ ) AND pH GRADIENT ( $\Delta\text{pH}$ ) IN MITOCHONDRIA DURING STEADY-STATE OXIDATIVE PHOSPHORYLATION. B.D. Jensen\* and T.E. Gunter, University of Rochester, Rochester, New York 14642.

The chemiosmotic theory identifies  $\Delta\psi$  and  $\Delta\text{pH}$  as the driving forces of oxidative phosphorylation. They are usually assumed to be equivalent. A steady-state theory was derived relating the overall phosphorylation efficiency to the individual contributions due to the membrane potential and pH gradient. State III measurements were performed at 10°C on isolated rat liver mitochondria.  $\Delta\psi$ ,  $\Delta\text{pH}$  and the free energy of phosphorylation were measured according to well established procedures and, under control conditions, were typically 160 mv, 49 mv and 10.2kcal/mole, respectively. The rates of respiration and phosphorylation were typically 14.5 and 21.5 nmoles/mg/min, respectively. Respiration was corrected for proton leakage, which was estimated to be 10 to 11 percent under control conditions. All measurements were made rapidly and as close to simultaneously as possible. The phosphorylation efficiency was examined under conditions where  $\Delta\psi$  and  $\Delta\text{pH}$  were caused to vary. These variations were caused by treating the mitochondria with low levels of organic acids. Significant changes in the membrane potential or pH gradient did not give rise to statistically significant changes in the phosphorylation efficiency. Further, the ratio of the phosphorylation efficiency due to the pH gradient to that of the membrane potential ( $E_{\text{pH}}/E_{\psi}$ ) was found to be  $1.14 \pm 0.4$ . We have concluded that  $\Delta\psi$  and  $\Delta\text{pH}$  are equivalent in the process of oxidative phosphorylation.

\*Present Address: Smith Kline & French Labs, Swedeland, PA 19479

This work supported by DOE Contract DE-AC02-76EV03490 and NIH grant AM-20359.



**W-PM-F10** THE PERMEABILITY OF RAT LIVER MITOCHONDRIA TO IONS. Chang-Jie Zhang, Huazhong Normal University, Wuhan, China and Henry Tedeschi, State University of New York at Albany, Albany, NY 12222.

The permeability of isolated rat mitochondria to ions was examined using the osmotic photo-metric method of Tedeschi and Harris (1958, Biochem. Biophys. Acta 28, 392-402). The apparent permeability constants to isosmotic concentration of various ions have been calculated. The results allow the following conclusions. (a) The apparent permeability constants are in the range of 5 to  $10 \times 10^{-9}$  cm/sec for  $K^+$  and approximately 3 to  $10 \times 10^{-8}$  cm/sec for  $Na^+$ . The values for  $K^+$  are in reasonable agreement with those calculated from the available flux data. (b) The apparent permeability constants for  $SO_4$ ,  $SO_3$ , and  $NO_3^-$  are in the range of  $\frac{1}{2}$  to  $7 \times 10^{-7}$ , whereas those for  $Cl^-$  are lower by an order of magnitude. The permeability to  $SO_4$  was studied in more detail. The uptake of  $SO_4$  was found to follow saturation kinetics with a  $K_m$  of  $2.45 \pm 0.9$  mM and a  $V_m$  ranging from 2 to 20 nmol sec<sup>-1</sup> mg protein<sup>-1</sup>. The results suggest a competition between  $SO_4$ ,  $SO_3$ , and  $NO_3^-$  but not  $PO_4$  or  $Cl^-$ . Our observations also indicate that the permeability of the mitochondria to ions is very variable suggesting the presence of unknown factors which are not controlled in these experiments. Aided by NIH grant GM 27043.

**W-PM-F11** ATP SYNTHESIS BY SINGLE GIANT MITOCHONDRIA OR MITOPLASTS. M.L. Campo and H. Tedeschi, Department of Biological Sciences and the Neurobiology Research Center, State University of New York at Albany, Albany, NY 12222

The ATP synthesized by single mitochondria has been determined under a variety of conditions using the luciferin-luciferase assay. The ATP synthesis was found to be comparable to those of conventional isolated mitochondrial preparations. Impalement with microelectrodes, the electrophoretic microinjection of Lucifer Yellow or, alternatively, pyranine does not interfere with the ability of the mitochondria to phosphorylate. Comparable results were obtained with mitoplasts. Most of the phosphorylation of ADP, represents oxidative phosphorylation since it is blocked by antimycin A. In most cases, the electric potentials across the mitochondrial membrane were continuously monitored and were found to be very low in magnitude. These results agree with the previous reports of Maloff *et al.*, 1978 (J. Cell Biol. 78, 214 - 226) and Bowman *et al.*, 1978 (in: Frontiers of Biological Energetics: From Electrons to Tissues, P.L. Dutton, J.S. Leigh, and A. Scarpa, eds., 1, 413-421). Together with the demonstration that the microelectrodes are in the internal mitochondrial or mitoplast space (e.g., Bowman and Tedeschi, 1980, Science 209, 1251-1252; 1983, Biochim. Biophys. Acta 731, 261-266) these experiments support the notion that a significant membrane potential is not required for oxidative phosphorylation. Aided by NIH grant GM 27043.

**W-PM-F12** THE PROTON GRADIENT IN SINGLE GIANT MITOCHONDRIA. M.L. Campo and H. Tedeschi, Department of Biological Sciences and the Neurobiology Research Center, SUNYA, Albany, NY 12222.

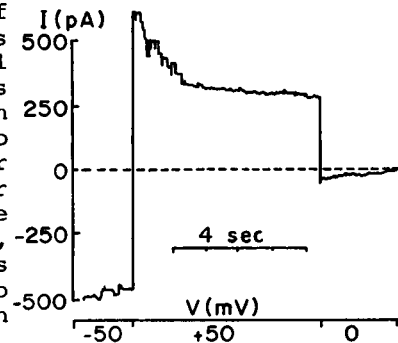
We have previously shown (these abstracts) that the ability of single giant mitochondria to synthesize ATP is not affected by electrophoretic microinjection of the fluorescent pH indicator pyranine. This finding opens the way for determining the pH gradient produced by metabolism in these mitochondria using pyranine. After the microinjection of pyranine the fluorescence change corresponding to a given pH can be calibrated in individual mitochondria by measuring the fluorescence as a function of pH changes in the presence of the protonophore FCCP. Over a wide range of pH the relationship between fluorescence and  $\Delta$  pH was found to be linear. Comparison of the fluorescent changes accompanying the addition of succinate to mitochondria, in the presence of rotenone, to those observed in the calibration curve, permits estimating the pH change induced by metabolism. This change was found to be in the range of 0.28 to 0.30 units, alkaline inside. These results together with those previously reported support the notion that the protonmotive force does not have a direct role in oxidative phosphorylation. Aided by NIH grant GM 27043.

**W-Pos1** INTRACELLULAR  $K^+$  AND  $Na^+$  ACTIVITY IN LIVER SLICES. Robert Wondergem\* and Lisa M. Chapman\*. Physiology Department, College of Medicine, East Tennessee State University, Johnson City, TN. 37614. (spon. W. McD. Armstrong).

As a step toward further understanding the regulation of transmembrane potential ( $E_m$ ) in liver, we measured hepatocyte  $E_m$  and intracellular  $K^+$  and  $Na^+$  activities ( $a_K^i$  and  $a_{Na}^i$ ) under steady-state conditions. We also measured  $E_m$  and  $a_K^i$  under conditions that stimulate the Na-K pump. Mouse liver slices were suffused (15 ml/min) with Krebs' physiologic salt solution (PSS) equilibrated with 95%  $O_2$ -5%  $CO_2$ .  $E_m$  was measured with open-tip microelectrodes filled with 3 M KCl (10-20 Mohms), and  $E_m = -40 \pm 1.4$  mV ( $n = 10$  animals).  $K^+$  and  $Na^+$  selective liquid ion-exchanger microelectrodes were used to measure  $a_K^i$  and  $a_{Na}^i$ .  $a_K^i = 104 \pm 3.6$  mM ( $n = 10$  animals) and  $a_{Na}^i = 17 \pm 1.6$  mM ( $n = 10$  animals).  $E_K$  and  $E_{Na}$  were -88 and 48 mV, respectively. This demonstrates that  $K^+$  and  $Na^+$  are not in electrochemical equilibrium across the hepatocyte plasma membrane, and we conclude that an active Na-K exchange pump maintains the steady-state. When the tissue equilibrated for 1 hr with PSS in which KCl was substituted with an equivalent amount of additional NaCl, the  $E_m$  and  $a_K^i$  were not different than control values. When control PSS was restored (15 min) the  $E_m$  hyperpolarized 4 mV and  $a_K^i$  increased 32 mM compared with control values,  $P < 0.05$ . This is further evidence that hepatocyte  $E_m$  and  $a_K^i$  depend upon the activity of the Na-K pump. Supported by VA grant 1A(74)111-43.

**W-Pos2** A VOLTAGE GATED  $Cl^-$  CHANNEL IN CULTURED MAMMALIAN URINARY BLADDER EPITHELIUM: A PATCH CLAMP STUDY. John W. Hanrahan, William P. Alles and Simon A. Lewis. Dept. of Physiology, Yale Univ. Sch. Med., 333 Cedar St., New Haven CT 06510

The patch clamp technique has been used to study ion channels in cultured epithelial cells from the rabbit urinary bladder. Cells were dissociated without using enzymes and grown on collagen for 1-3 weeks. Single channel currents were recorded from inside-out and outside-out patches excised from the accessible cell surface. One type of channel was selective for  $Cl^-$  over cations, as determined by its reversal potential in asymmetric solutions. The mean slope conductance in symmetrical 150 mM KCl was 374 pS (13 patches). The probability of the channel being open was not affected noticeably by  $[Ca^{++}]_i$  but was markedly voltage dependent, being open most of the time over a cell potential range of -80 to +20 mV and closed at more positive values (see Figure). The rate of inactivation increased dramatically with larger positive voltage steps. The results are consistent with two closed states corresponding to brief intraburst closures and longer interburst periods; and two open states, one of which has a lower conductance (70 - 90 pS). Since this channel is only seen in the surface membrane of cultures that are presumed to be non-polarized, i.e. when sub-confluent or just after confluence (less than ~18 days old), it might be a basolateral membrane channel that contributes to the large basolateral membrane  $Cl^-$  conductance previously measured in the intact epithelium. Supported by NSERC(Canada) and NIH AM20851.



**W-Pos3** MEMBRANE REORGANIZATION INDUCED BY CHEMICAL TRANSFORMATION IN CULTURE. Beverly S. Packard<sup>PO</sup>, Mina J. Bissell<sup>P</sup>, and Melvin P. Klein<sup>B</sup>. Divisions of Chemical Biodynamics<sup>B</sup> and Biology and Medicine<sup>P</sup>, Lawrence Berkeley Laboratory, University of California, Berkeley, CA. 94720. (Intr. by Melvin Calvin).

The idea of transformation to a malignant phenotype inducing a reorganization of the intra- and perimembranous macromolecular scaffolding of the plasma membrane is supported by a broad range of biophysical, biochemical, and morphologic studies. We are using the induction of a cell line (Madin-Darby Canine Kidney (MDCK)) to a transformed phenotype by exposure to phorbol ester tumor promoters as a model in which to study the plasma membrane perturbations brought about by the transformation process, in general. The appearance of an immobile fraction upon treatment with biologically active tumor promoters was connoted using the technique of fluorescence recovery after photobleaching (FRAP) with the synthetic fluorescent phospholipid Collarein as the probe molecule. To ascertain whether, under the conditions used for the photobleaching work, this putative reorganization affects the binding of a growth factor and, potentially, the growth perturbations observed upon transformation in general, we have determined the binding constants and affinities for epidermal growth factor (EGF). Using Scatchard plot analysis there appear to be three environments for the EGF receptor of MDCK cells: high affinity binding, low affinity binding, and nonbinding. Conversion from the high affinity and nonbinding state to the low affinity binding state is brought about by treatment with the biologically active phorbol ester 12-O-Tetradecanoyl phorbol 13-acetate (TPA).

**W-Pos4** INTRACELLULAR ACIDOSIS BLOCKS THE BASOLATERAL Na-K PUMP IN RABBIT URINARY BLADDER.

Douglas C. Eaton, Kirk L. Hamilton and Karen E. Johnson. Dept. of Physiology and Biophysics, University of Texas Medical Branch, Galveston, TX 77550.

We examined the effect of intracellular pH on the basolateral (Na,K)-ATPase of rabbit urinary bladder cells. To modify the intracellular pH, we permeabilized the apical membrane of the bladder cells with the polyene antibiotic, nystatin. To verify that the intracellular pH could be altered after nystatin treatment, the intracellular pH was monitored with pH sensitive microelectrodes. (The normal intracellular pH was  $7.1 \pm 0.11$ ,  $n=21$ .) After nystatin treatment, the intracellular pH over the range of pH 5.8 to 8.0 was indistinguishable from the mucosal pH. The cell-to-serosal ouabain-inhibitable sodium flux showed a strong dependence on intracellular pH with more acid pH values producing substantial block. The ouabain-insensitive  $\text{Na}^+$  flux showed little if any dependence on intracellular pH. The magnitude of the block obeyed a sigmoidal relationship with half block of  $\text{Na}^+$  flux occurring at pH 6.85. The steepness of the relationship suggested that  $\text{H}^+$  ion was interacting with more than one site. At the normal intracellular pH ( $7.1 \pm 0.1$ ), the Na pump was already partially blocked. This partial block, coupled with the steepness of the relationship between pump activity and intracellular  $\text{H}^+$  near pH 7.1, suggest that intracellular pH could be an important controlling factor for Na pump activity. Also, since similar effects of intracellular pH on Na pump activity are found in red blood cells, nerve cells, and muscle cells, it seems very possible that the blockage of the Na-K pump by intracellular hydrogen ion could explain the clinically observed relationship between plasma acidosis and elevated plasma potassium levels. (supported by DHHS AM-20068 and RCDA AM-00232 to D.C.E).

**W-Pos5** CELL SWELLING INCREASES A Ba-INHIBITABLE, K-CONDUCTANCE IN THE BASOLATERAL MEMBRANE OF NECTURUS SMALL INTESTINE. K.R. Lau, R. Hudson and S.G. Schultz, Department of Physiology & Cell Biology, University of Texas Medical School, Houston, Texas 77025.

Previous studies from this laboratory (Gunter-Smith et al, J. Membrane Biol. 66:25-39, 1982) have shown that immediately following the addition of galactose or alanine to the solution bathing the mucosal surface of Necturus small intestine there is a rapid increase in the conductance of the mucosal membrane and a depolarization of the electrical potential difference across that barrier ( $\psi^{\text{mc}}$ ) due to the activation of rheogenic Na-coupled entry mechanisms for these solutes. This initial response is followed by a slow repolarization of  $\psi^{\text{mc}}$  that is paralleled by an increase in the conductance of the basolateral membrane ( $g^{\text{s}}$ ) and inferential evidence has been presented that this is due to an increase in the K-conductance of that barrier (Grasset et al, J. Membrane Biol. 71:89-94, 1983).

We now report that: (i) The presence of 5 mM Ba in the serosal solution reduces  $g^{\text{s}}$  and blocks the increase in  $g^{\text{s}}$  following the addition of galactose to the mucosal solution; and, (ii) Exposure of the tissue to a hypotonic (12%) bathing solution results in a slow hyperpolarization of  $\psi^{\text{mc}}$  and an increase in  $g^{\text{s}}$ . However, when the hypotonic solution contains Ba,  $\psi^{\text{mc}}$  depolarizes and  $g^{\text{s}}$  decreases. These findings strengthen the conclusion that the increase in  $g^{\text{s}}$  following the addition of sugars or amino acids to the mucosal solution is due to an increase in the K conductance of that barrier and suggests that the "signal" for this response is cell swelling resulting from the intracellular accumulation of these solutes in osmotically active forms (Schultz et al, J. Gen. Physiol. 49:849-866, 1966).

**W-Pos6** CONCENTRATION DEPENDENCE OF K UPTAKE IN ISOLATED EPITHELIA OF FROG SKIN. Thomas C. Cox.

Dept. of Physiology, Southern Illinois University School of Medicine, Carbondale, IL 62901

Previous studies have shown that 1 mM ouabain inhibits greater than 95% of K uptake into the isolated epithelium of frog skin (Cl free Ringer). It is not likely that this is caused by a direct effect of ouabain on the K channel because 1) ouabain increases K efflux as might be expected due to membrane depolarization and 2) ouabain has no significant effect on basolateral membrane resistance (Biophysical J. 37:269a, Am. J. Physiol. 245:F321). Since K can apparently leave but not readily enter the cell in the presence of ouabain, it was thought that the nature of the K channel might be responsible for this rectification of K flux. The possibility that the K channel may function as a long, single filing pore was checked for by changing the electrochemical gradient for K across the tissue. Isolated epithelia of *Rana pipiens* were short circuited and K uptakes were measured across the basolateral membrane. In the presence of 1 mM ouabain and 1 mM furosemide (Cl free Ringer, 2.4 mM K), short circuit current ( $I_{\text{sc}}$ ) was  $17.0 \pm 1.4 \mu\text{A}/\text{cm}^2$  and K uptake was  $0.07 \pm 0.02 \mu\text{A}/\text{cm}^2$  (6). When K was 24 mM in the presence of ouabain and furosemide,  $I_{\text{sc}}$  was  $9.2 \pm 0.6 \mu\text{A}/\text{cm}^2$  and K uptake was  $0.66 \pm 0.06 \mu\text{A}/\text{cm}^2$  (6). A second set of studies was done in the presence of 0.1 mM amiloride, ouabain, and furosemide. When K was 2.4 mM, K uptake was  $0.59 \pm 0.03 \mu\text{A}/\text{cm}^2$  (3). When K was 24 mM, K uptake was  $5.0 \pm 0.6 \mu\text{A}/\text{cm}^2$  (4). Rough estimates made using the flux ratio equation suggest that influx and efflux are not independent. These results suggest that ouabain insensitive K uptake is dependent on the electrochemical gradient for K in a manner consistent with a single filing mechanism.

**W-Pos7 BASOLATERAL MEMBRANE Cl CONDUCTANCE IN NECTURUS GALLBLADDER IS SENSITIVE TO Na TRANSPORT.** C. William Davis and Arthur L. Finn, Depts. of Physiology and Medicine, University of North Carolina, Chapel Hill, NC 27514.

We have used changes in the volume of individual cells of the gallbladder epithelium, as measured by quantitative light microscopy, to probe the permeability properties of the apical and basolateral cell membranes. Cell swelling occurred when the mucosal perfusate was switched from 105 mM N-methyl-D-glucamine (NMDG)-Cl Ringer to 95 mM K, 10 mM Na-Cl Ringer, at a rate of  $2.86 \pm 0.36$  % original cell volume/min ( $n=4$ ; the serosal perfusate is NaCl Ringer at all times). If all mucosal Na is removed, however, K-induced cell swelling is totally inhibited. The Na-dependent swelling process is abolished by  $10^{-4}$  M amiloride or by  $10^{-4}$  M bumetanide. To distinguish between solute entry by means of mucosal electrically-silent processes and by electrically-coupled K and Cl entry, we studied the effects of mucosal Cl removal on the swelling process. Thus, when the mucosal perfusate was switched from 105 mM NMDG-cyclamate to 95 K, 10 Na-cyclamate Ringer, the cells still swelled, albeit at a lower rate ( $1.45 \pm 0.22$  %/min;  $n=6$ ). In this situation Cl can enter the cell only from the serosal solution, so solute entry must be accomplished via the electrically-coupled apical entry of K and the basolateral entry of Cl. Cell swelling in mucosal Cl-free media was abolished by removal of all Na from, or by the addition of either amiloride or bumetanide to, the mucosal medium. Since swelling in the presence of 10 mM Na is limited by a low basolateral membrane Cl conductance, and since apical membrane conductance is increased by K-for-Na substitutions, we conclude that inhibition of Na transport results in a decreased basolateral membrane Cl conductance. Supported by NIH grant AM25483.

**W-Pos8 TURN-OFF OF ADH-INDUCED WATER FLOW: ROLE OF AN OSMOTIC GRADIENT.** R.H. Parsons, L. Hakim, A. Patel, L. Coluccio. Biol. Dept., RPI, Troy, NY 12181

Turn-off in the presence and absence of an osmotic gradient was examined using the glutaraldehyde fixation method of Eggena (Endocrinology 91:240, 1972). This method allows the ADH water flow response to be fixed. Paired *Bufo marinus* hemibladders were stimulated (20mU/ml) for 30 minutes in the absence of an osmotic gradient. The serosal bathing solution in both bladder preparations was then replaced with ADH-free solution for either 15 or 60 minutes of ADH washout. During the washout the control was exposed to an osmotic gradient, while the experimental had its luminal solution replaced with fresh full-strength Ringer's and was thus never exposed to an osmotic gradient. The bladders were fixed at the end of the washout period and the osmotic water flow determined. With 0 min. of washout there was no difference between the two bladder preparations ( $6.29 \pm 0.59$  vs  $6.02 \pm 0.56$ ,  $N=6$ ,  $\text{mg} \cdot \text{cm}^{-2} \cdot \text{min}^{-1}$ ). After 15 or 60 min. of ADH washout, the control preparation, exposed to an osmotic gradient throughout the washout period showed essentially a complete turn off of the hormone response ( $1.11 \pm 0.47$  and  $1.10 \pm 0.24$ ,  $N=6$  respectively). However the bladder with no exposure to an osmotic gradient during 15 min. washout showed little turn-off ( $4.38 \pm 0.72$ ,  $N=6$ ). At 60 min. of washout there was a drop in the non-gradient hemibladder indicating that even in the absence of a gradient there is a slow decay of water flow during washout. Thus, the presence of a gradient, and presumably water flow, appears to be needed to cause the rapid turn-off of transbladder water flow upon ADH-washout.

**W-Pos9 TWO TYPES OF POTASSIUM CHANNEL IN THE BASOLATERAL MEMBRANE OF TURTLE COLON**

William J. Germann and David C. Dawson, Dept. of Physiology, Univ. of Michigan, Ann Arbor, MI 48109

Potassium currents across the basolateral membrane of turtle colon can be measured in tissues treated with serosal ouabain (to inhibit the Na/K ATPase) and mucosal amphotericin-B (to reduce the resistance and cation selectivity of the apical membrane) (Kirk et. al., Nature, 287:237, 1980). In the presence of an M to S K gradient (mucosal  $\text{K}_2\text{SO}_4$  Ringers) the nature of the basolateral K conductance was highly dependent on the serosal anion. In the presence of serosal Na Benzene Sulfonate Ringers  $I_{\text{sc}}^{\text{K}}$  was abolished by quinidine but when the serosal solution was NaCl Ringers  $I_{\text{sc}}^{\text{K}}$  was unaffected by this drug. Under these two conditions the basolateral membrane also differed markedly in its selectivity for K over Rb.  $I_{\text{K}}/I_{\text{Rb}} = 5.2$  with NaBS and  $I_{\text{K}}/I_{\text{Rb}} = 1.6$  with NaCl. Measurements of  $^{42}\text{K}$  fluxes showed that in either condition  $I_{\text{sc}}^{\text{K}}$  was equal to the net K flow but the ratios of the M to S and S to M rate coefficients differed under these two conditions.  $\lambda_{\text{ms}}^{\text{K}}/\lambda_{\text{sm}}^{\text{K}} = 5.52$  for the quinidine-sensitive conductance and  $\lambda_{\text{ms}}^{\text{K}}/\lambda_{\text{sm}}^{\text{K}} = 1.03$  for the quinidine-insensitive conductance. These results are consistent with the notion that the basolateral membrane of turtle colon can contain at least two populations of K channels which differ in their pharmacology, ion selectivity and degree of cation interaction. Anion substitution experiments showed that simply removing serosal chloride was not sufficient to induce the quinidine-sensitive K conductance. Furthermore, the quinidine-sensitive conductance was induced in the presence of serosal chloride under conditions thought to be associated with cell swelling, i.e. permeant mucosal anions or urea. This observation raises the possibility that induction of the quinidine-sensitive K conductance is a response to cell swelling (NIH support).

**W-Pos10** CHLORIDE MOVEMENT ACROSS THE BASOLATERAL MEMBRANE OF NECTURUS GALLBLADDER EPITHELIUM: EVIDENCE AGAINST ELECTRODIFFUSION. Richard S. Fisher, Walter Reed Army Institute of Research, Washington, D.C. 20307.

The relative Cl and K sensitivity of the basolateral membrane potential of the in vitro Necturus gallbladder epithelium was determined. Tissues were punctured with two conventional, glass microelectrodes to measure simultaneously the intracellular PD ( $V_{cs}$ ) and the voltage across the subepithelial connective tissue ( $V_{se}$ ). Increasing the serosal K concentration from 2.5 to 25 mM caused a rapid, monotonic depolarization of  $V_{cs}$  without changes of  $V_{se}$ . Reduction of serosal Cl concentration (98 to 8 mM) caused a transient change of  $V_{se}$ . Thus, the difference between  $V_{cs}$  and  $V_{se}$  more accurately reflected the basolateral membrane PD ( $V_c$ ) after Cl concentration changes. The changes of  $V_c$  were small and biphasic. Perfusion of a low ionic strength solution in the mucosal chamber eliminated the current loop which normally passes through the epithelium. Consistent with the notion that the basolateral PD changes under control conditions are attenuated by parallel pathways, the K-induced depolarization increased by 80% after breaking the current loop. The changes of  $V_c$  in response to Cl substitutions were not different from those of tissues bathed in control solution in the mucosal chamber. Thus, the basolateral membrane PD is relatively insensitive to changes of serosal Cl concentration. It is concluded that Cl movement across the basolateral membrane is not attributable to simple electrodiffusion, and Cl exit from these cells at this membrane is most likely electroneutral.

**W-Pos11** ANIONS MODULATE THE BASOLATERAL MEMBRANE POTASSIUM CONDUCTANCE IN TOAD URINARY BLADDER. Simon A. Lewis\*, A. Grant Butt, M. Joanne Bowler, John P. Leader\*, Anthony D.C. Macknight. Depts. of Physiology Yale Med. Sch. New Haven Ct. 06510\*; Otago University Dunedin, New Zealand.

Sodium transport across the toad urinary bladder is altered by replacement of serosal chloride. The direction of this change depends on the replacement anion. Gluconate decreases net  $Na^+$  transport (as indicated by a decrease in the short circuit current,  $I_{sc}$ ), transepithelial conductance ( $G_T$ ) and abolishes the inhibitory effect of serosal  $Ba^{+2}$  on  $I_{sc}$ . Acetate increases  $I_{sc}$ ,  $G_T$  and enhances the inhibitory effect of serosal  $Ba^{+2}$  on  $I_{sc}$ . Equivalent circuit analysis of the epithelium using nystatin (Lewis et al, J. Gen. Physiol. 70) yielded the following result: 1) the mean basolateral membrane electromotive force (e.m.f) was estimated as 31.5 mV for gluconate and 72.6 mV for acetate (cell interior negative). 2) there is a linear relationship between basolateral membrane conductance and e.m.f. 3) serosal  $Ba^{+2}$  addition to the nystatin treated preparations decreases basolateral membrane e.m.f only when acetate is the chloride replacement. Morphological analysis indicates that gluconate causes cell shrinkage and acetate cell swelling. We conclude that cell volume regulates basolateral membrane  $K^+$  conductance by activation/insertion (for swollen cells) or inactivation/withdrawal (for shrunken cells) of  $Ba^{+2}$  blockable  $K^+$  channels. (Supported by grant # AM20851 to S.A.L, and the New Zealand M.R.C)

**W-Pos12** STOPPED-FLOW KINETICS OF NON-ELECTROLYTE TRANSPORT THROUGH RENAL APICAL MEMBRANE VESICLES. A.S. Verkman, J.A. Dix and J.L. Seifter, Brigham and Women's Hospital, Boston, MA 02115 and Dept. Chemistry, S.U.N.Y., Binghamton, N.Y. 13901

The non-electrolyte permeability properties of brush border membrane vesicles (BBMV), prepared from rabbit renal cortex by Mg aggregation and differential centrifugation, were determined. The time course of BBMV volume change following a hypertonic osmotic shock, measured by 90° light scattering (550 nm), consisted of a rapid volume decrease due to water efflux (10-50 ms) followed by a slower volume increase due to non-electrolyte influx. Urea influx and efflux rates exhibited identical self-inhibition kinetics; a single exponential rate constant fitted to the slower time course, corresponding to urea transport, decreased from 0.45/s ([urea]=0), to 0.18/s ([urea]=1300 mM) at 37°C with a single site  $K_{1/2}$  ~1200 mM (37°C) and 630 mM (25°C). Urea, preincubated with BBMV, inhibited thiourea flux with  $K_{1/2}$  ~370 mM (37°C), while thiourea (800mM) accelerated urea flux three-fold. Urea transport was not altered by 1 mM amiloride, 1 mM furosemide, 200  $\mu$ M phloretin, 25  $\mu$ M DBDS, 1 M acetamide, 1 M ethylene glycol or 1 M glycerol. At 37°C, non-electrolyte permeabilities were (in cm/s  $\times 10^{-6}$ ): urea 0.8, thiourea 1.3, ethylene glycol 11, glycerol 0.6, formamide 15, acetamide 13 and butyramide 35. The urea reflection coefficient,  $\sigma$ , estimated from the interpolated external urea concentration at which no initial volume change occurs (internal BBMV volume contains 200 mM mannitol, an impermeant), was  $1.1 \pm 0.1$ , suggesting little interaction between BBMV water and urea transport pathways. These studies suggest BBMV urea transport is mediated by a symmetric, saturable carrier which may also mediate thiourea transport but is independent of osmotic water transport.

**W-Pos13** VISCOSITY AND LOCAL OSMOSIS IN FROG GASTRIC MUCOSA. L. Villegas (Intr. by L. Sananes) Instituto Venezolano de Investigaciones Científicas, IVIC, Apartado 1827, Caracas 1010A, Venezuela.

Non-stimulated frog (*Rana pipiens*) gastric mucosa was used to measure the effects of viscosity changes of the solution at the serosal surface on the transmucosal water filtration and diffusion. Viscosity of the solution was increased 3 times by adding 5.5 mM of dextran with a mean M.V.=18,100. Fluxes are expressed in  $\mu\text{l cm}^{-2} \text{ h}^{-1}$ . When isosmotic (220 mOsm) solutions were used at both surfaces the spontaneous  $9.3 \pm 0.4$  net water flux was reduced to  $7.0 \pm 0.9$  by addition of dextran at the serosal surface, being the difference  $\Delta\phi_{\text{iso}} = -2.3 \pm 0.7$  ( $P < 0.01$ ). When hyperosmotic (520 mOsm) solution was used at the mucosal surface the mean  $28.7 \pm 2.2$  net water flux, formed by the spontaneous and the osmotically induced fluxes, was reduced by addition of dextran at the serosal surface to  $25.0 \pm 1.7$ , being the difference  $\Delta\phi_{\text{hyper}} = -3.7 \pm 0.9$  ( $P < 0.01$ ). Addition of the osmotically induced flux does not significantly change the effect produced by the use of dextran ( $\Delta\phi_{\text{iso}} - \Delta\phi_{\text{hyper}} = 1.4 \pm 1.1$ ;  $P > 0.20$ ). THO diffusion permeability was measured and is expressed in  $10^{-7} \text{ cm sec}^{-1}$ . Two independent groups of experiments were performed to measure unidirectional water diffusion. Using isosmotic solution at both surfaces the serosal-to-mucosal diffusion permeability was  $855 \pm 58$ . After addition of dextran at the serosal surface the mean permeability was  $943 \pm 25$ , being the difference  $88 \pm 73$  ( $P > 0.20$ ). The mucosal-to-serosal diffusion permeability was  $979 \pm 76$  and  $812 \pm 45$  after addition of dextran, being the difference  $-167 \pm 41$  ( $P < 0.01$ ). From these results it is proposed that increments of the viscosity of the solution at the serosal surface reduce and even reverse (AJP: 226:1338, 1974) the transmucosal net water flux by changing the composition of the extracellular space content without any effect in the transmucosal permeability to water.

**W-Pos14** THE UNIQUE ADVANTAGES OF NETWORK THERMODYNAMICS OVER EQUIVALENT CIRCUITS FOR THE STUDY OF ION TRANSPORT IN EPITHELIA. D.C. Mikulecky and M.L. Fidelman, Box 551, MCV/VCU, Richmond, VA 23298.

The inadequacies of the equivalent circuit approach for modeling ion transport in epithelia are not yet obvious. Recent correspondence from the Renal Physiology program director and Physiology Study Section Secretary of the Division of Research Grants of NIH state that "...the network thermodynamic approach does not provide unique advantages over more conventional equivalent circuit analysis for the study of ion transport." Since these are behind the scenes statements of anonymous reviewers, it is important that this issue be opened once more to public scientific debate. In an earlier work (Biophys. J. 25:323-340, 1979) great pains were taken to demonstrate that network thermodynamics could do a number of significant things that no version of equivalent circuit analysis could do. To further establish this point a number of popular equivalent circuit models have been examined thoroughly to demonstrate their failings in describing ion transport through epithelia. In each case, it is shown that a network thermodynamic model can be demonstrated to solve the problem when the equivalent circuit failed. Areas in which the network thermodynamic approach handles problems insurmountable in equivalent circuits are: (1) coupling (2) volume flow. (3) nonlinearity (4) volume changes in compartments. (4) carrier and channel models in various membrane structures in the system. (6) regulation and control of pumps. (7) Feedback mechanisms (8) The movement of uncharged substances (coupled to ion transport). (9) Time dependent events.

**W-Pos15** BASOLATERAL OUABAIN, AMPHOTERICIN AND CYANIDE EFFECTS ON AMILORIDE-INDUCED CURRENT FLUCTUATIONS. T. Hoshiko, Robert A. Grossman, Dept. of Physiol., School of Medicine, and Stefan Machlup, Dept. of Physics, Case Inst. Technology, Case Western Reserve Univ., Cleveland OH 44106, U.S.A.

Earlier studies of amiloride-induced current fluctuations were carried out in the presence of high basolateral K in order to reduce the resistance and potential across the basolateral membrane (Lindemann and Van Driessche, Science 195:292,1977). We have compared the amiloride corner frequency ( $f_c$ ) when the *R. pipiens* abdominal skin is bathed in (115 mEq/l Na, 5 K) vs. (120 K), with sulfate as the anion. In 59 paired determinations, no significant difference was found at apical Na = 120 mEq/l. Thus high basolateral K under these circumstances seems unnecessary. We previously reported (Arch.Int.Physiol.Biochim.89:58,1981) that  $f_c$  was lower at high apical Na. This effect is small or absent when the basolateral surface is exposed to high K. To test the possibility that  $f_c$  was decreased because of increased intracellular Na in high basolateral Na,  $f_c$  was determined in the presence and absence of the inhibitors cyanide (N=39) and ouabain (N=37) which should increase intracellular [Na]. We found no significant difference in  $f_c$  in paired comparisons. Of course current and plateaus were decreased. Moreover, a water-soluble preparation of amphotericin B added to the basolateral bathing solution in 115 Na had no significant effect on  $f_c$  (N=50), but in 120 K, addition of amphotericin B significantly increased  $f_c$  (N=53). These results suggest that basolateral K may affect more than simply the electrical properties of the basolateral membrane. (Supported by PHS grant AM5865).

**W-Pos16** ONE-SITE VS TWO-SITE CLOGGING MODELS FOR SODIUM CHANNELS IN EPITHELIA: SHORT-CIRCUIT CURRENT AND NOISE.

Stefan Machlup, Dept. of Physics, and T. Hoshiko, Dept. of Physiology, Case Western Reserve University, Cleveland, OH 44106.

Sodium-induced "channel clogging" is analyzed as the mechanism of short-circuit current saturation as well as of the "sodium noise" in the apical membrane. Define a clogging transition as a configurational change triggered by one or more  $\text{Na}^+$  ions which closes the sodium channel. If one  $\text{Na}^+$  at one binding site suffices for triggering, then the short-circuit current  $I_{sc}$  has Michaelis-Menten form, i.e., it is linear in apical  $[\text{Na}]$  at low  $[\text{Na}]$  and bends over monotonically to an asymptote at high  $[\text{Na}]$ . The noise power curve has a  $[\text{Na}]^3$  foot, a point of inflection, and an asymptote. On the other hand, if cooperation of more than one  $\text{Na}^+$  ion is needed, e.g., if the clogging transition is triggered by two  $\text{Na}^+$  at two binding sites, the predicted  $I_{sc}$  has a peak, then falls to a finite asymptote as apical  $[\text{Na}]$  is increased.  $[\text{Na}]^2$  terms occur in numerator and denominator. The noise power has a  $[\text{Na}]^4$  foot, peaks, and goes to zero at high  $[\text{Na}]$ . 3-site models have  $[\text{Na}]^3$  terms in the  $I_{sc}$  formula, and n-site models have  $[\text{Na}]^n$ , with curve shapes much like the 2-site. The  $I_{sc}$  peak reported by Benos *et al* (J.Gen.Physiol. 81:667-685 (1983)) in bullfrog skin may rule out 1-site clogging. [Supported by USPHS Grant AM 05865]

**W-Pos17** Single K<sup>+</sup> channels behaviour during voltage step. E. Rousseau, M.D. Payet and R. Sauvé, Département de Biophysique, Univ. de Sherbrooke, J1H 5N4 and Département de Physiologie, Univ. de Montréal, H3T 1J7, Canada.

Currents from single K<sup>+</sup> channels were recorded on freshly isolated myocardial cells from newborn rats. The experiments were performed at 22°C in Mc Ewen solution with KCl filled pipettes: 10.8, 75, 150 and 300 mM. The channel shows inward rectification with a 25 to 30 pS conductance insensitive to [K]<sub>o</sub>. No outward currents were recorded with 150 or 300 mM KCl filled pipettes. The channel kinetic is voltage and [K]<sub>o</sub> dependent as demonstrated by the linear relation between  $\log(P_o/1-P_o)$  and membrane voltage. The  $\log(P_o/1-P_o)$ -V curves has a positive slope which is reduced as [K]<sub>o</sub> is lowered. At high [K]<sub>o</sub> (150 mM KCl) and positive voltages above the zero current voltage the probability to find the channel in the open state is near unity. Voltage pulses were applied during the channel opening or closing, to test that hypothesis. The voltage was abruptly changed from a membrane potential of -70 mV to potentials negative or positive toward the zero current voltage level (0 mV). Behaviours of the channel at the onset, during and at the offset of the pulse were analysed. We conclude that the rate constants of the channel are instantaneously changed according to the new voltage but that the channel state (open or closed) is not an instantaneous function of voltage.

Supported by MRC, FQMC, FCMC and FRSQ.

**W-Pos18** KINETIC PROPERTIES OF SINGLE CA-ACTIVATED POTASSIUM CHANNELS ACTIVATED BY STRONTIUM IONS. Owen B. McManus and Karl L. Magleby, Dept. of Physiology and Biophysics, Univ. Miami School of Medicine, Miami, FL 33101.

The patch clamp technique was used to study the kinetic properties of single Ca-activated K channels from cultured rat muscle cells. At +30 mV, the [Sr]<sub>i</sub> required for the channel to be open 10% of the time (100 μM) was ~200 times the [Ca] required for the same level of activity. Hill plots suggested a power of 1.2-2 for the relationship between the percent of time a channel was open and [Sr]<sub>i</sub>, indicating that two or more Sr ions are typically bound for channel opening. The distribution of all open intervals observed during 100 s of data in 100 μM Sr at +30 mV was described by the sum of two exponentials suggesting a minimum of two open states. The distribution of all shut intervals during the same segment of data was described by the sum of four exponentials, suggesting a minimum of 4 closed channel states. The channel readily enters three of these closed states during normal activity. The fourth state most likely represents an inactivated state. The mean number of openings/burst for this data was 2.3. The distributions of open and shut intervals in 0.5 μM Ca, were similar to those observed in 100 μM Sr, where the percent of time open is similar. These observations suggest that the decreased efficacy of Sr in activating the channel, when compared to Ca, is mainly due to a marked decrease in the forward rate constant for Sr binding, and not from marked changes in channel kinetics after Sr is bound. Supported by grants AM 32805 from NIH and a grant from the Muscular Dystrophy Association to KLM. OBM is a recipient of a Muscular Dystrophy Fellowship.

**W-Pos19** ION CONDUCTANCE AND SELECTIVITY OF SINGLE CALCIUM-ACTIVATED POTASSIUM CHANNELS IN CULTURED RAT MUSCLE. Andrew L. Blatz and Karl L. Magleby, Department of Physiology and Biophysics, University of Miami School of Medicine, Miami, FL 33101.

Shifts in reversal potential of single channel currents when various cations were substituted for K<sub>i</sub> were used with the Goldman-Hodgkin-Katz equation to calculate relative permeabilities. The selectivity was Tl > K > Rb > NH<sub>4</sub>, with permeability ratios of 1.2, 1.0, 0.67, 0.11. Na, Li, and Cs were not measurably permeant, with permeabilities < 0.05 that of K. Currents with the various ions were typically less than expected on the basis of the permeability ratios suggesting that the movement of an ion through the channel was not independent of the other ions present. With 100 mM K<sub>o</sub> plots of single channel conductance and current vs. activity of K<sub>i</sub> were described by a simple two barrier model with a single saturating site with an empirically determined dissociation constant of 100 mM. At most, only one ion occupied the channel at any time in this model. The maximum calculated conductance for symmetrical solutions of K was 640 pS. TEA, (tetraethylammonium ion) reduced single channel current amplitude in a voltage dependent manner. This effect was accounted for by assuming voltage dependent block by TEA (apparent dissociation constant of 60 mM at 0 mV) at a site located 26% of the distance across the membrane potential starting at the inner side. TEA was much more effective in reducing single channel currents, with an apparent dissociation constant ~ 0.3 mM. Supported by grants NS 07044, NS 10277, AM 32805, and NS 12207 from the National Institutes of Health, and a Grant from the Muscular Dystrophy Association.



**W-Pos20** VOLTAGE-SENSITIVE K<sup>+</sup> CHANNEL CURRENTS IN THE SOMAL AND DENDRITIC MEMBRANE OF CULTURED CEREBELLAR PURKINJE NEURONS. D.L. Gruol, A.V. Davis Center for Behavioral Neurobiology, The Salk Institute, P.O. Box 85800, San Diego, CA 92138.

Anatomical and electrophysiological evidence suggest that on a cellular level CNS neuronal function is regionally specialized both with respect to the type of synaptic input and the intrinsic electrical capabilities of the neuronal membrane. We are exploring these topographic differences in a well characterized CNS neuronal type, the cerebellar Purkinje neuron (PN). Initial studies have focused on identifying the intrinsic ionic mechanisms which underlie the electrical capabilities of the somatic and dendritic membrane. To facilitate these studies, an in vitro model system, cultured PNs, was used in conjunction with the "gigaohm seal" patch clamp technique. Cell-attached and outside-out recording configurations were used. In the somal membrane, channel activity mediating outward currents appears to result from 3 different types of voltage-sensitive K<sup>+</sup> channels, identified by their single channel conductance, voltage sensitivity and sensitivity to TEA, a K<sup>+</sup> channel blocker. One channel type, thought to be a Ca<sup>++</sup> activated K<sup>+</sup> channel, has a single channel conductance around 100 pS and is blocked by 1 mM TEA. The second channel type has a single channel conductance of 40 pS and is blocked by 10 mM TEA. The third channel type has a single channel conductance of 20 pS and is resistant to 10 mM TEA. Voltage-sensitive K<sup>+</sup> channels, including one similar to the somal Ca<sup>++</sup> activated K<sup>+</sup> channel, were also identified in the dendritic membrane. In both regions K<sup>+</sup> channel activity was associated with the falling phase of spontaneous action potentials, suggesting a role in the repolarizing phase of the action potential. These data suggest that Ca<sup>++</sup> and K<sup>+</sup> mediated electrical events occur in both the somatic and dendritic regions of PNs. (Supported by NIAAA 03504)

**W-Pos21** CHARACTERIZATION OF K CURRENTS RECORDED BY PATCH ELECTRODE VOLTAGE CLAMP IN GH<sub>3</sub> CELLS. F. Barros, G. Katz, R. Vandlen, G. Kaczorowski and J. P. Reuben. Merck Institute for Therapeutic Research, Rahway, N.J. 07065

This study was undertaken in view of the report that thyrotropin-releasing hormone (TRH) attenuates K currents in GH<sub>3</sub> cells (Kaczorowski et al. 1983, J. Mem. Biol. 71; 109). In order to ascertain whether TRH acts on the early transient K current (I<sub>K<sub>v</sub></sub>) or a slowly developing K current (I<sub>K<sub>Ca</sub></sub>) criteria have been established for identifying and separating the outward currents in GH<sub>3</sub> cells (see Dubinsky and Oxford 1982, Soc. Neurosci. Abstr.; Katz et al. these Abstr.). When the patch electrode contains 140 mM KCl or 80 mM K<sub>2</sub>SO<sub>4</sub>, 0 EGTA, 2 mM MgCl<sub>2</sub>, 5 mM HEPES, pH 7.3, and 0.5 to 2.0 mM tetrabutylammonium (TBA) I<sub>K<sub>v</sub></sub> is reduced to a brief transient (see Katz et al., this Abstr.), and inward Ca currents are observed followed by large (200 to 1000 pA for -60 to 0 mV pulses) outward I<sub>K<sub>Ca</sub></sub>. Starting with 100 msec pulses (-60 to 0 mV) I<sub>K<sub>Ca</sub></sub> increases with pulse duration (up to ~ 700 msec) and with pulse frequency. This late current is reduced (< 100 pA) by adding 5-10 mM EGTA to the electrodesolution or by lowering Ca<sup>2+</sup> from 10 to 0.1 mM. Furthermore, I<sub>K<sub>Ca</sub></sub> approaches zero at potentials near the apparent Ca reversal potential (E<sub>Ca</sub>; +70 to +90 mV). A high noise level is another characteristic of I<sub>K<sub>Ca</sub></sub>. To study I<sub>K<sub>v</sub></sub>, cells are bathed in TEA, and EGTA (5-55 mM) is added to the TBA-free electrode solution. In some cells, I<sub>K<sub>v</sub></sub> is totally inactivated (-60 to 0 mV) after ~ 400 msec and reactivates slowly (~ 30 sec) at -60 mV. This property of I<sub>K<sub>v</sub></sub> has been used to separate it from I<sub>K<sub>Ca</sub></sub>. TRH attenuates I<sub>K<sub>Ca</sub></sub> and shifts (10 to 30 mV) E<sub>Ca</sub> to more positive potentials. This suggests that Ca bound to the inner membrane surface is reduced.

**W-Pos22** BLOCKAGE OF K CURRENTS BY QUATERNARY AMMONIUM (QA) IONS IN GH<sub>3</sub> CELLS UNDER PATCH ELECTRODE VOLTAGE CLAMP. G. Katz, F. Barros, G. Kaczorowski, R. Vandlen and J. P. Reuben, Merck Institute for Therapeutic Research, Rahway, N.J. 07065

Two overlapping K currents, an early transient one (I<sub>K<sub>v</sub></sub>) and a slowly developing outward current (I<sub>K<sub>Ca</sub></sub>) (-35 to +100 mV) have been identified (see Dubinsky and Oxford, 1982, Soc. Neurosci. Abstr. and Barros et al. these Abstr.). Addition of QA ions to either the intracellular or extracellular medium is one means for separating I<sub>K<sub>v</sub></sub> from I<sub>K<sub>Ca</sub></sub>. Under the condition with 5-10 mM EGTA, 140 mM KCl or 80 K<sub>2</sub>SO<sub>4</sub>, 2 mM MgCl<sub>2</sub>, 5 mM HEPES, pH 7.3 in the electrode and 25 mM TEA in the bathing solution, I<sub>K<sub>Ca</sub></sub> is blocked and I<sub>K<sub>v</sub></sub> attains peak values of 500-2000 pA (-60 to + 80 mV) which inactivate with  $\tau_{1/2}$  of ~ 100 msec. Within ~ 10 sec following disruption of the membrane patch, TBA in the electrode (0.5 to 2.0 mM) rapidly reduces I<sub>K<sub>v</sub></sub> to a brief transient ( $\tau_{1/2}$  ~ 10 msec.) and attenuates the peak current to 50-300 pA. Higher concentrations of TEA (20 to 50 mM) are required to obtain comparable results. I<sub>K<sub>v</sub></sub> is not affected in cells bathed in TEA or TBA for several minutes. I<sub>K<sub>Ca</sub></sub> (maximized by deleting EGTA from the electrode), however, is blocked rapidly following external application of QA ions, but the order of effectiveness is reversed. TEA acts in a range from 2 to 30 mM whereas TBA at 10 mM has essentially no effect on I<sub>K<sub>Ca</sub></sub>. The blockage of I<sub>K<sub>Ca</sub></sub> by QA ions also possesses a defined polarity; high intracellular concentrations of QA ions do not effect I<sub>K<sub>Ca</sub></sub>. When QA ions are present and essentially all K currents are blocked, large inward Ca currents (up to 1000 pA in a 20  $\mu$  cell) are revealed whose reversal potentials range from +70 to +90 mV.

**W-Pos23** A POTASSIUM CHANNEL THAT OPENS DURING THE CARDIAC ACTION POTENTIAL. R. Levi and L. J. DeFelice, Dept. of Anatomy, Emory University, Atlanta, Georgia 30322

We are studying membrane currents in cell-attached patches during spontaneous action potentials in ventricular cells from 7-day chick embryo (top figure). The preparation was bathed in 3.5 K/100 Na/1.5 Ca buffered with HEPES at pH 7.35 and 23°C. The patch pipette solutions were either the bathing solution or 100 K/38 Na/EGTA. With both we observed fast outward pulses of current (bottom figure) during the plateau and repolarization of action potentials that reversed during the diastolic part only with high K solution. The *i(V)* curve of this channel was obtained by plotting the open channel current against an action potential. In 3.5 K solution *i(V)* showed a linear portion with a slope and a reversal potential of about 60 pS and 75 mV. This channel seems to be the same one studied by Clapham and DeFelice (*Biophys. J.* 45), which has properties in common with the delayed rectifying current.

Supported by NIH grant HL27385.

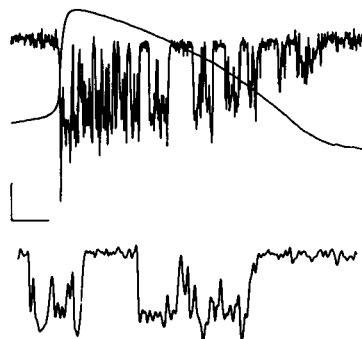
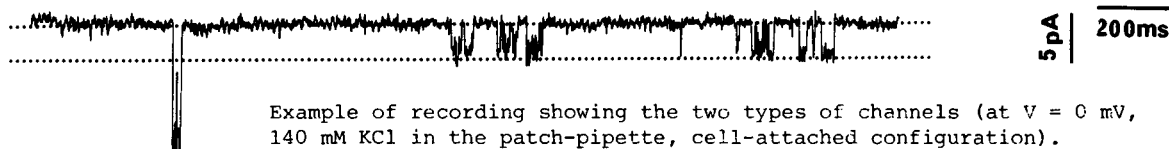


(Fig.: 3.5 K pipette solution. VERTICAL: 2.5 pA or 25 mV  
HORIZONTAL: 40 mS. (TOP) 6 mS. (BOTTOM) OUTWARD CURRENT IS DOWN.)

**W-Pos24** IONIC CHANNELS IN MOUSE EMBRYONIC MULTIPOTENTIAL CARCINOMA CELLS.

Michel Simonneau. Département de Biologie Moléculaire, Institut Pasteur, 75015 Paris & Laboratoire de Neurobiologie Cellulaire, CNRS, 91190 Gif sur Yvette, France. (Intr. by Y. Pichon).

Single channels currents were recorded with the patch-clamp technique from mouse embryonic multipotential carcinoma (E.C.) cells which have been extensively used for the studies of early mammalian embryogenesis (Jacob, F., 1978 *Proc. Roy. Soc. London B*, 201, 249-270). High resolution measurements of ionic currents were obtained using whole cell clamp and cell-attached patch recording configurations. Non-differentiated 1003 E.C. cells present two types of voltage-dependent unit currents which have been identified as: (1) a Ca<sup>++</sup> activated K<sup>+</sup> channel. This channel has characteristics (as slope conductance, ionic selectivity, effect of cytoplasmic Ca<sup>++</sup>, kinetics and pharmacology) similar to those described for other Ca<sup>++</sup> activated K<sup>+</sup> channels; (2) a less frequent second class of unitary current of larger conductance (450 pS at 0 mV holding potential, when the patch pipette contained 140 mM KCl, cell-attached configuration), identified as a Cl<sup>-</sup> channel. Single channel recordings were also obtained under whole cell clamp configuration, suggesting a low density of channels. (Supported in part by M.I.R. grant n°8299 and Fondation pour la Recherche Médicale Française).



Example of recording showing the two types of channels (at V = 0 mV, 140 mM KCl in the patch-pipette, cell-attached configuration).

**W-Pos25** SINGLE CHANNEL RECORDING FROM BILAYERS DERIVED FROM ISOLATED SEA URCHIN PLASMA MEMBRANES FORMED AT THE TIP OF A PATCH ELECTRODE. A. Darszon, A. Liévano and J. Sánchez. Depts. of Biochem. and Neuroscience, CINVESTAV-IPN, Mexico City.

Changes in the plasma membrane permeability of equinoderm sperm play a fundamental role in the acrosome reaction. This process, a prerequisite for fertilization, involves a complex series of events. The reaction in vivo is triggered by a glycoprotein "jelly" surrounding the egg, which induces among other aspects, an increase in the intracellular levels of Ca<sup>++</sup> and Na<sup>+</sup> and an efflux of H<sup>+</sup> and K<sup>+</sup>. Using the patch clamp technique (Hamill et al, 1981), we obtained gigaseals by forming bilayers at the tip of a patch electrode (Wilhelm, 1982) from a monolayer derived from a mixture of lipid vesicles and sea urchin sperm plasma membranes (12-50 µg protein/ml) isolated according to Cross (1982). The external solution was Mg<sup>++</sup> free artificial sea water containing 5 mM CaCl<sub>2</sub>. The patch electrode contained the same media without CaCl<sub>2</sub>.

Currents were recorded using a 10GΩ resistance and voltage steps in the ± 100 mV range for 10-20 sec were applied. The signal was stored on magnetic tape in analog form and later analyzed by microcomputer. Single channel currents were observed in almost every membrane formed. Various channels with different conductances (100 and 140 pS) and lifetimes were recorded. I/V curves show a linear conductance for the currents we have analyzed. Substitution of Na<sup>+</sup> for TMA in one experiment did not change the reversal potential indicating that Na<sup>+</sup> is not the main permeant ion. This is consistent with data obtained on whole sea urchin sperm where the membrane potential appears to be determined by K<sup>+</sup>. This was partially supported by CONACyT and NSF grants.

**W-Pos26** PHARMACOLOGY OF VOLTAGE-GATED K CHANNELS IN NEUROBLASTOMA CELLS. Fred N. Quandt, Dept. of Medical Physiology, University of Calgary, Faculty of Medicine, Calgary, Alta., Canada T2N 1N4.

Membrane patches of N1E-115 cells exhibit three classes of voltage-gated open states giving rise to outward current in response to depolarization. All three are considered to be K channels, since each became nonconducting when K was substituted with Cs. The three classes could be distinguished on the basis of conductance. One class exhibited a conductance of 10-12 pS (150 mM K/5 mM Cs, 10°C), while a second class exhibited a lower conductance of 3-4 pS. A third class of open state had a conductance of up to 100 pS. The high and medium conductance open states have a different pharmacology since the internal application of 100 μM 4-aminopyridine (4-AP) blocked the current due to the latter, while 0.5 mM 4-AP did not block the former state. The medium and low conductance states have a similar pharmacology since both types were blocked by the internal application of either 100 μM 4-AP or 1 mM Ba, or by the external application of 15 mM tetraethylammonium (TEA). In contrast to external TEA, internal application of TEA caused a concentration-dependent reduction in conductance of the open state for either medium or high conductance open states. 15 mM TEA produced a 30% decrease in open channel conductance. The 100 pS open state likely represents the opening of "Ca-dependent K-channels" which contribute to voltage-clamp currents recorded from whole N1E-115 cells. The similar pharmacology of the medium and low conductance open states suggests a common state having receptor sites for blockers. The medium and low conductance open states would then represent multiple open states for a single type of delayed-rectifier K channel. Supported by the Alberta Heritage Foundation for Medical Research and the Medical Research Council of Canada.

**W-Pos27** ELECTROGENIC MECHANISMS OF SLOW EXCITATORY POTENTIALS IN BULLFROG SYMPATHETIC GANGLIA. Stephen W. Jones and Paul R. Adams. Dept. Neurobiology & Behavior, SUNY at Stony Brook, NY 11794.

The large B cells of bullfrog sympathetic ganglia have both slow muscarinic and "late, slow" peptidergic EPSPs. Single electrode voltage clamp analysis of either slow potential shows two underlying mechanisms: (1) an inward current due to inhibition of the M-current, a voltage-dependent  $K^+$  current that is activated by depolarization in the region between rest and threshold, and (2) an additional inward current, associated with an increased conductance with a positive reversal potential. The proportion of the two currents varies from cell to cell; some cells show only M-current inhibition.

The combined B and C cell inputs were stimulated by a suction electrode on the preganglionic trunk above the 8th or 9th ganglion. Slow EPSCs resulted from trains of 1-4 V stimuli. Stimulation for 2 sec at 50 Hz produced 53±3% M-current inhibition (mean±sem, 14 cells, 6 frogs). Longer trains produced up to 90% M-current inhibition. Short trains could produce 1-5% M-current inhibition per stimulus, and slow EPSCs were occasionally observed to single stimuli. Late, slow EPSCs were obtained from trains at 10-40 V in the presence of 1  $\mu$ M atropine. Stimulation for 4-5 sec at 10 Hz produced 49±5% M-current inhibition (13 cells, 4 frogs). For comparison, the  $I_{50}$  for bath application of teleost LHRH, the putative transmitter for the late, slow EPSP, was 0.35  $\mu$ M. LHRH antagonists block the M-current inhibition due to the late, slow EPSP. Late, slow EPSCs appear to be faster and smaller in ganglia that have been treated with trypsin.

(Supported by NIH grant NS 18579 and an NIH Postdoctoral Fellowship to SWJ.)

**W-Pos28** BLOCK OF SINGLE ACETYLCHOLINE-ACTIVATED CHANNELS BY GUANIDINE DERIVATIVES. Stephen M. Vogel, Jerry M. Farley, and Toshio Narahashi. Northwestern Univ. Med. Sch., Chicago, IL and Univ. of Mississippi Med. Center, Jackson, MS.

Methyl- and ethylguanidine ( $C_1$  and  $C_2$ ) have been shown to preferentially block inward end-plate currents (Farley et al., 1981, *J. Gen. Physiol.* 77, 273) in a manner dependent on the direction of the current (Vogel et al., *J. Gen. Physiol.*, in press). To further characterize the block, we have examined the actions of  $C_1$  and  $C_2$  on currents through single acetylcholine-activated ionic channels in membrane patches excised from cultured chick myotubes. Both inside-out and outside-out patches were formed, allowing drug to be applied either internally (cytoplasmic membrane) or externally. The single channel current-voltage relationship was linear from -100 to +100 mV in symmetrical internal and external Cs solutions. The single channel conductance was 42 pS in 120 mM Cs and 54 pS in 360 mM Cs.  $C_1$  (10 or 20 mM) and  $C_2$  (2 mM) applied externally (120 mM Cs) markedly depressed inward currents. At -100 mV,  $C_1$  and  $C_2$  decreased the amplitude of the single channel currents by 50 to 70%.  $C_2$  was without effect on outward currents, whereas  $C_1$  caused a small reduction. When applied internally,  $C_2$  blocked outward-going currents, but exerted no effect on inward currents. The degree of block was similar for internally and externally applied  $C_2$ . Raising the internal Cs concentration to 360 mM completely removed the blocking effect of internally applied  $C_2$ . In summary, (1)  $C_1$  and  $C_2$  reduce the conductance of single channels; this explains at least partially the block of inward end-plate currents in the frog caused by  $C_1$  and  $C_2$ ; (2) the block can be antagonized by Cs; and (3) the block is symmetrical for internally and externally applied  $C_2$ , implying that the energy profile in the channel is symmetrical.

**W-Pos29**  $Ca^{++}$  MEDIATED OPENING OF  $K^+$  CHANNELS IN CILIARY GANGLION CELLS EVOKED BY ACh. J.M. Tang and D.J. Nelson; Department of Physiology, Rush Medical College, Chicago, Illinois 60612.

Properties of the response of nicotinic receptors to ACh in parasympathetic ganglion cells were studied in cultured ciliary ganglion neurons using whole cell and single channel recording techniques. The response of the somal membrane to ACh obtained in whole cell recordings was an immediate decrease in cell input resistance from an average of 71 M $\Omega$  to 38 M $\Omega$ . The ACh-dependent conductance increase is due to a  $K^+$  current with a reversal potential at approximately 60 mV in a 12.5 mM  $K^+$  solution. On-cell and excised patch clamp records in the absence of ACh revealed two different types of  $Ca^{++}$ -activated  $K^+$  selective channels (344 pS and 232 pS in symmetrical high  $K^+$  solutions) exhibiting different sensitivities to  $Ca^{++}$  and membrane potential. For clarity we termed the larger conductance the  $Ca^{++}$ -activated  $K^+$  channel and the smaller, the voltage sensitive  $K^+$  channel. Single channel currents were observed in on-cell membrane patches from  $K^+$  depolarized cells prior to and during micropipette application of ACh onto the somal membrane outside the patch area. The probability of opening  $Ca^{++}$ -activated  $K^+$  channels and to a lesser degree, voltage sensitive- $K^+$  channels increased significantly following ACh application; activation of both channels was blocked by the removal of  $Ca^{++}$  from the bath. ACh activation was blocked by the presence of 25  $\mu$ M D-600 and 30  $\mu$ M D-tubocurarine but not by 100 nM atropine in calcium containing solutions. No increase in channel activity was observed following micropipette application of ACh to the extracellular membrane surfaces of outside-out patches. The results demonstrate that ACh controls ion channel opening in isolated ciliary ganglion neurons indirectly via an intracellular messenger presumed to be calcium. Supported by NIH Grant NS18587.

**W-Pos30** EFFECT OF ANTIRECEPTOR MONOCLONAL ANTIBODIES ON SINGLE CHANNEL CURRENTS OF PURIFIED ACETYLCHOLINE RECEPTOR RECONSTITUTED IN LIPID BILAYERS. Y. Blatt<sup>†</sup>, M.S. Montal<sup>†</sup>, J. Lindstrom<sup>\*</sup> and M. Montal<sup>†</sup>. University of California at San Diego<sup>†</sup> and The Salk Institute<sup>\*</sup>, La Jolla, CA 92093.

Purified acetylcholine receptor (AChR) from *Torpedo californica* electric organ, composed of  $\alpha_2\beta\gamma\delta$ , was reconstituted, first into lipid vesicles and subsequently into planar lipid bilayers formed both in a teflon aperture [1] or at the tip of patch pipets [2]. The effect of subunit specific monoclonal antibodies (mAbs) [3] on single channel currents activated by ACh (1-10  $\mu$ M) was tested. MABs were added to the same compartment as ACh both before or after the agonist. MAB 35 and mAb 6 raised against intact AChR [4] and reactive with the  $\alpha$ -subunit main immunogenic region altered neither the single channel conductance nor the channel open lifetimes. In contrast, mAb 10, generated against  $\beta$ -subunit but reactive also with  $\alpha$ -subunits, inhibited single AChR channels. Screening the activity of the existent library of anti-AChR mAbs directed against distinct AChR subunits and subunit domains may provide an assay for the functional role of the AChR subunits in channel function. [1] Nelson, et al., PNAS, 77: 3057 (1980); [2] Suarez-Isla, et al., Biochemistry, 22:2319 (1983); [3] Tzartos & Lindstrom, PNAS, 77:755 (1980); [4] Tzartos, et al., J. Biol. Chem., 256:8635, (1981). Supported by DAMR, NIH and MDA.

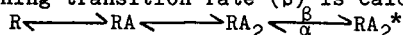
**W-Pos31** FOURIER TRANSFORM INFRARED SPECTROSCOPY OF THE NICOTINIC ACETYLCHOLINE RECEPTOR FROM *TORPEDO CALIFORNICA*, Thomas N. Earnest and Kenneth J. Rothschild, Departments of Physics and Physiology, Boston University, Boston, MA 02215

Fourier transform infrared (FTIR) spectroscopy can be used to probe aspects of the structure and function of biomembrane components. The infrared vibrational modes are sensitive to various parameters such as hydration, membrane fluidity, temperature and isotopic labeling. Information can be obtained about membrane protein secondary structure as well as the orientation of specific protein components such as  $\alpha$ -helices. In addition, it has recently been demonstrated that individual groups in a membrane undergoing conformational change can be detected and characterized (K.J. Rothschild and H. Marrero, Proc. Natl. Acad. Sci. USA 79, (1983) and K.J. Rothschild, W.A. Cantore and H. Marrero Science 219, 1333 (1983)). We have performed FTIR spectroscopy on acetylcholine receptor (AChR) enriched membranes from *T. californica* which have been incorporated into well oriented multilamellar films. In the dehydrated state, these films exhibit peaks at 3296  $\text{cm}^{-1}$  (NH stretch), 1657  $\text{cm}^{-1}$  (C=O stretch) and 1543  $\text{cm}^{-1}$  (NH bending) which correspond to the amide A, I and II modes, respectively. These frequencies correspond to those found for predominantly  $\alpha$ -helical proteins such as rhodopsin. However, hydration and hydrogen-deuterium exchange produce peak shifts which indicate the presence of  $\beta$ -structure which is exposed to the aqueous environment. The implication of these results will be discussed in terms of current models of AChR structure. (We thank G. Hess of Cornell University for the AChR enriched membranes. This work was supported by a grant from the AHA to KJR)

**W-Pos32** KINETICS OF AChR CHANNELS IN A MUSCLE CELL LINE. S. Hestrin, J.I. Korenbrot, and A.V. Maricq. Dept. of Physiology, U.C.S.F., S.F., CA 94143.

We have recorded single channel events, in the presence of ACh, from the membranes of myotubes of a mouse skeletal muscle cell line (c2). Recordings either "on-cell" or "inside out", were within the first week following myotube formation. Generally, the ACh sensitivity was uniform over the cell membrane surface. Current amplitude histograms indicated that the unitary channel events belong to a single channel type.

At low agonist concentrations (range: 0.2-1.0  $\mu$ M), the histograms of the closed time intervals could be fit with three exponents. The fast exponent of the fit (range: 0.1-0.2 msec) corresponded to the brief gaps which separate openings within a burst. We found that only 10-20% of the bursts contained a gap. If the gaps arise from a shut state which the channel occupies just before opening, then the opening transition rate ( $\beta$ ) is calculated to be 1000-2000  $\text{sec}^{-1}$



The above model for AChR activation predicts that as the agonist concentration increases the mean closed time interval would converge to the opening transition ( $\beta$ ). Under high agonist concentration (10-100  $\mu$ M), we observed bursts of activity which contained several openings in rapid succession. Histograms of the closed time intervals were fitted with a multiexponential function. The majority (50-80%) of the closed time intervals belonged to a fast exponent. The time constant of that exponent became shorter as the agonist concentration increased. It appears then that  $\beta$  is as fast as 8000  $\text{sec}^{-1}$  (or faster). The discrepancy of the calculated  $\beta$  under low and high agonist, will require a modification of the model.

**W-Pos33** Structural Studies of the Acetylcholine Receptor from *Torpedo nobiliana*

David G. Rhodes<sup>1</sup>, R. Preston Mason<sup>1</sup>, Yvonne M. H. Vant Erve<sup>1</sup> and Leo G. Herbet<sup>1,2</sup>,  
U. of Conn. Health Center, Departments of Medicine<sup>1</sup> and Biochemistry<sup>2</sup>, Farmington, CT 06032.

Acetylcholine receptor membranes were isolated from *Torpedo nobiliana* electroplax tissue and purified on a sucrose density gradient. A fraction from this gradient had a lipid to protein ratio of  $0.81 \pm 0.23$  (SD) umoles phosphorus per mg protein, and a receptor content equal to  $41 \pm 2\%$  of the total protein based on capacity for binding [<sup>125</sup>I]- $\alpha$ -bungarotoxin. Fluorescence measurements of these preparations were made in the absence and presence of carbamylcholine and  $\alpha$ -bungarotoxin. Addition of carbamylcholine caused no detectable change in the intrinsic fluorescence. If the fluorescence was enhanced with quinacrine, however, addition of carbamylcholine caused a decrease in the fluorescence maximum at 334 nm, but no consistent change in the maximum at 500 nm. The concentration dependence of the fluorescence changes indicated that these effects are ligand specific and that the apparent dissociation constant is 0.1  $\mu$ M. Addition of  $\alpha$ -bungarotoxin causes a large increase in the fluorescent intensity at 334 nm, again with inconsistent results for the maximum at 500 nm. The effects with carbamylcholine were qualitatively reproduced in partially dehydrated, oriented multilayers of receptor enriched vesicles by atomizing the multilayers with concentrated carbamylcholine solutions. Lamellar x-ray diffraction data has been obtained from these multilayers, and preliminary studies indicate that a photoactivated agonist could replace the atomizing technique, allowing these techniques to be combined for use in kinetic measurements. This combination will allow detailed investigation of the interaction of drugs with membrane bound receptors. (Supported by NIH HL-27630, NIH HL-07420 and the American Heart Association)

**W-Pos34** Mechanism for Cardiovascular Drug Binding to Membrane Associated Receptors: Approach to the Binding Site Through the Lipid Bilayer. L. G. Herbet<sup>1,2</sup>, J. G. Sarmiento<sup>1</sup> and D. G. Rhodes<sup>1</sup>, U. Conn. Health Center, Depts. of Medicine<sup>1</sup> and Biochemistry<sup>2</sup>, Farmington, CT 06032.

Several observations have been made in this laboratory regarding interactions of cardiovascular drugs with receptors in the cardiac sarcolemmal membrane: (1) The receptor site density is very low, approximately one site per square micron. (2) Many cardiovascular drugs that interact with these membrane associated receptor sites are very lipid soluble and some are amphiphilic. (3) For one such drug, propranolol (a beta blocker), neutron diffraction measurements showed that the primary nonspecific site of interaction was the lipid bilayer of the sarcoplasmic reticulum membrane. In view of these findings, the binding data for radiolabelled dihydropyridine calcium channel blockers was interpreted in terms of a kinetic mechanism. The measured forward rate constant for the binding of nitrendipene to the high affinity sarcolemmal membrane site is  $10^6$ - $10^7$ (Ms)<sup>-1</sup>. The maximum forward rate constant calculated for the model of a small isotropic drug approaching a receptor site on a vesicle through bulk solvent was found to exceed the measured rate by about  $10^2$ . A relation was derived to predict the maximum forward rate constant for a two-stage mechanism which involves partition of the drug into the membrane followed by lateral diffusion of the drug through the lipid bilayer to a site on a protein receptor. This model was also consistent with the experimental data, but the maximum forward rate constant was  $10^5$  faster than the measured rate constant. This "membrane pathway" model suggests novel criteria to be considered in the design of new cardiovascular drugs.

(Supported by NIH HL-27630, NIH HL-07420, and the American Heart Association)

**W-Pos35** CURARE-INDUCED SINGLE CHANNEL EVENTS IN CELLS WHICH DO NOT DEPOLARIZE IN RESPONSE TO CURARE. M.R. Montpetit & C.E. Morris, Biology Dept., U. of Ottawa, Ont. K1N 6N5.

The depolarizing effect of curare on embryonic rat muscle (Ziskind & Dennis, Nature 276: 622 (1978)) gave the first indication of this drug's partial agonist action. A curious feature of this action is that curare does not depolarize the cells beyond about -50 mV even though curare-activated single-channel events are readily detected at -50 mV. This disparity between the macroscopically and microscopically observed effects of curare deserves attention since it suggests that cells which show no depolarizing response to curare might nevertheless possess acetylcholine receptors for which curare is an activating agent. Curare has its customary antagonistic action on cells of the mouse skeletal muscle cell line, C8:  $10^{-5}$ M curare in the bath abolishes the depolarizing action of pressure-applied  $10^{-5}$ M suberyldicholine (control depolarizations  $23.1 \pm 2.2$  mV, n = 21; in the presence of curare  $0.50 \pm 0.26$  mV, n = 12). The cells do not, however, depolarize in response to  $10^{-5}$ M pressure-ejected curare, even when hyperpolarized to -90 mV prior to drug application. One might conclude that the cells lack acetylcholine receptors with the "embryonic" property of curare activation. And yet when these cells are probed with  $10^{-6}$ M or  $10^{-5}$ M curare-filled patch pipettes, they consistently display curare-activated single-channel currents with conductance and kinetic characteristics similar to those found in rat myotubes by Trautmann, 1982 (Nature 298: 272) - 2 major conductance states with the larger events having the briefer mean open time. These events are observed in cell-attached and outside-out configurations. Frequency of activation is voltage dependent between -100 mV and -150 mV, but little further increase in activation frequency is seen at higher voltages.

**W-Pos36** THE ROLE OF SULFHYDRYL GROUPS IN RAT BRAIN MUSCARINIC RECEPTOR BINDING SITES, El.A.M., Abdallah, F.A. Morsy, and A.E. Shamoo, University of Maryland, School of Medicine, Membrane Biochemistry Research Laboratory, Dept. of Biological Chemistry, 660 W. Redwood Street, Baltimore, Maryland 21201

The mechanism of rat brain muscarinic receptors inhibition by methylmercury (MeHg) and mercuric chloride ( $\text{HgCl}_2$ ) has been investigated using the binding of potent antagonist L-( $^3\text{H}$ )quinuclidinyl benzilate ( $^3\text{H}$ )QNB to the muscarinic receptors. The results emphasized that MeHg or  $\text{HgCl}_2$  interact with the membrane sulfhydryl groups (-SH) at the receptor binding sites. In the case of simple mono thiol compound (cysteine),  $\text{HgCl}_2$  and o-iodosobenzoic acid (IOB) showed the same potency to inhibit the -SH with the ratio 2:1 on a molecular basis (slope = 3.82,  $r=0.977$ ; slope = 4.09,  $r=0.98$ ; for  $\text{HgCl}_2$  and IOB respectively), and form a dimercaptide bond. Inhibition of ( $^3\text{H}$ )QNB binding of the receptor due to IOB treatment cannot be reversed by D-penicillamine nor dimercaptosuccinic acid and this suggests that the -SH groups undergo an oxidation reaction to sulfenic acid groups (-SOH) rather than forming a dimercaptide bond. However, addition of  $\text{HgCl}_2$  to the reaction medium containing IOB does not increase the ( $^3\text{H}$ )QNB binding inhibition. The greatest inhibition of ( $^3\text{H}$ )QNB binding by  $\text{HgCl}_2$  indicates the presence of two -SH groups within close proximity in the active site which forms a dimercaptide ring structure with the mercuric ion and causes allosteric changes of the binding site and magnifies the inhibition effect. Supported by the National Institutes of Environmental Health Sciences (ES-1248), and the Department of Energy (DE-AS0580 EV 10329).

**W-Pos37** PROTECTIVE EFFECT OF DIMERCAPTOSUCCINIC ACID ON METHYLMERCURY AND MERCURIC CHLORIDE INHIBITION OF RAT BRAIN MUSCARINIC ACETYLCHOLINE RECEPTORS El.A.M. Abdallah, and A.E. Shamoo, University of Maryland, School of Medicine, Membrane Biochemistry Research Laboratory, Department of Biological Chemistry, 660 W. Redwood Street, Baltimore, Maryland 21201.

The reactivation of the rat brain muscarinic acetylcholine receptor (mACh-R) bindings with dimercaptosuccinic acid (DMSA) after *in vitro* and *in vivo* inhibition by mercuric chloride ( $\text{HgCl}_2$ ) and methylmercuric chloride (MeHg) was investigated. Receptor binding was estimated by the potent and specific antagonist L-( $^3\text{H}$ )quinuclidinyl benzilate ( $^3\text{H}$ )QNB. At  $1 \times 10^{-4}$  M,  $\text{HgCl}_2$  caused complete inhibition of the ( $^3\text{H}$ )QNB binding. The inhibition of ( $^3\text{H}$ )QNB binding by  $\text{HgCl}_2$  was still higher than 50% at  $1 \times 10^{-8}$  M. MeHg caused less inhibition of ( $^3\text{H}$ )QNB binding than  $\text{HgCl}_2$ . The inhibited receptor showed a significant degree of reactivation when treated with DMSA. The recovery was almost complete after MeHg inhibition or with the lower  $\text{HgCl}_2$  concentrations. Generally, the reactivation was dependent on the concentration of DMSA. When rats injected with either early or delayed doses of DMSA following administration with five consecutive daily doses (8 mg/kg body weight gavage method), of MeHg or  $\text{HgCl}_2$ , the inhibition of ( $^3\text{H}$ )QNB binding was less than untreated ones. The early treatment with DMSA decreased the inhibition of ( $^3\text{H}$ )QNB binding due to MeHg or  $\text{HgCl}_2$  intoxication. However, DMSA was more effective in reducing  $\text{HgCl}_2$  inhibition than reducing MeHg inhibition either in an *in vitro* or in an *in vivo* treatment. The ability of DMSA to reactivate the mACh-R after inhibition with the mercurials emphasizes the involvement of essential sulfhydryl groups in ( $^3\text{H}$ )QNB binding sites and also shows that these sulfhydryl groups are the primary target for the MeHg and  $\text{HgCl}_2$  inhibition of the rat brain muscarinic receptors. Supported by the National Institute of Environmental Health Sciences (ES-1248), and the Department of Energy (DE-AS0580 EV 10329).

**W-Pos38** SPECIFIC INTERACTIONS BETWEEN GANGLIOSIDES AND ENKEPHALINS. M. Myers and E. Freire, Department of Biochemistry, University of Tennessee, Knoxville, TN 37996-0840.

The interactions of the opioid peptides [D-Ala<sup>2</sup>]methionine enkephalinamide and [D-Ala<sup>2</sup>,D-Leu<sup>5</sup>]enkephalin with dipalmitoyl phosphatidylcholine (DPPC) large unilamellar vesicles containing gangliosides  $\text{GM}_1$ ,  $\text{Gd}_{1a}$  and  $\text{Gt}_{1b}$  have been investigated using high sensitivity differential scanning calorimetry. In the absence of ganglioside the addition of enkephalin does not induce any change in the heat capacity function of DPPC over the entire concentration range studied ( $0-.5 \times 10^{-3}\text{M}$ ). In the presence of gangliosides, however, changes in the heat capacity function were observed with as little as micromolar concentrations of the enkephalins. The magnitude of these changes as well as the nature of the enkephalin effect depends on the type of ganglioside studied. For DPPC vesicles containing ganglioside  $\text{GM}_1$  only a slight broadening in the heat capacity function and a small upward shift in the transition temperature were observed. For DPPC vesicles containing ganglioside  $\text{Gd}_{1a}$  the effect was dramatic; enkephalin concentrations lower than  $10^{-5}$  M were able to induce phase separation of the ganglioside as judged by the appearance of two well defined peaks in the heat capacity function. In the absence of enkephalin the heat capacity function of this system is characterized by a single peak. For DPPC vesicles containing ganglioside  $\text{Gt}_{1b}$  the enkephalin effect was also seen at micromolar concentrations. In this case, however, the effect of the enkephalin was to shift to higher temperatures the intrinsically phase separated ganglioside peak characteristic of DPPC vesicles containing  $\text{Gt}_{1b}$ . These results provide evidence for the existence of high affinity interactions between specific gangliosides and enkephalins and suggest that gangliosides may play a role in the biological functioning of opiate receptors. (Supported by NIH Grant GM-30819).

**W-Pos39** LIGHT SCATTERING CHANGES ACCOMPANY SECRETORY ACTIVITY AT THE NERVE TERMINALS OF VERTEBRATE NEUROHYPOPHYSES. B.M. Salzberg, A.L. Obaid, R.K. Orkand, and H. Gainer. University of Pennsylvania, Philadelphia, PA. and N.I.H., Bethesda, MD.

The ability to monitor directly both the secretory events at vertebrate nerve terminals and the local membrane potential changes that regulate them should contribute to our understanding of excitation-secretion coupling. We have found changes in the opacity of frog (*Xenopus laevis*) and mouse (CD-1) neurohypophyses, following membrane potential changes known to trigger the release of peptide hormones. These optical signals, recorded without averaging as transmitted intensity changes in the image plane of a compound microscope, reflect variations in large angle light scattering rather than absorbance. They are characterized by a very weak wavelength dependence, and their behavior closely parallels secretion. The magnitude of the light scattering changes depends upon the frequency of stimulation, the duration of the nerve terminal action potential, and  $[Ca^{++}]_o$ . Calcium channel blockers such as  $Cd^{++}$ ,  $Co^{++}$ , and  $Mn^{++}$  reduce or eliminate the scattering signal while secretagogues such as 4-aminopyridine, tetraethylammonium and  $Ba^{++}$  dramatically enhance the effect.

In the mouse, but not in the frog, the change in light scattering also exhibits a fast component which resembles the action potential. Identification of the event(s) responsible for the opacity changes must await precise measurements of light scattering *per se*. However, the weak dependence on wavelength of the signal reflecting secretion, contrasted with the strong wavelength dependence of the extrinsic absorption signal provided by linear potentiometric probes (e.g., merocyanines), permits one to monitor simultaneously, in a stained preparation, the voltage changes in the nerve terminals and the release of secretory products. Supported by USPHS grant NS 16824.



**W-Pos40** FUSION OF LIPOSOMES INTO SARCOPLASMIC RETICULUM. W.B. Van Winkle, R.J. Bick and M.L. Entman. Depts. of Medicine and Biochemistry, Baylor College of Medicine, Houston, Tx 77030.

Alterations in phospholipid (PL) constituents of isolated sarcoplasmic reticulum (SR) membrane have a pronounced effect on various aspects of SR  $\text{Ca}^{2+}$ ATPase. Changing the PL composition of SR is most often accomplished by detergent solubilization in the presence of excess exogenous PL followed by dialysis or gradient centrifugation. Two disadvantages of this method are: disruption of freeze fracture membrane asymmetry of  $\text{Ca}^{2+}$ ATPase and any adhering PL and ionic leakiness of resultant vesicles. We have adapted the liposome fusion techniques of Schneider et al (PNAS 77:442, 1980) to alter PL composition of SR using native SR PL as well as dioleoylphosphatidylcholine (DOPC) liposomes. Incorporation of liposomes from either PL source is time and pH dependent but reaches a maximum level of only 2-3x normal SR PL amounts.  $\text{Ca}^{2+}$ ATPase activity diminishes with increased PL in contrast to detergent reconstitution using the same PL:SR ratios. Freeze fracture electron microscopy reveals an increase in vesicular dimensions with increasing PL incorporation. Unlike native SR and control, non-liposome fused SR, fused SR vesicles do not exhibit  $\text{Ca}^{2+}$ ATPase particle asymmetry; and large particle-free areas, representing fused liposomes, are seen in both fracture faces. Despite the fluid nature of DOPC, which can account for as much as 85% of fatty acyl chains in fused preparations, the inhibition of  $\text{Ca}^{2+}$ ATPase suggests structural hinderance following fusion. Supported by HL22856, HL13870 and AHA (Texas Affiliate).

**W-Pos41** PROPERTIES OF THE  $\text{Ca}^{2+}$ -MgATPASE OF SARCOPLASMIC RETICULUM FROM VASCULAR SMOOTH MUSCLE. George D. Ford, Luc Raeymaekers, Frank Wuytack and Rik Casteels. Laboratorium voor Fysiologie, Campus Gasthuisberg, KUL, Leuven, Belgium.

A subcellular fraction, highly enriched in sarcoplasmic reticulum (SR), was prepared from bovine aortic muscularis by a combination of differential and isopyknic centrifugation followed by density loading with calcium phosphate. This fraction was highly enriched in NADPH cytochrome-c reductase but contained only small amounts of 5'-nucleotidase or  $(\text{Na}^+ + \text{K}^+)$ -MgATPase. This fraction, and its precursor, exhibited a  $\text{Ca}^{2+}$ -dependent,  $\text{La}^{3+}$ -sensitive phosphorylated intermediate of 98,000 daltons molecular weight analogous to that found in striated muscle SR. For the first time in smooth muscle SR preparations, the basal MgATPase activity was low enough to allow determination of the influence of ATP and  $\text{Mg}^{2+}$  on the  $\text{Ca}^{2+}$ -MgATPase relationship. The apparent  $K_{\text{Ca}^{2+}}$  increased from 1.40  $\mu\text{M}$  to 13.7  $\mu\text{M}$  with increasing  $\text{Mg}^{2+}$  suggesting some form of competition for cationic sites. With increasing levels of ATP, the  $K_{\text{Ca}^{2+}}$  decreased from 4.18  $\mu\text{M}$  to 1.07  $\mu\text{M}$ , while the  $V_{\text{max}}$  increased from 12.1 to 90.6 nmoles/mg, min. Optimal activity was found at 3 mM  $\text{Mg}^{2+}$  and 3 mM MgATP. These results suggest that vascular smooth muscle SR activity may be subject to variations in intracellular levels of  $\text{Mg}^{2+}$  and ATP. (This work was performed, in part, while George D. Ford was a Fulbright-Hayes research scholar at KUL.)

**W-Pos42** SPECIFIC LABELING OF A SINGLE THIOL RESIDUE IN SARCOPLASMIC RETICULUM ATPase BY PYRENE MALEIMIDE. S.Verjovski-Almeida and Eleonora Kurtenbach\*. Department of Biochemistry, Federal University of Rio de Janeiro, 21910 Rio de Janeiro, Brazil.

Sarcoplasmic reticulum ATPase purified from the skeletal muscle microsomal fraction can be selectively labeled by N-1-pyrene maleimide (NPM). The label reacts specifically with one mol thiol residues per mol ATPase in the range of concentrations from 0.1 to 1.5  $\mu\text{M}$  NPM, independent of the ratio protein/label, which was varied from as low as 1/100 up to 1/1 on a molar basis. The apparent affinity for NPM is ~0.3  $\mu\text{M}$ . The rate of labeling exhibits two components, a fast one completed within 2-3 min and a slow one which last up to 120 min. The fast component can be eliminated by the presence of 5 mM ATP in the labeling medium, which however does not affect the maximal level of labeling. On the other hand inclusion of 20 mM Pi-Mg in the presence of EGTA greatly enhances the fast component and exposes an additional thiol residue. The probe appears to react with the thiol residues of the catalytic site of the enzyme. The fluorescence quenching of the pyrene-ATPase adduct with acrylamide and Cesium ions was studied to determine the access of these hydrophilic quenchers to the probe on the enzyme. Quenching in the presence of EGTA was less effective than in the presence of 100  $\mu\text{M}$   $\text{Ca}^{2+}$ , revealing that in the presence of EGTA the probe is less exposed to the solvent. This is in line with the view that upon saturation of the high affinity  $\text{Ca}^{2+}$  sites the ATPase undergoes a conformational change which exposes its catalytic site to the medium solvent. Supported by CNPq-FINEP(Brazil) and MDA.

**W-Pos43** EFFECTS OF CYCLIC GMP (cGMP) ON FUNCTIONALLY SKINNED MYOCARDIAL CELLS OF RABBITS. J.Y. Su, Department of Anesthesiology, University of Washington, Seattle, WA 98195

The muscarinic effect of choline esters on myocardial contractility has been shown to be either associated with (e.g., *Proc. Nat. Acad. Sci.* 66:398, 1970) or dissociated from (e.g., *J. Cyclic Nucleotide Res.* 3:407, 1977) the increases in cGMP. The purpose of his study was to test the hypothesis that cGMP was a second messenger for choline esters by studying the direct effect of cGMP on intracellular sites of muscle contraction. We used functionally skinned fiber preparations to study the effect of cGMP on  $\text{Ca}^{2+}$  activation of the contractile proteins (CP), and  $\text{Ca}^{2+}$  uptake and release from the sarcoplasmic reticulum (SR) separately at the same time that "tension" was monitored. Papillary muscle was isolated from rabbits. Pieces of the muscle were homogenized (sarcolemma disrupted). A fiber bundle was dissected from the homogenate and mounted on forceps and one end attached to a tension transducer. The bathing medium contained 1 mM (for CP), 0.1 mM (for SR) free  $\text{Mg}^{2+}$ ; 2 mM  $\text{MgATP}^{2-}$ ; 70 mM  $\text{K}^+ + \text{Na}^+$ ; 15 mM creatine phosphate; 7 mM (for CP), 7 or 0.05 mM (for SR) EGTA total; and varying amounts of free  $\text{Ca}^{2+}$ . Ionic strength = 0.15 and pH =  $7.00 \pm 0.02$  at  $23 \pm 2^\circ \text{C}$  with imidazole. Propionate (for CP) and methanesulfonate (for SR) were major anions. Caffeine-induced tension transient was used to measure the amount of  $\text{Ca}^{2+}$  released from the SR. We found that cGMP (0.001-1  $\mu\text{M}$ ) did not significantly change the pCa-tension relation, increased (30-55%) the  $\text{Ca}^{2+}$  uptake by the SR, and only increased (18%)  $\text{Ca}^{2+}$  release at 1  $\mu\text{M}$  cGMP. There was no dose-response relation. The increased  $\text{Ca}^{2+}$  uptake by the SR was also observed with cAMP (*Pflugers Arch.* 394:48, 1982). We conclude that these intracellular effects of cGMP cannot contribute to the negative inotropic action of choline esters. Supported by NIH Grants HL 20754 and HL 01100 (RCDA).

**W-Pos44** STERIC HINDERANCE OF TNP-AMP IN THE PHOSPHORYLATED SITE OF SARCOPLASMIC RETICULUM ATPase. Robert K. Nakamoto and Giuseppe Inesi, Department of Biological Chemistry University of Maryland School of Medicine, Baltimore, MD 21201

TNP-nucleotides are found to interact directly with the ATPase active site competing with phosphorylating substrates and occupying catalytic sites in exchange with ADP even after formation of intermediate phosphoenzyme (Nakamoto and Inesi, *JBC*, submitted).

The fluorescence yield of TNP-AMP is 8-10 times higher, the emission peak is blue shifted from 535 to 525 nm, and  $\tau_{fl}$  increases from <0.1 nsec to 0.8 nsec upon formation of E-P from Pi in absence of  $\text{Ca}^{2+}$ .

In control solvent conditions, the increase in fluorescence intensity and blue shift of emission peak is obtained either by lowering solvent polarity or sterically constraining the analogue in highly viscous solvents without lowering polarity. However, a substantial increase in  $\tau_{fl}$  is measured in conditions of increased viscosity (3.4 nsec, propylene glycol,  $-50^\circ \text{C}$ ) whereas decreased polarity increases  $\tau_{fl}$  much less (0.1 - 0.2 nsec, dioxane).

Extrapolation of these characteristics to TNP-AMP bound to the enzyme indicates that following E-P formation, the binding domain confers steric hinderance upon the analogue probably in part by excluding solvent molecules. This is contrasted with the non-phosphorylated enzyme site which confers less constraints upon bound analogue and greater access to solvent molecules. The fluorescence effects are much more pronounced where enzyme phosphorylation is obtained with Pi in the absence of  $\text{Ca}^{2+}$ , then with ATP in the presence of  $\text{Ca}^{2+}$ .

Supported by USPHS (HL27867) and the Muscular Dystrophy Association of America.

**W-Pos45** LIPID DISTRIBUTION IN SPIN LABELED SR AS DETERMINED BY PARAMAGNETIC BROADENING AGENTS. C. Coan & S. Keating, Physiology Dept., U. of the Pacific Dental School, San Francisco CA. 94115

The distribution of a stearic acid spin probe between the inner and outer leaflets of the SR bilayer is determined by the accessibility of the probe to Ni-EDTA, a spin broadening agent. The spin probe used contains the spin moiety on the 4th carbon from the carbonyl group, and is known to incorporate into SR with the spin moiety at the membrane-solvent interfaces. Ni-EDTA does not penetrate SR vesicles, and thus the fraction of spin probes exposed on the exterior interface can be determined directly by titration. We find this fraction to be 35%. On the other hand, when  $\text{Ni}^{2+}$  is allowed to freely enter the vesicles by use of the ionophore X-537A, all spin probe signal is reduced, indicating that all probes are on either the inner or the outer interface. Further evidence indicates that the probe is evenly distributed among the lipids in the bilayer, suggesting a 35% inner to 65% outer lipid asymmetry. This is in accordance with the observed ATPase asymmetry favoring location of the enzyme on the vesicular exterior.

EDTA is unique in its ability to tightly chelate transition metals, and hence EGTA and  $\text{Ca}^{2+}$  may be used without altering the chelation of  $\text{Ni}^{2+}$ . Thus we have been able to probe the effect of ligand binding to the ATPase on the spin probe asymmetry. We find a 5% increase in the protected fraction of spin probe on enzyme phosphorylation with  $\text{P}_i$ , indicating a change in the macromolecular conformation which affects the lipid phase at this step in the enzymatic cycle.

**W-Pos46** CALCIUM FLUXES IN FAST-TWITCH SKELETAL MUSCLE SARCOPLASMIC RETICULUM. A. Chu, P. Volpe, B.R. Costello, and S. Fleischer. Dept. of Molec. Biol., Vanderbilt Univ., Nashville, TN 37235.

Heavy (H) and light (L) sarcoplasmic reticulum (SR) vesicles, corresponding to terminal and longitudinal cisternae regions of SR, have been described. Previous studies (Ohnishi, S.T., J. Biochem. 86, 1147, 1979; Miyamoto, H. and Racker, E., FEBS Lett. 133, 235, 1981) indicated that ruthenium red (RR) enhanced energized  $\text{Ca}^{2+}$  uptake and decreased  $\text{Ca}^{2+}$  release in HSR, but had little effect in LSR. Recently, a terminal cisternae fraction (TC) with intact junctional feet structures has been prepared (Saito, A., Seiler, S., Chu, A., Fleischer, S., submitted), and is the focus of this study. Passively loaded TC vesicles exhibited  $\text{Ca}^{2+}$ -dependent  $\text{Ca}^{2+}$  efflux, with a maximum between pCa 5-6 over a range of pCa 4-8.  $\text{Ca}^{2+}$  efflux was diminished by RR or high  $[\text{Mg}^{2+}]$ . Compared to HSR, the TC had a low  $\text{Ca}^{2+}$  uptake rate that was greatly increased by RR, whereas the  $\text{Ca}^{2+}$ ,  $\text{Mg}^{2+}$ -dependent ATPase activity measured in the presence of A23187 was unaffected by RR. The  $\text{Ca}^{2+}$ -dependent  $\text{Ca}^{2+}$  efflux and the low  $\text{Ca}^{2+}$  uptake rate of TC are unique characteristics of TC as compared to longitudinal cisternae. Our study supports the localization of RR-sensitive  $\text{Ca}^{2+}$  channels in terminal cisternae region of SR [supported by NIH grant AM 14632, fellowships from NIH (AM 07016, GM 08198) and MDA].

**W-Pos47** ADENINE NUCLEOTIDES,  $\text{Ca}^{2+}$ ,  $\text{Mg}^{2+}$ , AND  $\text{H}^+$  CONTROL A  $\text{Ca}^{2+}$  RELEASE CHANNEL IN SARCOPLASMIC RETICULUM: Gerhard Meissner, Edward Darling, and Julia Eveleth, Department of Biochemistry, University of North Carolina, Chapel Hill, NC 27514

Rabbit skeletal muscle sarcoplasmic reticulum was fractionated into a " $\text{Ca}^{2+}$ -release" and "control" fraction by differential and sucrose gradient centrifugation. The " $\text{Ca}^{2+}$ -release" fraction was recovered from the 32%-38% region of a sucrose gradient that contained membranes sedimenting at 2,600-10,000xg. The "control" fraction sedimented in the 29%-35% region of a sucrose gradient containing membranes obtained by differential pelleting at 35,000-130,000xg. At 37° C, external  $\text{Ca}^{2+}$  (2-20  $\mu\text{M}$ ) caused the release of 300 nmol  $\text{Ca}^{2+}$ /mg protein/s from  $\text{Ca}^{2+}$  release vesicles passively loaded at pH7 with an internal "physiological"  $\text{Ca}^{2+}$  concentration of 5 mM.  $\text{Ca}^{2+}$ -induced  $\text{Ca}^{2+}$  release was half-maximally activated at  $6 \times 10^{-7}$  M  $\text{Ca}^{2+}$ , had an approximate pK value of 6.6, and was half-maximally inhibited at an external  $\text{Ca}^{2+}$  concentration of  $2 \times 10^{-4}$  M and  $\text{Mg}^{2+}$  concentration of  $7 \times 10^{-5}$  M.  $^{45}\text{Ca}^{2+}$  efflux from "control" vesicles was slightly inhibited at external  $\text{Ca}^{2+}$  concentrations that stimulated the rapid release of  $\text{Ca}^{2+}$  from  $\text{Ca}^{2+}$ -release vesicles. Adenine, adenosine and derived nucleotides AMP-PCP, ADP, AMP and c-AMP reversed the  $\text{Mg}^{2+}$  inhibition of  $\text{Ca}^{2+}$ -dependent  $\text{Ca}^{2+}$  release in media containing a "physiological" free  $\text{Mg}^{2+}$  concentration of 0.6 mM. Other nucleoside triphosphates and caffeine were minimally effective in increasing  $^{45}\text{Ca}^{2+}$  efflux from passively loaded vesicles.  $\text{La}^{3+}$ , ruthenium red and procaine inhibited  $\text{Ca}^{2+}$ -induced  $\text{Ca}^{2+}$  release.  $\text{Ca}^{2+}$  flux studies with actively loaded vesicles also indicated that a subpopulation of sarcoplasmic reticulum contains a  $\text{Ca}^{2+}$  release system that is regulated by  $\text{Ca}^{2+}$ ,  $\text{Mg}^{2+}$  and adenine nucleotides. (Supported by USPHS Grant AM 18687).

**W-Pos48** AN ATTEMPT TO CORRELATE THE MEMBRANE LOCALIZATION OF ETHANOL WITH FUNCTIONAL PERTURBATIONS IN THE CALCIUM-PUMP ATPASE OF SARCOPLASMIC RETICULUM. C.A. Napolitano and L.G. Herbert, U. Conn. Health Ctr., Farmington, CT 06032; Brookhaven Natl. Lab., Upton, NY 11973.

Calcium transport by sarcoplasmic reticulum (SR) membrane vesicles was inhibited by ethanol in a linear and concentration-dependent manner over a range of 0-1% (v/v). The level of ethanol associated with the SR membrane as determined by a centrifugation procedure was  $0.07 \pm 0.04$  moles ethanol/mole lipid (mean  $\pm$  S.D.) at 0.1% ethanol and increased linearly ( $r=0.9$ ) to  $0.55 \pm 0.22$  moles ethanol/mole lipid at 1% ethanol. These data are corrected for ethanol partitioning into the water space and were used to calculate an apparent partition coefficient of  $5 \pm 2$  for ethanol in SR. To correlate the functional effects of ethanol on calcium transport with the possible site of ethanol interaction with the SR membrane, lamellar meridional neutron diffraction was recorded from hydrated oriented SR membrane multilayers that were exposed to protonated or deuterated ethanol vapor. Radiochemical analysis indicated that under these conditions  $11 \pm 3$  moles ethanol/mole  $\text{Ca}^{2+}$ -pump ATPase (0.1 moles ethanol/mole lipid) were associated with the membrane. The neutron scattering difference profile for ethanol when compared to the profile for water showed that ethanol is distributed primarily throughout the aqueous regions hydrating the SR membrane and may allow for an interpretation of the calculated partition coefficient. Under conditions which allow ethanol to diffuse out of the multilayer, ~ 1 mole ethanol/mole  $\text{Ca}^{2+}$ -pump ATPase (1 mole ethanol/110 moles lipid) remains associated for more than 30 hrs. Neutron diffraction data are currently being collected in an attempt to locate this "tightly" bound ethanol component and to relate this to possible effects on the functional properties of the calcium-pump ATPase. (Supported by NIH HL27630, HL26903, HL07420, HL22135 and HL21812.)

**W-Pos49** SARCOPLASMIC RETICULUM (S.R.)  $\text{Ca}^{2+}$ -ATPase FUNCTION: POTENTIAL ROLE OF THE 53,000 DALTON GLYCOPROTEIN IN COUPLING  $\text{Ca}^{2+}$ -TRANSPORT TO ATP HYDROLYSIS. Kenneth S. Leonards and Howard Kutchai, Dept. of Physiology & Biophysics Program, Univ. of Va. Medical School, Charlottesville, VA. 22908.

An essential feature of S.R.  $\text{Ca}^{2+}$ -ATPase function is the close coupling between  $\text{Ca}^{2+}$  transport and ATP hydrolysis (2  $\text{Ca}^{2+}$  transported/ATP split in intact S.R.). To investigate the interactions involved in this coupling, the ATPase activity of reconstituted  $\text{Ca}^{2+}$ -ATPase/lipid vesicles and reconstituted SR (R-SR) vesicles were examined in the presence and absence of the  $\text{Ca}^{2+}$  ionophore A23187. Cholate purified  $\text{Ca}^{2+}$ -ATPase, reconstituted into lipid vesicles (egg PC and egg PC/egg PE mixtures) was highly active, but completely uncoupled ( $\Delta\text{ATPase}/\text{A23187}=0$ ). Control S.R. preps were tightly coupled under the same conditions. These results led us to re-examine how the methods used to isolate, purify, and reconstitute the  $\text{Ca}^{2+}$ -ATPase alter  $\text{Ca}^{2+}$  transport/ATPase coupling. The degree of coupling in R-SR was found to depend on the  $[\text{K}^+]$  and temperature used during cholate solubilization and reconstitution. R-SR vesicles, solubilized and reconstituted in high  $[\text{K}^+]$  buffer were extensively uncoupled, whereas those prepared in low  $[\text{K}^+]$  buffer only slightly less coupled than, control SR. The conditions which uncouple  $\text{Ca}^{2+}$ -transport from ATP hydrolysis also irreversibly solubilize the 53,000 dalton glycoproteins. The protein composition of these R-SR preps demonstrate a correlation between the 53,000 dalton glycoprotein content (relative to  $\text{Ca}^{2+}$ -ATPase), and the degree of coupling, and suggest that the 53,000 dalton glycoprotein may be intimately involved in regulating coupling of ATP hydrolysis to  $\text{Ca}^{2+}$  transport in S.R. This work supported by an American Heart Association (Virginia affiliate) Research Fellowship (to K.S.L.).

**W-Pos50** BLOCKING OF  $\text{K}^+$ -CHANNELS IN SR-MEMBRANES CAN INCREASE NET  $\text{Ca}^{2+}$ -LOADING. R.H.A. Fink and D.G. Stephenson, Department of Zoology, La Trobe University, Melbourne, Australia 3083.

Sarcoplasmic reticulum (SR) membranes contain  $\text{K}^+$ -selective channels which can be blocked with tetra-ethyl-ammonium (TEA), 4-aminopyridine (4AP) or procaine (Coronado & Miller, J. Gen. Physiol. 79, 529-547, 1982). As the physiological function of the SR- $\text{K}^+$ -channels is generally unknown we carried out experiments on mechanically skinned fibres from the iliofibularis muscle of the toad, *Bufo marinus*, (Moisescu & Thieleczek, J. Physiol. 275, 241-262, 1978) to test the effects of  $\text{K}^+$ -channel blockers. The preparations with intact SR were loaded at a pCa of 6.5 in the presence and in the absence of 4AP, TEA and procaine.  $\text{Ca}^{2+}$  was then released by 30mM caffeine in a solution containing 0.75 to 1mM EGTA. Peak tension and the area under the tension transient during  $\text{Ca}^{2+}$  release were used as a relative measure of the stored  $\text{Ca}^{2+}$ . Both parameters were substantially increased after loading in the presence of the  $\text{K}^+$ -channel blockers used. After loading in 1.6mM 4AP, peak tension during the  $\text{Ca}^{2+}$  release was larger by c.60% than the average control value of the  $\text{Ca}^{2+}$  release in the absence of the blocker, and the area under the tension transient was even more markedly increased by c.80% compared with the control values. Similarly, after loading in 10mM TEA and in 1mM procaine, peak force and area of the  $\text{Ca}^{2+}$  release transient were significantly increased by between 10 to 50% compared to the controls. Our main conclusion is that  $\text{K}^+$ -channels are involved in modulating  $\text{Ca}^{2+}$  movements across the membranes of the SR.

Supported by NH&MRC (Australia) and ARGS.

**W-Pos51** IDENTIFICATION AND ISOLATION OF AN ENDOGENOUS PROMOTOR FOR THE FORMATION OF THE TRIAD JUNCTION IN SKELETAL MUSCLE. Adrian M. Corbett and Anthony H. Caswell, Dept. of Pharmacology, University of Miami School of Medicine, P.O. Box 016189, Miami, Florida 33101.

The triad of skeletal muscle consists of the transverse tubule and two terminal cisternae which are physically joined by junctional feet. The junction of isolated triads can be mechanically broken by passage through a French press and subsequently rejoined by incubation of the isolated organelles with certain salts of weak acids (e.g. K cacodylate, K acetate,  $\text{KHCO}_3$ ). We recently discovered an endogenous factor which acts in the same manner as these artificial compounds. When rabbit skeletal muscle is homogenized in KCl and centrifuged, an endogenous factor is extracted into the high speed supernatant which can cause the rejoining of mechanically broken triads. A three stage purification of this factor has been achieved using: 1) Ammonium sulfate fractionation, 2) ion exchange chromatography, and 3) molecular sieve chromatography. SDS-PAGE showed that this protein was purified to homogeneity and has a  $M_r$  of 34,000. This protein has the following characteristics: 1) it runs as a polymeric substance with an  $M_r$  of 134,000 on molecular sieve chromatography, 2) it promotes the formation of triadic vesicles from the isolated organelles in a low ionic strength medium, and 3) both this protein and cacodylate share the property of specifically catalyzing the association and aggregation of junctional proteins which had previously been dissolved in neutral detergent and salt. SDS-PAGE demonstrates that identical proteins are preserved in each case. While the physiological role of this protein is still not known, these results suggest that the triad junction is a dynamic association of proteins which may play a role in muscle excitation. (Supported by NIH Grant AM2160 and Training Grant HL07188).

**W-Pos52** RAPID KINETICS OF CALCIUM RELEASE FROM SARCOPLASMIC RETICULUM ISOLATED FROM NORMAL AND MALIGNANT HYPERTHERMIA SUSCEPTIBLE PIGS. Do Han Kim, Frank A. Sreter and Noriaki Ikemoto. (Intr. by Hartmut Wohlrab) Dept. of Muscle Res., Boston Biomed. Res. Inst.; Dept. of Neurol., Harvard Med. School, Boston, MA 02114

Several recent reports suggest that abnormalities in malignant hyperthermia susceptible (MH) muscles are at least partly ascribable to altered  $\text{Ca}^{2+}$  release functions of sarcoplasmic reticulum (SR). We have investigated the time course of  $\text{Ca}^{2+}$  release from SR isolated from normal (N) and MH muscles using stopped flow spectrophotometry and arsenazo III as  $\text{Ca}^{2+}$  indicator. Several methods were used to trigger  $\text{Ca}^{2+}$  release; a) addition of halothane (e.g. 0.2 mM), b) an increase of extravesicular  $\text{Ca}^{2+}$  concentration ( $[\text{Ca}_0^{2+}]$ ), c) combination of a and b, and d) replacement of ions (K-gluconate to choline Cl) to produce membrane depolarization. The initial rates of  $\text{Ca}^{2+}$  release induced by halothane or  $\text{Ca}^{2+}$  alone, or both are at least 70 per cent higher in MH SR than in N SR. The amount of  $\text{Ca}^{2+}$  released by halothane at low  $[\text{Ca}_0^{2+}]$  in MH SR is about two times as large as in N SR. Membrane depolarization led to biphasic  $\text{Ca}^{2+}$  release in both MH and N SR. The rate constant of  $\text{Ca}^{2+}$  release in the rapid phase, which is triggered via depolarization of the T-tubule (Ikemoto et al, this meeting), is significantly higher in MH SR ( $k = 100 \text{ s}^{-1}$ ) than in N SR ( $k = 25 \text{ s}^{-1}$ ). Although all types of  $\text{Ca}^{2+}$  release investigated have higher rates in MH SR than N SR but the T-tubule content is about the same in MH and N SR. Thus, it appears that  $\text{Ca}^{2+}$  release channels located in the SR moiety rather than triggering mechanisms have been altered in MH SR. Supported by grants from NIH (AM16922, GM15904-16, HL23961) and MDA, D.H.K. is a postdoctoral fellow of MDA.

**W-Pos53** COMPOSITION OF SARCOPLASMIC RETICULUM AND MITOCHONDRIA DURING CAFFEINE CONTRACTURE (CC). T. Yoshioka and A.P. Somlyo, Univ. of Pennsylvania, Philadelphia, PA 19104.

Calcium release from the terminal cisternae (TC) of tetanized frog muscle is associated with an uptake of Mg and K into the TC: only in the presence of valinomycin is the counter movement of K and Mg sufficient to completely compensate for the charge released as  $\text{Ca}^{2+}$  (1,2). Frog semitendinosus fiber bundles were rapidly frozen either at rest or 1 min. after addition of 5mM caffeine. The main results of electron probe analysis of cryosections are shown in the Table; the total fiber Ca was unchanged during CC.

Terminal cisternae	n	Mg	K	Ca
Control	111	56±12	610±72	115.4±28.4
Caffeine	134	88±21	671±133	41.8±13.9
Paired I-band cytoplasm				
Control	111	52±17	451±109	2.9±4.8
Caffeine	134	58±16	512±122	7.2±4.2

The fraction of calcium released from the TC (64% of resting value) was slightly greater than during tetanus (59%; 1). Mitochondrial Ca also increased to 15mmol/kg dry mitochondrial wt, probably as the result of the long duration of the CC. In previous studies showing Mg uptake by the TC of tetanized muscle we could not exclude the possibility that

Mg was accumulated by the TC not during the period of increased Ca permeability (release), but during the time between action potentials when, presumably, Ca pumping takes place. The present results show that this is unlikely to be the case, and that Mg is also accumulated ( $P < 0.001$ ) during the maintained increase in SR permeability caused by caffeine. 1) Somlyo, A.V. et al., J. Cell Biol. 90: 577-594, 1981; 2) Kitazawa, T. et al., J. Physiol. In Press. Supported by HL15835 to the Pa. Muscle Institute.

**W-Pos54** DANTROLENE NA BINDING SITES INVOLVED IN INHIBITION OF CALCIUM RELEASE FROM SR IN VITRO. Stefania Danko, and Noriaki Ikemoto. (Intr. by Philip Graceffa) Dept. of Muscle Res., Boston Biomed. Res. Inst.; Dept. of Neurol., Harvard Med. School, Boston, MA 02114

An accumulated physiological evidence suggests that dantrolene Na (DAN) works as a muscle relaxant by acting either on a) T-tubule/SR coupling or b)  $\text{Ca}^{2+}$  release from SR, or both. Several  $\mu\text{M}$  DAN inhibits caffeine-induced  $\text{Ca}^{2+}$  release from rabbit skeletal muscle SR (cf. Kim and Ikemoto, Biophys. J., 41, 232a, 1983), as determined by stopped-flow spectrophotometry. Ten to 20  $\mu\text{M}$  dantrolene Na also decreases the rate constant of rapid  $\text{Ca}^{2+}$  release induced by membrane depolarization (K-gluconate to choline Cl replacement) from the control value of 100-140s<sup>-1</sup> to 35-80s<sup>-1</sup>. In an attempt to identify the DAN binding sites which are responsible for the above effects, we have determined DAN binding to various membrane fractions using fluorescent technique (Dehpour et al, Biochem. Pharmacol., 31, 965, 1982). Capacity ( $n$ , nmol mg<sup>-1</sup>) and affinity ( $K$ , M<sup>-1</sup>) of binding as determined by Scatchard plots are as follows: microsomal fraction enriched in the T-tubule/SR complex, 7.43,  $1.0 \times 10^5$ ; purified SR, 8.0,  $2.3 \times 10^5$ ; purified T-tubule, 18.0,  $0.91 \times 10^5$ . DAN binding to the SR moiety is inhibited by 2--10 mM caffeine. However, there is no effect of caffeine (2--5mM) on the DAN binding to the purified T-tubule. DAN binding sites of SR and those of the T-tubule are also distinguishable in that the fluorescence intensity per unit binding is about five times higher in the T-tubule than SR. These results suggest that DAN binding sites of SR are localized in the SR components involved in caffeine-induced  $\text{Ca}^{2+}$  release, while those of the T-tubule are related to the inhibition of the T-tubule mediated rapid  $\text{Ca}^{2+}$  release. Supported by grants from NIH (AM16922) and MDA.

**W-Pos55** MEMBRANE FLUIDITY OF SARCOPLASMIC RETICULUM REGULATES THE CALCIUM EFFLUX. S. Tsuyoshi Ohnishi\*, Alan J. Waring\*\* and Tomoko Ohnishi\*\*. Dept. of Hematol./Oncology, Hahnemann University School of Medicine, Phila., Pa. 19102\*; and Dept. of Biochemistry and Biophysics, University of Pennsylvania, Phila., Pa. 19104\*\*.

It is known that malignant hyperthermia (MH) is triggered by general anesthetics such as halothane, and that the symptom is alleviated by dantrolene. However, the mechanism of triggering of MH and the mechanism of inhibition by dantrolene are not elucidated. We demonstrated that skeletal sarcoplasmic reticulum (SR) prepared from pig with MH has abnormally high Ca-induced Ca-release and halothane-induced Ca-release (ref. 1), and that halothane-induced Ca-release is inhibited by dantrolene. These findings indicate that SR may play a key role in the pathogenesis of MH. We also found that halothane fluidizes the MH-SR membrane (as measured by spin-probe EPR) and that dantrolene inhibits that fluidization. Ethanol also fluidizes the SR membrane. However, the effect of ethanol was the same in both MH-SR and normal SR, suggesting that the halothane fluidization of MH-SR may be related to the abnormally high halothane-induced Ca-release. The SR prepared from alcoholic rats is resistant to the ethanol-fluidizing effect (similar to mitochondria, ref. 2); the Ca-efflux of this SR is also resistant to ethanol. Data suggest that membrane fluidity regulates Ca-efflux. (Supported in part by NIH GM30703, HL 26903, AA 5662).  
Ref.1:FEBS Letters 161:103 (1983). Ref.2:Proc.Natl.Acad.Sci.(USA) 78:2382 (1981).

**W-Pos56** MOLECULAR DYNAMICS AND ENZYMIC ACTIVITY IN SARCOPLASMIC RETICULUM: A COMPARISON OF THE EFFECTS OF ETHER AND TEMPERATURE. Diana J. Bigelow and David D. Thomas, Dept. of Biochemistry, University of Minnesota, Minneapolis, MN 55455.

We have used EPR (both conventional and saturation transfer) to investigate the rotational dynamics of proteins and lipids in sarcoplasmic reticulum (SR) as a function of two activating conditions: diethyl ether and increased temperature. The addition of 5% (v/v) diethyl ether to skeletal SR activates both the Ca-ATPase and Ca uptake activities (Salama and Scarpa, 1980, J. Biol. Chem. 255:6525). We have found that this ether addition increases the nsec rotational motion of lipid hydrocarbon chains, as determined from EPR spectra of spin-labeled fatty acid and phospholipid analogs in SR membranes. Moreover, spectral subtractions show that, at the ether concentration required for maximal enzymatic activation, both the restricted spectral component (presumably corresponding to boundary lipid) and the mobile component are substantially mobilized, resulting in the same high lipid mobility observed in the absence of protein. Microsecond protein mobility (measured by saturation transfer EPR of a maleimide spin-label attached to the enzyme) is also increased by ether. A 10-degree increase in temperature has similar effects to those of ether on all three properties (enzyme activity, lipid mobility, and protein mobility). However, the rates of motion of protein and bulk lipid increase by only modest amounts. Only the mobility of the restricted (boundary) lipid component increases by a factor comparable to that of the enzymatic activity.

**W-Pos57** A Catheter NMR Probe for IN VIVO NMR Measurements of Internal Organs. H.L. Kantor, R.W. Briggs, and R.S. Balaban NIH, NHLBI Bethesda, MD. Milton Hershey Medical Center, Dept. of Radiology Hershey, PA.

We report the in vivo measurement of  $^{31}\text{P}$  NMR spectra from the canine heart using an NMR probe placed within the heart using peripheral blood vessels. This permitted the acquisition of NMR signals from distinct regions of the heart with excellent signal/noise characteristics. The coil is a 2cmX7mm two turn flat elliptical solenoid, which was passed through a cutdown of either the jugular vein or carotid artery to the heart. The coil was positioned under fluoroscopic monitoring into either the left or right ventricle. The magnet was shimmed on the water signal, which had a line width of less than 30 Hz. The experiment was performed at 1.89 tesla yielding an  $^1\text{H}$  resonance of 80 MHz and  $^{31}\text{P}$  of 32.5 MHz. The coil was elliptical in shape in order to be inserted in the vessels. Field maps of the coil demonstrated that even with this geometry a nearly spherical field was produced.  $^{31}\text{P}$  spectra were collected with a  $90^\circ$  flip of 6  $\mu\text{sec}$ . A 6 minute collection yielded resolved peaks for inorganic phosphate, phosphodiesteres, phosphocreatine (PCr), and all of the phosphates of ATP, with a signal to noise ratio for PCr of approx. 12:1. No distinct resonance was observed for 2,3 DPG in blood, possibly due to the rapid flow of blood past the coil. However, 2,3 DPG in the blood may make some contribution to the spectra collected. The calculated intensity ratio of PCr/ATP in the right ventricle was 1.7/1. Over the course of several hours, no change in the NMR spectra were observed attesting to the preparation's stability. In addition, during placement of the coils the animals experienced no changes in pulmonary artery wedge pressure, peripheral blood pressure or EKG. The dogs survived the procedure with no harmful effects.

**W-Pos58** MULTIFREQUENCY CROSS-CORRELATION PHASE FLUOROMETRY USING SYNCHROTRON RADIATION.

E GRATTON\*, D.M. JAMESON, N. ROSATO and G. WEBER, Dept. of Physics and Dept. of Biochemistry, University of Illinois, Dept. of Pharmacology, University of Texas Health Science Center at Dallas.

The construction and operation of a cross-correlation phase and modulation fluorometer using the synchrotron radiation facility at the ADONE-Frascati electron storage ring is described. In the frequency domain the pulsed source gives a large series of equally spaced harmonic frequencies. Use of cross-correlation techniques in conjunction with a high repetition rate pulsed light source permits one to isolate one harmonic frequency from the adjacent frequencies with high precision. The cross-correlation frequency required for the analysis of the phase delay and modulation ratio is obtained using two coupled frequency synthesizers, one of which drives the radiofrequency cavity of the storage ring and the other which modulates the response of the photomultipliers used for the signal detection. The accuracy, reproducibility and sensitivity of the instrumentation have been determined experimentally. A study of measurement artifacts related to the color error of the photomultipliers has been carried out and no sensible color error was detected. Tryptophan emission was investigated in different pH conditions and at several excitation and emission wavelengths. Results of experiments on energy transfer between tyrosine and tryptophan in bovine serum albumin (BSA) and between tryptophan-tryptophan and bis-anilino-naphthalenesulfonate (bis-ANS) adsorbed to BSA are also presented. Energy transfer causes a definite lengthening of the measured phase angle due to the delayed emission of the acceptor excited through the donor relative to direct excitation.

**W-Pos59** SPATIAL LOCALIZATION OF TISSUE METABOLITES BY P-31 NMR ROTATING FRAME ZEUGMATOGRAPHY. T. Schleich, G.B. Matson<sup>+</sup>, M. Garwood, and G. Acosta, Dept. of Chemistry, Univ. of California, Santa Cruz, CA 95064 and <sup>+</sup>NMR Facility, Univ. of California, Davis, CA 95616.

We have employed surface coils for rotating frame zeugmatography experiments designed to accomplish one-dimensional P-31 metabolic mapping in eye phantoms and bovine eyes. High resolution metabolite spatial localization depends on the  $B_1$  field gradient produced by a surface coil in the presence of a homogeneous  $B_0$  field. Chemical shift information is thus preserved. The basic experiment is designed such that 20 to 32 RF pulses of increasing equally incremented durations are applied to the sample producing magnetization precession away from the z-axis in the rotating frame. The degree of precession away from the z-axis defines the distance from the coil, such that the "dimension" is a curved surface of constant  $B_1$  strength. Two dimensional Fourier transform processing of the data results in a suite of spectra displayed as a function of mapping distance. All experiments were performed at 80.96 MHz on a wide-bore NT-200 spectrometer system. Two-turn planar circular surface coils were employed. Calculation of the  $B_1$  field isocontour profile for a surface coil is necessary for the establishment of the initial pulse and incremental duration times and for the estimation of resolution. Experiments with bovine eye phantoms reveal that  $T_1$  discrimination produces a loss of resolution due to smearing in the mapping dimension. Resonance offset effects are also implicated. A phase cycling saturation pulse sequence was devised to circumvent  $T_1$  discrimination effects. The method has been applied to the intact bovine eye. Metabolite maps delineating contributions from constituent tissues of the bovine eye have been obtained. Techniques for the correction of intensity distortion due to  $T_1$  discrimination and  $B_1$  field strength variation are currently being explored. (Supported by the National Eye Institute.)

**W-Pos60** IMAGING OF CHIRAL STRUCTURES USING CIRCULARLY POLARIZED LIGHT. M.F. Maestre\*, C. Bustamante†, D. Keller§, and I. Tinoco, Jr.§ \*Lawrence Berkeley Laboratory, Berkeley, CA 94720; †Chemistry Dept., U. of New Mexico; §Chemistry Dept., U. of California, Berkeley.

If a microscopic object is illuminated with circularly polarized light, a differential image can be obtained that is related to the circular dichroism of the sample. A theoretical investigation was done for the differential image obtained by subtracting the images formed under right and left circularly polarized light. Two types of images are obtained: a) darkfield images formed from light reflected or scattered by the sample, and b) brightfield images formed from light transmitted through the sample. The sign and magnitudes of each feature in a circular differential image strongly depend on the structure of the sample. The sign and magnitude of the darkfield differential images are sensitive to the large features with dimension of the order of the wavelength of light, and the brightfield differential images are sensitive to the short-range molecular order.

**W-Pos61** ULTRAVIOLET RESONANCE RAMAN STUDIES OF PEPTIDE COMPONENTS. Leland Mayne, Tarik Ramahi, Terry Oas and Bruce Hudson, Molecular Biology Institute and Department of Chemistry, University of Oregon, Eugene, Oregon 97403.

Modern laser techniques make ultraviolet radiation available with sufficient intensity for Raman spectroscopy at wavelengths to 188 nm. Raman spectra of N-methylacetamide show a strong amide II band when excited below 220 nm. This band is not seen at all when spectra are obtained with visible or near UV excitation. Deuterium exchange of the amide proton results in a substantial change in the intensity distribution of the amide bands so that the amide II' band becomes the largest peak. Recent studies of isotopically substituted N-methylacetamide in which the peptide bond has been labeled with C13 and N15 have also been performed. The isotopic shift of the deuterated version of this molecule shows that the amide II' vibration is essentially a pure C-N stretch. These studies indicate that such isotopic substitution may be sufficient to identify Raman bands due to specific peptide bonds in proteins. Overtone and combination bands of normal and isotopic peptide bands will also be discussed. Relative intensity differences are observed between the isotopic species.

Ultraviolet Raman scattering appears to be a useful technique for the determination of the content of proline isomers in peptide chains. Studies of model cyclic proline peptides reveal that those species which must have proline peptide bonds in the cis conformation have Raman amide II bands above 1500  $\text{cm}^{-1}$ . Molecules with predominantly trans proline conformations have their strong UV Raman bands well below 1500  $\text{cm}^{-1}$ .

ABSTRACT  
WITHDRAWN



**W-Pos63** ANALYSIS OF IN SITU LIGNIN DEGRADATION BY PHOTOACOUSTIC SPECTROSCOPY. R. V. Greene, S. H. Gordon, and J. M. Gould. Northern Regional Research Center, ARS/USDA, Peoria, Illinois 61604

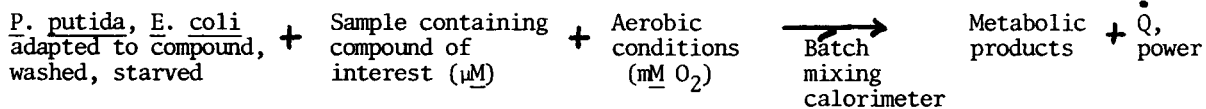
Photoacoustic spectroscopy (PAS) is a promising analytical technique for characterizing insoluble materials. Because the photoacoustic spectrum of a given material is theoretically and empirically the same as its absorption spectrum, interpretation of the spectrum is straightforward. Lignin, which composes up to 30% of the dry weight of woody plants, is a three-dimensional polymer of essentially infinite molecular weight, comprised of a variety of phenylpropane monomeric units randomly coupled through an assortment of carbon-carbon and ether linkages. PAS is one of the few analytical techniques available for studying lignin in situ. In nature, lignin is degraded by a variety of environmental factors. Among them are reactions involving activated oxygen species and biodegradation by fungi. Fungal lignin degradation also appears to involve an oxidant ( $H_2O_2$ ), which is excreted from the mycelia. Results will be presented in which modification of native lignin by some of these factors are characterized utilizing UV-visible and Fourier-transform-IR photoacoustic spectroscopy.

**W-Pos64** ELECTROCHEMICAL IMMUNOASSAYS WITH ENZYME AMPLIFICATION. H. B. Halsall, K. R. Wehmeyer, M. J. Doyle, W. R. Heineman, Department of Chemistry, University of Cincinnati, Cincinnati, OH 45221.

Heterogeneous assays have been developed for both (i) haptenic and (ii) macromolecular systems. All assays use alkaline phosphatase (AP) as the enzyme label to convert phenyl phosphate to phenol, which is then measured amperometrically at a carbon paste electrode after passage through a C-18 reverse phase column. The detection limit for phenol was  $5.0 \times 10^{-9}M$  with a linear range of three orders of magnitude. (i) AP-labeled digoxin used as the competitive tracer in human serum allowed the determination of digoxin throughout its therapeutic range with a detection limit of 50 pg/ml. An excellent correlation existed between digoxin concentrations in 54 patient samples determined by RIA and this method. This configuration used  $\alpha$ -digoxin as the adsorbed phase. (ii) a. A similar strategy for human orosomucoid as the antigen gave a detection limit of 1 ng/ml with a most sensitive range between 1 and 10 ng/ml. (ii) b c AP-labeled goat  $\alpha$ -rabbit IgG was used as a model tracer in both b competitive and c sandwich assays for rabbit IgG. For b the rabbit IgG was present both as the adsorbed phase and soluble analyte. This assay had a detection limit of 5 ng/ml and a dynamic range of two orders of magnitude. Configuration c had  $\alpha$ -rabbit IgG as the adsorbed phase and AP- $\alpha$ -rabbit IgG as the outer layer of the sandwich. This assay was very sensitive, with a detection limit of 10 pg/ml and a dynamic range of four orders of magnitude. These assays are rapid, simple, sensitive and inexpensive and place electrochemical immunoassay closer to the clinical laboratory. Supported by grants NIH HD-13207 and NSF CHE-8217045.

**W-Pos65** MICROBIAL-MICROCALORIMETRIC METHOD FOR AQUEOUS COMPOUND ANALYSIS.

Rex Lovrien, Biochemistry and Biotechnology Dept., Univ. of Minnesota, St. Paul, MN 55108  
Adapted bacteria used in heat conduction calorimetry provide a new basis for assay of dilute compounds in water:



Lower organic acids, alcohols, sugars and hydrocarbons commonly generate 50-500 Kcal/mole of aerobic metabolic heat (J. Exp. Zool. 228, in press (1983); Biotech. Bioeng. 22, 1249-69 (1980)). Nanomole amounts of such compounds in 0.5-2 ml. of aqueous sample can be quantitated. The bacteria are grown on the compound of interest, which induces the necessary enzymes by large factors. Induction provides for two needs, specificity, and rapidity in driving the analytical reaction. One may grow one's own "specific reagents", which are washed, starved, but still fully functional microorganisms. About 1 mg. of such organisms usually are capable of combusting several dozen nanomoles of benzene, acetate, methanol, etc. in water, in 200-300 sec. at 25°. There are a number of useful features. (i) Flexibility; myriad organisms are probably useful, able to combust many compounds, (ii) Works under rugged conditions, raw soil, river water, broth, without need to derivatize or to extract the sought compound, (iii) Enables discernment of toxic agents when they disable organisms, (iv) Provides a basis for nondestructive assay of mammalian tissue, cells and metabolic compounds.

**W-Pos66** SEDIMENTATION COEFFICIENT DISTRIBUTIONS FROM ULTRACENTRIFUGE INTERFEROGRAMS. David A. Yphantis, Biochemistry and Biophysics Section, University of Connecticut, Storrs, CT 06268.

A new approach is described for determination of  $G(s)$ , the integral sedimentation coefficient distribution curve, from measurements of Rayleigh interferograms: For each set of measurements construct a curve of concentration corrected for radial dilution (as the integral of  $r^{*2} dc$  from the meniscus to the radius  $r$ ) versus position. The logarithm of the ratio of radii corresponding to the same corrected concentration then determines the sedimentation coefficient associated with this concentration. (In contrast, the usual methods estimate the sedimentation coefficient corresponding to a given concentration from the ratio of the radius to the original boundary position.) This new approach provides the following advantages: The concentration distribution before the first interferogram need not correspond to undisturbed sedimentation; convection-free sedimentation is only required in the time interval between the distributions used. The effects of diffusion on the apparent sedimentation coefficient distributions are significantly decreased since most diffusion occurs at early times; thus the extrapolations to infinite time are easier and less critical. The resultant  $G(s)$  for monodisperse solutes are significantly sharper (typically by a factor of 2-3) than the  $G(s)$  furnished by the usual approaches. These advantages are paid for in terms of two requirements: The absolute fringe displacement must be known and the fringe displacements used must be of higher precision than usually required. Implementations of this algorithm will be illustrated with both synthetic and experimental data. (Supported by NSF grant PCM 81-11484).

**W-Pos67** TECHNIQUE FOR PREPARING CELLS AND ORGANELLES FOR DEEP-ETCH STUDY. Alan Magid, M. J. Costello, J. M. Corless and H. P. Ting-Beall, Dept. Anatomy, Duke Med. Ctr., Durham, NC 27710

The rapid-freezing, deep-etch methodology pioneered by Heuser and coworkers (e.g., *J. Cell Biol.* 82: 150, 1979) is unnecessarily complex for many applications. We have developed a simpler method for freeze-etching aqueous suspensions of isolated cells, organelles, and similar materials based on the mica-carbon technique of Valentine et al. (*Biochemistry* 7: 2143, 1968) and the ultra-rapid freezing method of Corless and Costello (*Methods Enzymol.* 81: 585, 1982). A thin carbon film is floated onto the surface of a suspension of particles and is then picked up again on its mica support. Adsorbing specimens to a film conveys several advantages: 1) elongated specimens become oriented so that longitudinal fractures are much favored; 2) specimens may be conveniently exposed to various chemical treatments; 3) the thin film ( $\sim 10 \mu\text{m}$ ) insures freezing preservation. To limit swelling during the final pickup step from deionized  $\text{H}_2\text{O}$  (used to minimize salt artefacts during etching), most specimens were fixed on 2% buffered glutaraldehyde. Films are picked up finally with copper "hats", sandwiched with another hat, and excess  $\text{H}_2\text{O}$  blotted off. Alternatively, specimens may be picked up on coverslips or EM grids for supplemental study. The sandwich is then plunged into  $\text{LN}_2$ -cooled propane ( $-190^\circ\text{C}$ ) and stored under  $\text{LN}_2$ . Specimens were fractured in a Balzers 360 M, etched 20 min. at  $-95^\circ\text{C}$ , and rotary shadowed with Pt-C at a  $25^\circ$  angle. Replicas were removed with dilute chromic acid and cleaned with Clorox. In this pilot work we have examined myofibrils, isolated rod outer segments, rabbit sperm, and tropomyosin paracrystals. Micrographs of muscle, retina, and some common artefacts of the method will be shown. Supported in part by NIH grants to each author.

**W-Pos68** DETECTION AND AERODYNAMIC SIZING OF UNSTAINED AEROSOLIZED BACTERIA IN REAL TIME ON A SINGLE PARTICLE BASIS. A. J. Adams<sup>1</sup>, D. E. Wennerstrom<sup>2</sup>, and M. K. Mazumder<sup>1</sup>, <sup>1</sup>Electronics and Instrumentation, Graduate Institute of Technology, University of Arkansas, Little Rock, AR 72203; <sup>2</sup>Microbiology and Immunology, University of Arkansas for Medical Sciences, Little Rock, AR 72205.

Single particle aerodynamic relaxation time (SPART) analysis has been successfully applied to the study of three types of bacteria: *Bacillus subtilis*, *Escherichia coli*, and *Staphylococcus epidermidis*. The technique subjects aerosolized bacterial particles to a 24-kHz acoustic excitation field, monitors the resulting particle motion using a dual-beam, frequency-biased laser Doppler velocimeter, and aerodynamically sizes the particle in real time by measuring the phase lag of the particle motion relative to the driving field. We find that bacterial aerosols can be readily generated by the conventional technique of pneumatic atomization, that the SPART-analyzer detects and sizes individual bacterial cells, and that bacteria retain viability during the analysis. The method can distinguish the three types of organisms from the measured aerodynamic size distribution. The measured aerodynamic diameters agree with results predicted from microscopic observation. This study demonstrates the potential of the SPART technique in the rapid detection and characterization of airborne biological particles.

**W-Pos69** A REANALYSIS OF RADIATION-RELATED HEPATOCELLULAR TUMORS IN MICE: THE MALE/FEMALE SUSCEPTIBILITY AND NEUTRON/GAMMA RAY EFFICACY. Richard P. Spencer, Dept. Nuclear Medicine, University of Connecticut Health Center, Farmington, CT 06032.

Ionizing radiation is known to have little effect in inducing hepatocellular tumors in mice, unless a mitotic stimulant is also used (such as CC14 or partial hepatectomy). Fetal tissues are also mitotically active and Sasaki et al (Gann 69:451, 1978) demonstrated that radiation of mice in utero, at 17 days postcoitus, produced a high incidence of hepatocellular tumors. We analyzed their data separately for males and females after subtracting out the "spontaneous" occurrence of the tumor (which was higher in males). The incidence of hepatic malignancy, versus x-ray dose, was also higher in males than in females (at 300 R:38.3% versus 12.4%). The number of tumors in each sex, after "spontaneous" incidence correction, suggested passage of the line of incidence versus dose through the origin. When all hepatic tumors were considered (data in Gann 69:167, 1978), the incidence was again higher in males after 200 R in utero radiation at 16-18 days postcoitus (C57-BL/6 x WHT/Ht mice). Relative hepatic susceptibility was assessed for LAF1/Jax male mice from the data of Wiley et al (Radiat. Res. 54:284, 1973) by calculating: (tumors induced by neutrons-spontaneous)/(tumors induced by gamma rays - spontaneous). At 200 R the relative hepatic sensitivities were: 3.18, 7.43, 4.30 and 4.11 respectively, when: a) partial hepatectomy was carried out 8-13 weeks post radiation, or b) radiation was done 24, 36.5 or 43.5 hours after partial hepatectomy. Radiation at 24 hours after partial hepatectomy was most effective in enhancing neutron/gamma ray sensitivity. (Supported by USPHS CA 17802, National Cancer Institute).

**W-Pos70** THERMOREGULATION IN THE PRESENCE OF LOW INTENSITY RADIOFREQUENCY FIELDS. Eleanor R. Adair, (Intr. by A. Pharo Gagne). John B. Pierce Foundation and Yale University, New Haven, Connecticut 06519.

Maintenance of a constant internal body temperature is essential to the survival and optimal functioning of every warm-blooded organism. Radiofrequency electromagnetic radiation is an environmental energy source that can disturb normal thermoregulatory processes by generating heat in both peripheral and deep-body tissues. Experiments using squirrel monkeys as subjects have quantified the minimal intensity of 2450-MHz CW microwaves that will reduce metabolic heat production in the cold, initiate thermoregulatory sweating in the heat, alter peripheral vasomotor tone in thermoneutral environments, and stimulate behaving animals to select a cooler environment. The threshold power densities that altered all responses were remarkably similar (4-8 mW/cm<sup>2</sup>), representing a rate of whole-body energy absorption (~1.5 W/kg) that is equivalent to 15-20% of the resting metabolic rate of the squirrel monkey. Control experiments featuring exposures to comparable intensities of infrared radiation failed to provoke similar response changes, suggesting that thermosensitive tissue heated by radiofrequency radiation may be located deep in the body rather than in the skin. In general, whether the environment is warm or cool, warm-blooded organisms detect and respond immediately to low-intensity radiofrequency fields as they do to other environmental thermal stimuli resulting in precise regulation of the internal body temperature at the normal level. (Research supported by AFOSR Grant 77-3420.)